Syntheses and Polymerization of Bio-based Diketopiperazine Monomers and their Self-assembly

Thawinda HIRAYAMA

Japan Advanced Institute of Science and Technology

Doctoral Dissertation

Syntheses and Polymerization of Bio-based Diketopiperazine Monomers and their Self-assembly

Thawinda HIRAYAMA

Supervisor: Professor Tatsuo Kaneko

Graduate School of Advanced Science and Technology
Japan Advanced Institute of Science and Technology
Materials Science

March 2020

Abstract

High performance DKP-based biopolyimides with morphology control feature were here established. From the dimerization of biomass 4-amino-L-phenylalanine (4APhe), a newly-designed bio-based aromatic diamines having diketopiperazine (DKP) as a central core (DKP-4APhe) was generated. The polymerization of DKP-4APhe with various dianhydrides could introduce high rigidity from alicyclic building blocks to the polymer structures and help generate high thermal resistant polyimide (PIs). The developed bio-based PIs showed high thermal stability with highest T_{d10} of 432 ^{o}C and no glass transition below the thermal decomposition temperatures. The charge transfer characteristic to polyimides and hydrogen bonding between the imide group and DKP ring or between DKP moieties could be a reason for high thermal stability. However, due to flat structure of LL-DKP units, polyimides with low molecular weight was obtained as a result of highly dense packing of polymer chains.

By changing the conformation isomer of DKP-based polyimides to DL type, polyimide with greatly increased molecular weights could be generated. The prepared DL-polyimide film exhibited lower yellow index and higher transparency compared to the commercial PI, Kapton®. The DL-polyimide film derived from BTDA also showed ductile property with 10.5% elongation.

Due to superior hydrogen bonding ability of DKP and the embedded aromatic in the polymer chains, the self-assembly property could be bestowed on the developed PAAs and PIs. Here, the self-assembly of the DKP-based PIs was demonstrated. The uniform PIs nanospheres could be obtained using simple solvent displacement method and subsequent two-step imidization. High thermal resistance property of the generated PI particles still maintained. In addition, the thermoresistant biopolyamide particles have the ability to transform into different shapes such as spiky balls, flakes, or rods by external stimuli of solvent exchange. The PAA

particle morphologies were almost kept in PIs after two-step imidization. Such high-performance bio-based PIs with controllable particulation property could lead to their possible applications such as fillers reinforcing polymer matrix.

Keywords: Diketopiperazine, Bio-based, Polyimide, Self-assembly

Acknowledgements

Primarily, I would like to express my sincere appreciation to my respected advisor, *Professor Tatsuo Kaneko* for his sincere and tireless guidance and patience, generous encouragement and kind support at professional and personal level during the PhD program at JAIST.

I also sincerely thank the committee members: my second supervisor *Professor Masayuki Yamaguchi*, my advisor for minor research *Associate Professor Kazuaki Matsumura*, *Associate Professor Toshiaki Taniike* at JAIST and *Professor Supason Wanichwecharungruang* from Chulalongkorn University, for their time and valuable advice during the defense.

I am very grateful to *Dr. Maiko Okajima* for her kindness and concern that made it possible for me to complete my study without any difficulties in JAIST. I also thank *Assistant Professor Kenji Takada* for his kind support throughout my research at Kaneko Laboratory. My thankfulness also extends to all Kaneko lab members and all Thai friends at JAIST who I have known and worked with for 3 years. Thank you for providing me such a warm studying and working environment.

Importantly, I am affectionately thankful to my parents and my husband for thoughtful attention and continuous encouragements during study.

Finally, I also place on record, my sense of gratitude to all who, directly or indirectly, have lent their helping hand in this venture.

Spring 2020

Thawinda Hirayama

Contents

Pages

CHAPTER I

GENERAL INFORMATION

1.1 Bio-based polymers

Advances in petroleum-based fuels and polymers have benefited humanity in numerous ways. Petroleum-based plastics can be disposable and highly durable, depending on their composition and specific application. However, petroleum resources are finite, and prices are likely to continue to rise in the future. In addition, global warming, caused in part by carbon dioxide released by the process of fossil fuel combustion, has become as increasingly important problem. The disposal of household plastic made of petroleum-based materials, such as fast-food utensils, packaging containers, and trash bags also causes the environmental problems and the loss of natural resources. It is necessary to find new ways to secure sustainable world development. Renewable biomaterials that can be used for both bioenergy and bioproducts are possible alternative to petroleum-based and synthetic products.

Long time continuing overconsumption of nonrenewable resources due to human activities have caused a profoundly unfavorable impact on the environment and numerous problems [1] such as carbon dioxide emission into the earth's atmosphere which is a serious factor of enhancing global warming [2]. Most of household plastic waste which mostly comes from petroleum-based materials such as polyethylene, polypropylene, polyvinylchloride, polystyrene, etc. greatly play a part in the loss of natural resources and the limited amount of petroleum. Therefore, the use of environmentally friendly polymers originating from renewable starting materials is highly significant concerning the reduction of waste.

Bio-based polymers, the materials that are produced from renewable resources, are now of great interest due to environmental concerns and the realization that global petroleum is an exhaustible resource. Bio-based polymers offer important contributions by supplying a renewable alternative to the use of fossil fuel-based chemicals and through the related positive environmental impacts such as reduced carbon dioxide emissions. As a result, the development in bio-based polymers has accelerated in recent years.

The first generation of bio-based polymers focused on deriving polymers from agricultural feedstocks such as corn, potatoes, and other carbohydrate feedstocks. However, in recent years the focus has shifted due to a desire to move away from food-based resources and significant breakthroughs in biotechnology.There are three principal ways to produce bio-based polymers using renewable resources [3]:

1. Using natural bio-based polymers with partial modification to meet the requirements (e.g., starch)
2. Producing bio-based monomers by fermentation/conventional chemistry followed by polymerization (e.g., polylactic acid, polybutylene succinate, and polyethylene)
3. Producing bio-based polymers directly by bacteria (e.g., polyhydroxyalkanoates).

However, there are still some drawbacks that prevent the wider commercialization of bio-based polymers in many applications. This is mainly due to limited performance and higher price when compared with other conventional polymers, which remains a significant challenge for bio-based polymers.

In this section, examples of well-established bio-based plastics made from renewable resources are reviewed.

Polylactic acid or polylactide (PLA)

PLA belongs to the family of aliphatic polyesters with the basic constitutional unit lactic acid. The monomer lactic acid is the hydroxyl carboxylic acid which can be produced via bacterial fermentation from abundant naturally occurring renewable resources such as corn (starch) and sugars. PLA can be synthesized by direct polycondensation of lactic acid monomers or ring-opening polymerization of lactide monomer.

PLA is a commercially interesting polymer as it has many unique characteristics, including good transparency, glossy appearance, high rigidity, and ability to tolerate various types of processing conditions. PLA is a thermoplastic polymer which has the potential to replace traditional polymers such as PET, PS, and PC for packaging to electronic and automotive applications [4].

While PLA has similar mechanical properties to traditional polymers, the thermal properties are not attractive due to low T_g of 60°C. Heat-resistant PLA can withstand temperatures of 110 °C [5]. There has been reported a number of efforts to overcome such drawback for instance changing the stereochemistry of the polymer and blending with other polymers and processing aids to improve the performances [6]–[12].

Polyhydroxyalkanoates (PHAs)

PHAs are a family of polyesters produced by bacterial fermentation using several renewable waste feedstock such as cellulosic, vegetable oils, organic waste, municipal solid waste, and fatty acids with the potential to replace conventional hydrocarbon-based polymers.

PHA polymers are thermoplastic. The common T_g of the polymers varies from −40°C to 5°C, and the melting temperatures range from 50°C to 180°C, depending on their composition [13]. However, due to its stiffness, brittleness and narrow processing temperature

range, it is not attractive for many applications, requiring development in order to overcome these shortcomings [14] such as copolymerization with a second monomer. For example, the copolymer poly(3HB-*co*-3HV) has increased tensile strength and toughness compared to poly(3HB) while remaining biodegradable [15]. PHA and its copolymers are widely used as biomedical implant materials.

Polybutylene succinate (PBS)

PBS, an aliphatic polyester with similar properties to those of PET, is produced by condensation of succinic acid and 1,4-butanediol. PBS can be produced by either monomers derived from petroleum-based systems or the bacterial fermentation route.

Conventional processes for the production of 1,4-butanediol use fossil fuel feedstocks such as acetylene and formaldehyde. The bio-based process involves the use of glucose from renewable resources to produce succinic acid followed by a chemical reduction to produce butanediol.

PBS is a semicrystalline polyester with a melting point higher than that of PLA. The T_g is approximately −32°C. In comparison with PLA, PBS is tougher in nature but with a lower rigidity and Young's modulus. It is used in foaming and food packaging application. The relatively poor mechanical flexibility of PBS limits the applications of 100% PBS-based products. However, this can be overcome by blending PBS with PLA or starch to improve the mechanical properties significantly, providing properties similar to that of polyolefin [16], [17].

All the polymers mentioned above display low thermal and mechanical performances compared to petrochemical-based polymers. Many efforts are seen towards introducing new bio-based polymers with higher performance and value. One of the most effective strategies to improve the performances is incorporating aromatic component into the polymer backbone [9], [10], [18]–[21].

1.2 High performance polymers

High-performance polymers are polymers that provide improved set of properties and meet higher requirements than standard or engineering plastics due to their exceptional mechanical strength, higher chemical and/or a higher heat stability, electrical or sound insulation properties and superior flame resistance [22]. Because of the superior performance characteristics of high performance polymers and other economic advantages, they have been applied in many industries ranging from communication to medicine and also in many challenging areas like aerospace, energy electronics, automotive etc. as compared to the conventional polymers [23] and are also slowly replacing traditional materials such as aluminum or metals [24]. Therefore, the demand for this type of polymeric materials is increasing steadily.

Various categories of high performance polymers include poly(phenylene ether), polysulfones, poly(aryl ether ketone), polyoxadiazole, polyimide etc . Here, in this section, two kinds of high performance polymers were focused: polyimide and polyurea.

1.2.1 Polyimide

Polyimides (PIs), a class of super high-performance plastics, have been widely utilized inside of electronic devices and under the aerospace, because PIs are tolerate in such harsh environments [25]–[29] owing to their outstanding mechanical durability, thermal, and chemical stability.

According to the composition of their main chain, polyimides can be classified into aliphatic, semi-aromatic and aromatic. Aromatic polyimides constantly attract wider interest because of their thermal stability and mechanical properties surpass the others [30]–[32]. Generally, there are two types of degradation: thermal-oxidative degradation and thermal degradation. Both types of degradation proceed via a radical mechanism [33]. The increase in

temperature stability by incorporating aromatic units is because aromatic rings help stabilize free radicals by delocalization through π-system and consequently offer a good protection against chain scission. In this way, the thermal stability is strongly increasing. In spite of the increase in thermal stability, aromatics also provide the rigidity of the chains make the polymers difficult in processability. To find a balance between processability and stability, flexible units (e.g., O, S, $C(CH_3)$ and other rigid parts (e.g., O, S, $C(CH_3)$ can be alternatively incorporated into the polymer chains.

Preparation and structure of polyimides

Polyimides are generally synthesized via the most widely practiced two-step procedure from diamines and aromatic tetracarboxylic dianhydrides: 1.) low temperature condensation with formation of prepolymer, poly(amic acid) (PAA) and 2.) thermal cyclodehydration or imidization at 250- 300 °C, the most frequently employed method for PIs formation. This process has some limitations for example, the generation of water, which would create voids and stresses in the final products [23]. Additionally, high temperature leads to several undesirable side reactions, such as crosslinking or scissoring polymer chains that can result in brittle films [31], [32]. The imide ring closure may be alternatively proceeded via the catalytic cyclodehydration at room temperature using a mixture of acetic anhydride with tertiary amines. It is a much milder reaction conditions leading to the fabrication of less damaged PIs.

A classic example of polyimide is Kapton, which is produced by condensation of pyromellitic dianhydride (PMDA) and 4,4'-oxydianiline (ODA) under ambident conditions in dipolar aprotic solvents, such as N-methylpyrrolidone (NMP) or N,N-dimethylacetamide (DMAc). PAA precursors are cured by either thermal or chemical treatment to proceed polycyclodehydration reaction lead to final polyimide (Scheme 1) [34].

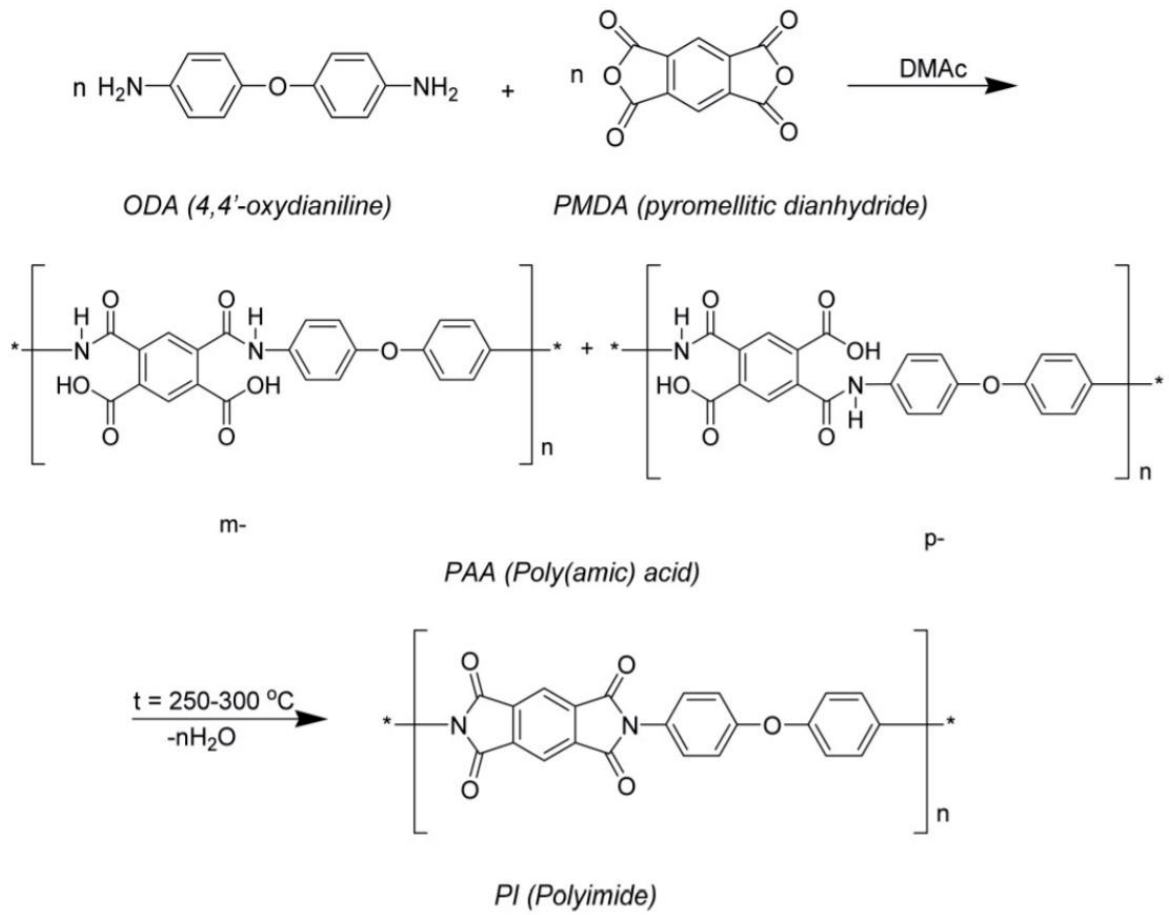

Scheme 1.1 Reaction between ODA and PMDA to PAA with following cyclodehidration to PI [35].

Reactions between cyclic anhydrides and primary diamines undergo SN_2Ac mechanism (bimolecular nucleophillic acyl substitution). The reaction running in two steps. First, the intermediate poly(amic acid) is formed by the nucleophilic attack of the amino group on the carbonyl of the anhydride. This reaction is irreversible because the amino group is strong nucleophilic agent (not a good leaving group) [36]. Second, nucleophilic ring closure due to dehydration leads to imide ring formation.

Physical properties of polyimides

Intramolecular interaction

The increased interchain attractive forces due to charge transfer complex (CTC) formated between dianhydride and diamine groups in polyimides is an important reason for effectively increasing in the chain rigidity and hence T_g of polyimides [37]. Due to the presence of electron donor (nitrogen atom) and electron acceptor (carbonyl group) in the polymer structure, it is natural to assume that electron moving and donor-accepter interaction undergoes in polyimides. Kapton-type polyimide, for instance, has a high T_g of 400^{o}C because of rigidity from pyromellitimide structure and strong charge transfer interaction between the electron-withdrawing part of pyromellitimide and the electron-donating part of diphenyl ether [35]. This interaction also attributes to the color and other, particularly semi-conductor, properties of polyimides [38], [39]. Figure 1.1 shows the idealized form of charge transfer interaction between the dianhydride and diamine groups.

Additionally, the existence of π–π interaction between aromatic also lead to parallel and planar chain conformations to each other [40]. It was also reported that T_g was strongly influenced by the presence of connecting bridges in the dianhydride as it changed its electron affinity and hence promoted/depromoted the possibility of CTC formation [41].

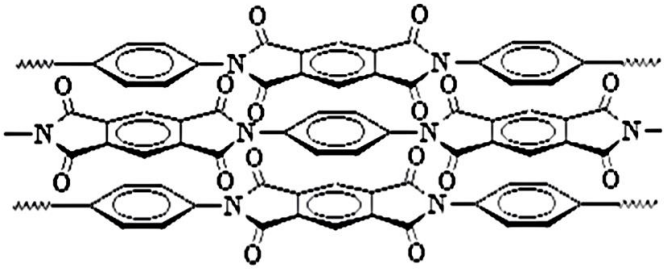

Figure 1.1 Idealized charge transfer complex formation between dianhydrides and diamines in polyimide [35].

Thermal properties and Optical property

Aromatic polyimide have been widely applied in many engineering fields due to their excellent high thermal and chemical resistance, high mechanical properties, and good dielectric features [42]–[45].

Thermal stability can be measured by a variety of methods. These have included measure of the amount of weight change of a material as a function of increasing temperature in air (thermos-oxidative degradation) or in an inert environment such as nitrogen atmosphere (thermal degradation) so called thermogravimetric analysis (TGA). In general, polyimides are stable up to a temperature of 440 °C in a nitrogen atmosphere [46].

However, in microelectronic and optoelectronic engineering which require colorless and high transparent PI films, conventional PI films generally show considerable coloration ranging from pale yellow to deep brown and poor optical transmittance originated from the formation CTC between the diamine donor moieties and dianhydride acceptor moieties in their highly-conjugated molecular structures [47], [48]. By introduction of heteroaromatic units, rigid and highly-conjugated substituents into polymer structure to obtain PI films with high thermal resistance, it usually inevitably deteriorate their optical transparencies at the same time. On the contrary, polyimides that contain flexible linkages, such as ether units, show high optical transparency by weaken CT interactions but low glass transition temperatures due to their flexible polymer backbones. Figure 1.2 summarized various molecular design procedures, including favorable and unfavorable designs in developing PI films with desired properties.

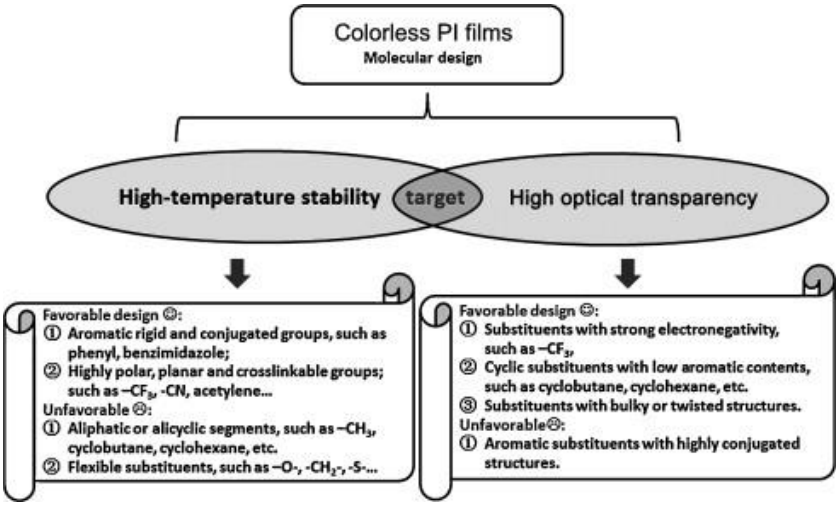

Figure 1.2 Molecular design for PI films [49].

Polyimide particles

Due to their combing excellent properties of PI together with the development of nanotechnology, the fabrication of such high performance engineering plastic into nanomaterials has become attractive. Recently, PI spherical nanoparticles have drawn much attention due to their potential as next generation materials such as nanoreactors, low dielectric fillers, coating materials, drug delivery carriers and ultra low-k materials [50]–[55]. However, due to their intractability, it is a challenged work how to control such rigid structure into desired nano- or micro-materials.

Chai *et al.* [56] and Xiong *et al.* [57] obtained PI spheres by the dropwise addition of the poor solvent (water or ethanol) into PI solutions. This method is not common as it could be applied only with soluble PIs. On the other hand, poly(amic acid) (PAA), the precursor of PI dissolved in some organic solvents such as NMP, is easily converted into PI by the imidization treatment. Therefore, PI particles are often fabricated from PAA solutions or PAA particles. One of the most common technique to fabricate PI particles from PAA solution is solvent displacement method or also known as reprecipitation method.

Suzuki *et al.* [58] prepared 6FDA-ODA typed polyimide particles through two-steps imidization of poly(amic acid) particles using reprecipitation method (Figure 1.3). The obtained PAA and PI nanoparticles were all spherical with size-controlled between ca. 20-500 nm by changing the experimental conditions such as temperature of the poor solvent, the composition of two kind of poor solvent, and PAA in NMP solution concentration.

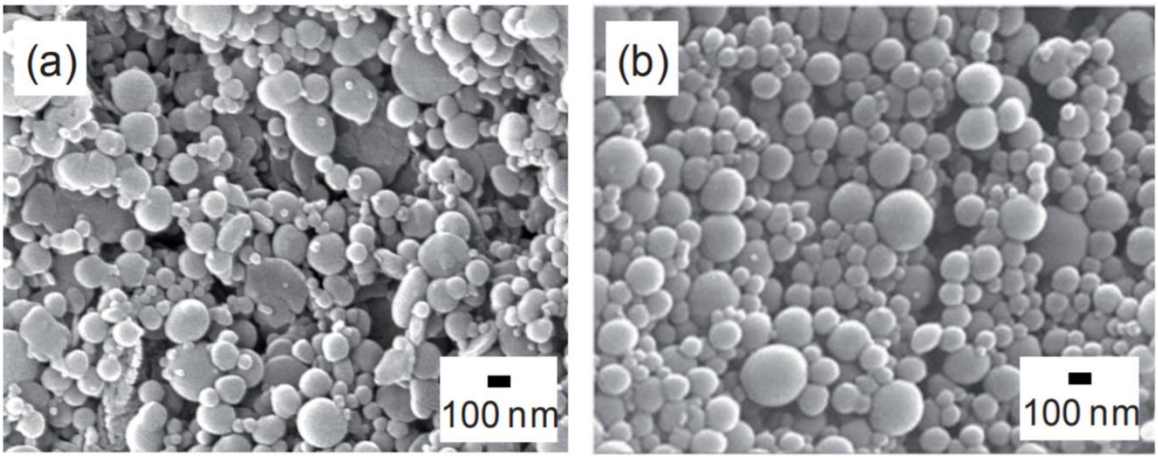

Figure 1.3. SEM images of 6FDA-ODA-type (a) PAA and (b) PI nanoparticles [58].

Recently increasing demand in the high technology industries such as space, micro/nano electronics, planes, automotive, membranes, fuel cells, etc. has been the driving force for the development of the diversity of polyimide materials with different characteristics. However, PIs were mainly developed with petrochemical-based monomers and only a few attempts have been made to prepare partial or completely bio-based PIs [59]–[65]. Recently we proposed the concept of bio-based PIs using a bio-based aromatic diamine, 4,4'-diaminotruxillic acid (4ATA), and various dianhydrides [59]. Attributed to the molecular design, we found that alicyclic structure sandwiched between two aromatic rings imparted rigidity to generate high thermoresistance polyimides with T_{d10} of 425 ^{o}C and T_g of 350 ^{o}C at maximum as well as functionality such as transparency in the case of 4ATA (Scheme 1.2).

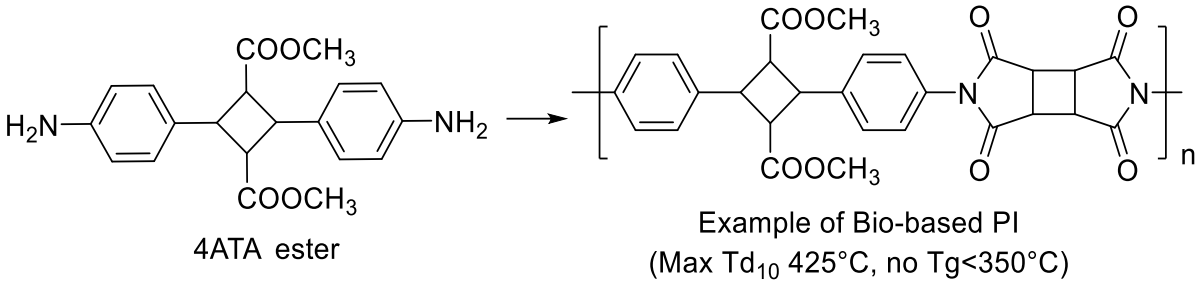

Scheme 1.2 Bio-based PI derived from 4ATA diamine monomer [59].

1.3.2 Polyurea

Polyurea (PU) is also one of the most successful materials used in the coating industry [66], [67], having multiple applications in many fields due to their good mechanical properties, fast curing, chemical resistance, hydrolytic stability, low flammability and excellent bonding properties to all type of surfaces, especially metals [68]–[72].

There are a number of methods have been used to prepare polyureas; however, the most common method is a rapid polyaddition reaction between two species: a diamine and a diisocyanate. The diisocyanate can be aromatic or aliphatic in nature. By simply mixing those two commercial components, the polyurea with urea linkages could be prepared (Scheme 1.3 (a)). Additionally, polyureas can also be formed via a carbamic acid intermediate by the reaction of isocyanates and water. This acid decomposes to an amine and carbon dioxide (Scheme 1.3 (b)). The amine then reacts further with another isocyanate group to form the polyurea linkage.

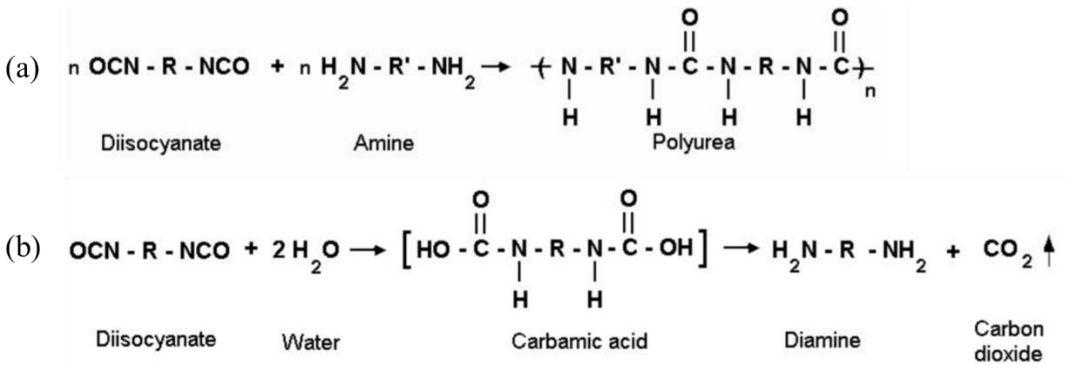

Scheme 1.3 (a) Polyurea chemistry and (b) Isocyanate/water reaction [73].

However, thermal degradation of conventional PU takes place at temperatures above 200 °C [74], which limits their usage as an engineering material. There have been a great number of studies about improving the thermal stability of PU such as introduction of rigid structure and blending or copolymerization with higher thermally stable polymers [75], [76].

1.3 Bio-based monomers

To generate bio-based polymer, one of possible approaches is producing bio-based monomers by fermentation/conventional chemistry from biomass followed by polymerization Biomass is organic material that comes from plants and animals, and it is a renewable source of energy. The conversion of biomass to useful materials such as polymers has considerable economic and environmental value, particularly in times of global warming and diminishing petroleum oil reserves. In previous reports, a few attempts have been made to prepare bio-based monomers for high-performance polymer syntheses [59]–[65]. The following are the bio-based monomers we have studied in our laboratory.

1.4.1 4-Aminocinnamic acid (4ACA)

Cinnamic acid is a white crystalline compound, soluble in many organic solvents but slightly soluble in water. Cinnamic acid and its derivatives are ones of bio-monomers existing

in plants such as Storax balsam [77]. Both *cis* and *trans* isomers of 4ACA are found; however, a latter is majority. 4ACA could also be obtained biosynthetically by the action of the enzyme phenylalanine ammonia-lyase (PAL) on phenylalanine – deamination of α-amino residue of phenylalanine (or its derivatives) to generate cinnamic acid (or its derivatives) [78], [79]. In addition, cinnamic acid also can be chemically modified to obtain 4ACA via nitration and followed by reduction to introduce amine functionality (Figure 1.5).

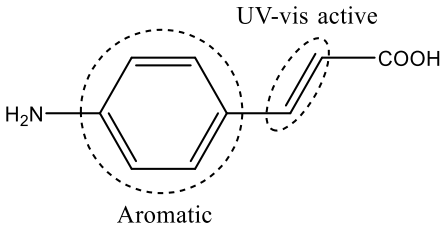

Figure 1.4 Chemical structure of 4ACA along with its property.

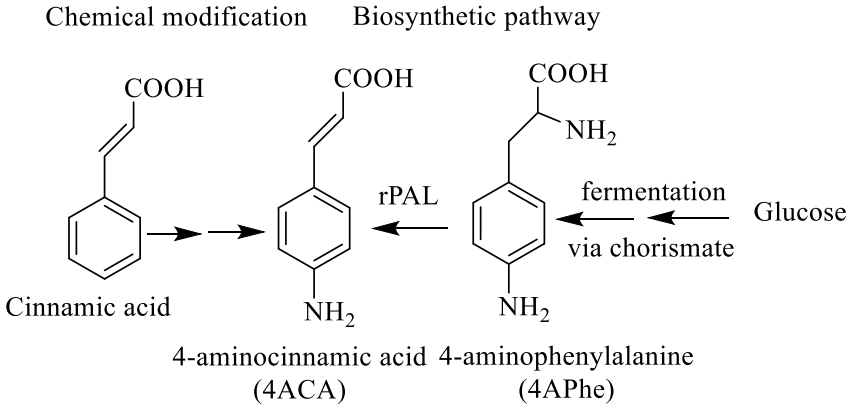

Figure 1.5 Chemical and biosynthetic pathways for the synthesis of 4ACA from cinnamic acid and 4-aminophenylalanine respectively.

In our previous work, we successfully prepared ultrahigh thermal resistant biopolyimide from a bio-based aromatic diamine, 4,4'-diaminotruxillic acid (4ATA), produced by a [2+2] photodimerization of 4ACA [59].

1.4.2 4-Aminophenylalanine (4APhe)

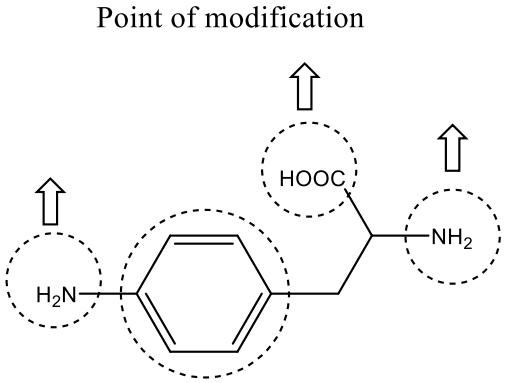

Figure 1.6 Chemical structure and ability modification of 4APhe.

4-Amino-L-phenylalanine (4APhe) is an amino derivative of amino acid phenylalanine, produced by bacteria as an intermediate of antibiotics [80] or via established systems for fermenting glucose or biomass [78], [79]. 4APhe also can be chemically produced from phenylalanine via nitration and followed by reduction to introduce amine group.

4APhe is an attractive starting material for further functionalization to achieve a novel bio-based monomer because it has three possible points of modification in the structure of 4APhe, which are carboxylic acid, aromatic amine and amine at α-carbon. One possible modification to obtain diamine monomer from 4APhe is the condensation rendering cyclodipeptide with two-amide linkage as a central core, named 2,5-diketopiperazines.

1.4 Diketopiperazine and its self-assembly property

2,5-Diketopiperazines (DKPs), forming from the condensation of two α-amino acids, are highly polar, symmetrical rings that can contain functional side chains, depending on the original amino acids. They not only abound in nature but also are often produced as degradation products of polypeptides, especially in processed food and beverages.

In the early 1900s, Fischer reported a simple, reliable synthesis route of DKP synthesis by converting the acid to a free-base methyl ester and cyclized it [81]. Other synthesis schemes also exist, with significant differences in complexity and yields [82].

The DKPs are semirigid molecules, and although they are conformationally constrained heterocycles, they are flexible because the six-membered ring can exist in an essentially flat conformation or a slightly puckered boat form, with only a few kcal/mol difference in energy between the boat and planar forms [83]. The crystal and molecular structures of 2,5-diketopiperazines have been examined extensively because these molecules are the simplest class of cyclic peptides. They contain 2 cis-amide bonds and as a result possess 2 H-bond acceptor and 2 H-bond donor sites important for binding to enzymes and receptors.

The cis-amide functionality in the 2,5-diketopiperazine ring forms intermolecular hydrogen bonds (N−H···O) between adjacent molecules that enable 2,5-diketopiperazines to take up higher-ordered supramolecular structures that are important in crystal engineering [84], [85] and as liquid gelators [86]–[88].

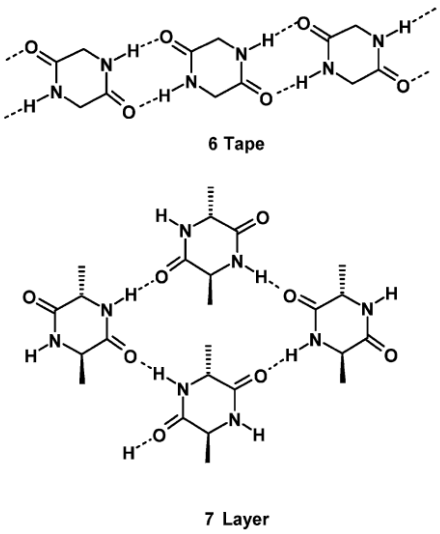

Figure 1.7 Schematic view of hydrogen bonding patterns observed for 2,5-diketopiperazines in the solid state [89].

Owing to such strong intermolecular interactions driven by unique hydrogen bonding patterns, DKP based-molecules tend to undergo molecular self-assembly forming various nano- and micro-architecture such as spheres, nanotubes, nanobelts, and fibers [90]–[92].

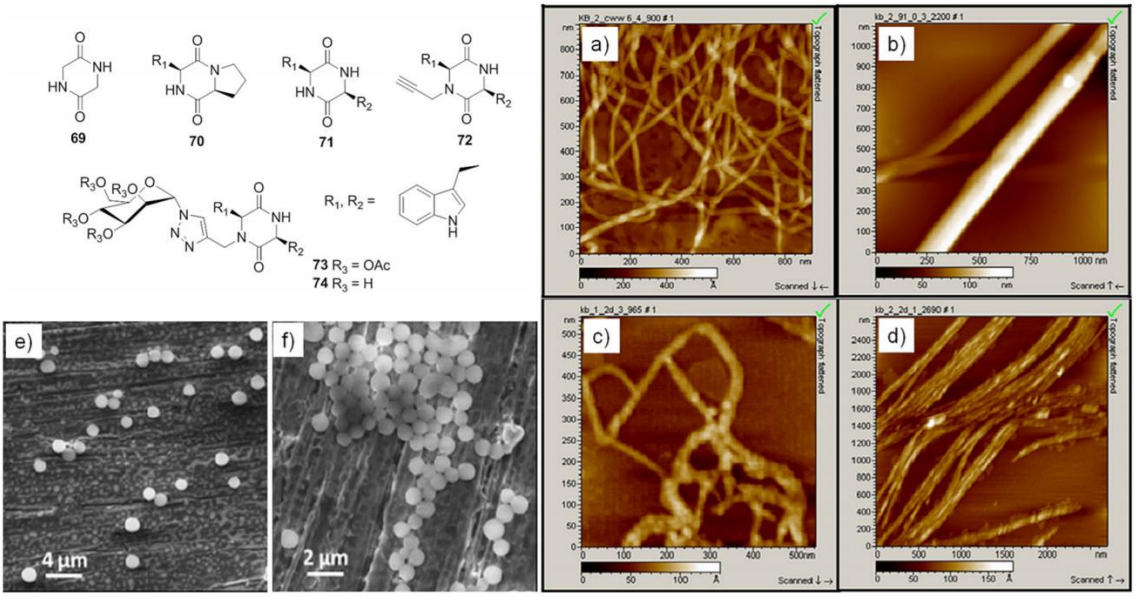

Figure 1.8 Chemical structures of cyclodipeptides (CDPs) 69–74 and AFM images of self-assembled fibrillar aggregates of CDPs 71, 73 and 74 (a–d) [92]. FESEM images showing self-assembled soft spherical structures of e) CDP 73 and f) 74 [93].

Despite the unique self-assembly property and stable heterocyclic structure, DKP rings are commonly found as the core structure of several drugs [83], [94], [95], but only few researches applied DKP for building blocks in functional polymeric materials [96]–[99]. In the presence of DKP embedded in the structure, particulation of the corresponding polymer chains into various morphologies through hydrogen bonding can be expected as a result of the chain self-assembly.

1.5 General Purpose

Here, we would like to generate a high-performance material from a renewable source for a sustainable green society. Bio-based polymer such as polyimide (PI) and polyurea (PU) is an attractive candidate for fabrication of such materials due to their combining outstanding properties. To wider their application potentials and increase their values, incorporating self-assembly property into such bio-based high performance polymers is also our target.

In this study, we are focusing on 4-aminophenylalanine (4-APhe), a bio-based aromatic amino acid derived from glucose fermentation, as a starting material to generate a novel bio-derived monomer for the synthesis of bio-based high performance polymer. Through the molecular design, the established monomer composes of two aromatic rings providing rigidity to the polymer structure and also 2,5-diketopiperazine (DKP) as a central core, a cyclic dipeptide having multiple sites for hydrogen bonding formation.

We study the synthesis of novel bio-based aromatic diketopiperazine diamine, 3,6-di(4-aminophenylmethyl)-2,5-diketopiperazine (DKP-4APhe), through a simple coupling process of stepwise protection and deprotection. The polymerization of two high performance polymers, polyimide and polyurea, from the obtained bio-based DKP monomers with commercialized counterparts is demonstrated. Particulation behavior of the corresponding PIs is also investigated.

CHAPTER II

SYNTHESIS AND CHARACTERIZATION OF BIO-BASED DIKETOPIPERAZINE MONOMERS

2.1 Introduction

The development of bio-based polymers has been advanced extensively to serve the need for sustainable green society. However, the conventional bio-based polymers were aliphatic such as polyester [100] and polycarbonates [101] exhibiting low thermal and mechanical performances, which limited their utilization. One strategy to overcome such limitations is to introduce biomass-derived aromatic monomers into the polymer backbone.

In previous report, we prepared a bio-based aromatic diamine, 4,4'-diaminotruxillic acid (4ATA), produced by a photodimerization of 4-aminocinnamic acid (4ACA), an aromatic amino acid obtained by a bio-conversion of 4-aminophenylalanine (4APhe) using genetically-engineered microbial cells [59]. Attributed to the molecular design, we found that alicyclic structure at the central core of 4ATA help impart high rigidity and consequently generate high thermo resistant polyimides with highest T_{d10} of 425 ^{o}C and T_g values over 350 ^{o}C. Despite their ultrahigh thermal performances, 4ATA syntheses required phenylalanine ammonia lyase (PAL)-catalyzed bioconversion of 4-aminophenylalanine (4APhe) which led to extremely low yield. This dilemma motivated us to render alternative biomass derived-diamine monomer based on the molecular structure concept of 4ATA.

The dimerization of biomass 4APhe could produce a diamine monomer with 2,5-diketopiperazine (DKP) as an alicyclic core, which corresponded to 4ATA molecular concept. DKP is the simplest class of cyclic peptides containing two *cis*-amide bonds and possessing

two H-bond acceptor and two H-bond donor sites. Considering our design, the presence of symmetrical amide functionality in DKP ring and aromatic moieties in the monomer structure, the DKP-based polymer chains were expected to undergo self-assembly through hydrogen bonding and π-π interaction [90], [92], [102], [103]. As a result, the incorporation of DKP into super engineering polymers such as PIs could render high-performance PIs with higher ordered supramolecular structures, which lead to the widening of PIs applications. For example, PIs spheres, one possible form of supramolecular self-assembly of polyimides, have recently attracted attention as fillers, heat resistant superhydrophobic coatings [104] and ultralow dielectric constant films [105].

Moreover, the diversity of DKP derivatives could also be extended by controlling their stereochemistry at α-carbon. The influence of stereochemistry of DKP based diamine monomers on the developed polymers' properties and their self-organization were also worth to explore.

In this chapter, we presented the syntheses of bio-based aromatic diketopiperazine diamines with different stereochemistry at two α-carbon (LL and DL type) from the dimerization of biomass 4-aminophenylalanine (4APhe) (**Figure 2.1**). The syntheses using simple stepwise protection and deprotection approach were demonstrated. The characterizations of these novel monomers were analyzed.

In the next chapters, the polymerization of these prepared monomers into high-performance polymers such as polyimides (PIs) and polyurea (PU) was demonstrated. Their self-organization study of the developed DKP- based polymers was also provided.

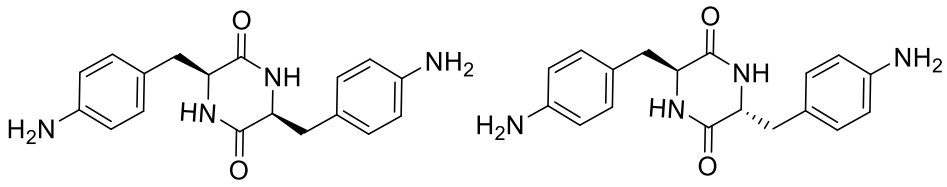

Figure 2.1 Chemical structure of bio-based aromatic diketopiperazine diamines derived from cyclodipeptide formation of 4-aminophenylalanine (4APhe) (DKP-4APhe) with LL (compound 1) and DL (compound 2) sterochemistry.

2.2 Experimental

2.2.1 Materials

4-amino-L-phenylalanine (L-4APhe: from Watanabe chemical), 4-amino-D-phenylalanine (D-4APhe: from Watanabe chemical), benzyl chloroformate (CbzCl: >96.0% from TCI), 1,4-dioxane (>99.5% from Kanto chemical), acetic acid (AcOH: >99.7% from Kanto chemical), trimethylsilyl chloride (TMSCl: from Shin-Etsu chemical), methanol (>99.8% from Kanto chemical), di-*tert*-butyl dicarbonate (Boc_2O: >95.0% from TCI), tetrahydrofuran (THF, >99.5% from Kanto chemical), sodium hydroxide (NaOH, >97.0% from Kanto chemical), *N,N'*-dicyclohexylcarbodiimide (DCC: >98.0% from TCI), hydroxybenzotriazole (HOBt: anhydrous from Dojindo), trimethylamine (>99.5% from Aldrich), formic acid (>98.0%, from Kanto chemical), 2-butanol (>99.0% from Kanto chemical), toluene (>99.0% from Kanto chemical), hydrogen bromide solution, 33 wt.% in acetic acid (33% HBr/AcOH: from Sigma-Aldrich), and NH_3 solution (conc. 28.0-30.0% from Kanto chemical) were used without further purification.

2.2.2 Characterization

^{1}H NMR were performed on a Bruker Biospin AG 400 MHz, 54 mm spectrometer using DMSO-d_6 as the solvent. The FT-IR spectra were recorded with a Perkin-Elmer Spectrum One spectrometer between 4000 and 400 cm^{-1} using a diamond-attenuated total reflection (ATR) accessory. The mass spectra were measured using a Fourier transform ion cyclotron resonance mass spectrometer (FT-ICR MS, Solarix) and scanned from *m/z* 50 to *m/z* 1000. The solubility of the monomer was investigated using 1 mg of sample in 1 mL of solvent at room temperature and at 60°C. Thermogravimetric analysis (TGA) was carried out by Seiko Instruments SII, SSC/5200 at a heating rate of 5 °C/min under a nitrogen atmosphere. Remaining solvent and absorbed moisture in samples were removed at 150^{o}C for 1 hour before TGA measurement.

2.2.3 Monomer syntheses

The schematic representation of synthesis of the bio-based aromatic diketopiperazine diamines from 4APhe is shown in **Scheme 2.1**. Both LL and DL typed DKP based-monomers were synthesized using similar protocol.

a) Synthesis of 4APhe-z: A solution of 4APhe (10.0 g, 0.040 mol) dissolved in 10% AcOH (340 mL) was added drop by drop with 5M NaOH to raise pH to 3. A solution of CbzCl (6 mL, 0.040 mol) in 1,4-dioxane (340 mL) was then slowly added and the mixture was stirred overnight at room temperature. The mixture was made to pH 7 by 5M NaOH before filtration and washed with water. The expected product was obtained as white shinny powder with 82% yield. The specification was as follows. ^{1}H NMR (400 MHz, DMSO-d_6, δ, ppm): 2.76 (dd, 1H, J = 8.8 Hz, 14.0 Hz), 3.08 (dd, 1H, J = 3.4 Hz, 14.0 Hz), 3.60 (t, 1H, J = 3.4 Hz), 5.15 (s, 2H), 7.18 (d, 2H, J = 8.4 Hz), 7.40 (m, 7H), 9.72 (s, 1H).

b) Synthesis of Methyl-4APhe-z: The milky mixture of 4APhe-z (5.0 g, 0.016 mol) in MeOH (80 mL) was added with TMSCl (8.5 mL, 0.067 mol). The mixture was stirred overnight at room temperature. The solvent was evaporated and the crude sample was further recrystallized from MeOH and diethylether to obtain the expected product with 90% yield. The specification was as follows. ^{1}H NMR (400 MHz, DMSO-d_6, δ, ppm): 3.15 (dd, 1H, J = 5.2 Hz, 14.0 Hz), 3.65 (s, 3H), 4.17 (t, 1H J = 5.2 Hz), 5.14 (s, 2H), 7.14 (d, 2H, J = 8.8 Hz), 7.40 (m, 7H), 8.47 (s, 3H), 9.82 (s, 1H).

c) Synthesis of Boc-4APhe-z: A stirred solution of 4APhe-z (4.5 g, 0.014 mol) in THF:H_2O (1:1, 62 mL) was added with NaOH (1.3 g, 0.033 mol) at room temperature followed by the addition of Boc_2O (3.5 g, 0.016 mol). The reaction mixture was stirred at room temperature for overnight. THF was then removed by evaporation and 1M HCl was added to bring pH to 4 and followed by filtration to obtain the product with 98% yield. The specification was as follows. ^{1}H NMR (400 MHz, DMSO-d_6, δ, ppm): 1.35 (s, 9H), 2.92 (d, 2H, J = 7.0 Hz), 3.59 (dd, 1H, J = 7.0 Hz,14.0 Hz), 5.13 (s, 2H), 5.71 (d, 1H, J = 6.1 Hz), 6.99 (d, 2H, J = 12.0 Hz), 7.25 (d, 2H, J = 8.0 Hz), 7.41 (m, 5H).

d) Synthesis of Linear dipeptide-4APhe-z: To a 0^{o}C solution of boc-4APhe-z (8.5 g, 0.021 mol) in DCM (120 mL), HOBt (3.05 g, 0.022 mol) was added followed by the addition of DCC (5.08 g, 0.025 mol). The reaction mixture was stirred for 1 hour and allowed it to room temperature. Then, a solution of methyl-4APhe-z (8.25 g, 0.023 mol) in DMF (23 mL) was added and followed by the addition of trimethylamine (3.4 mL, 0.024 mol). The reaction was stirred further at room temperature for overnight. To work up, the precipitated dicyclohexlyurea was filtered off and washed with little DCM. The filtrate was evaporated to obtain the crude compound, which was adjusted pH under ice condition with 1N HCl to pH 2-3. The acidified mixture was then washed with sat. $NaHCO_3$ and filtered. The crude product was obtained as yellowish powder with 70% yield. The specification was as follows. ^{1}H NMR

(400 MHz, DMSO-d_6, δ, ppm): 1.29 (s, 9H), 1.68 (d, 2H, *J* = 22.0 Hz), 2.89 (d, 2H, *J* = 21 Hz), 3.58 (s, 3H), 4.12 (dd, 1H, *J* = 7.0 Hz, 14.0 Hz), 4.46 (dd, 1H, *J* = 7.2 Hz, 14.0 Hz), 5.14 (s, 4H), 6.81 (d, 1H, *J* = 9.0 Hz), 7.12 (d, 4H, *J* = 8.0 Hz), 7.38 (m, 14H), 8.20 (d, 1H, *J* = 8.1 Hz), 9.68 (s, 1H), 9.70 (s, 1H).

e) Synthesis of Cyclic dipeptide 4APhe-z: To remove boc group, linear dipeptide-4APhe-z (7.77 g, 0.011 mol) was charged with 98% formic acid (466 mL), followed by stirring for 5 h at room temperature. Excess formic acid was then removed in vacuum (temperature less than 30 ^oC was maintained). The obtained crude was refluxed in the mixture of 310 mL of 2-butanol and 155 mL of toluene at 110 ^oC for 5 h, followed by the filtration and drying under vacuum to obtain the expected product with 58% yield. The specification was as follows. ^1H NMR (400 MHz, DMSO-d_6, δ, ppm): 2.14 (dd, 2H, *J* = 6.4 Hz, 13.6 Hz), 3.92 (dd, 2H, *J* = 4.4 Hz, 13.6 Hz), 5.12 (s, 4H), 6.94 (d, 4H, *J*= 8.4 Hz), 7.35 (m, 14H), 7.89 (s, 2H), 9.75 (s, 2H).

f) Synthesis of DKP-4APhe: 33% HBr/AcOH solution (38.5 mL) was added to cyclic dipeptide 4APhe-z (3.85 g, 0.0065 mol). The mixture was stirred at room temperature for 3.5 hours. Diethyl ether was added and decanted several times. The procedure was repeated several times to remove excess acid. The crude compound was dried under vacuum. After drying, the compound was dissolved in water followed by the addition of NH_3 solution drop by drop till the pH become 12 while stirring. The mixture was heated at 60^oC for 1 hour and kept for cooling before filtration to obtain the expected product with 98% yield. The specifications were as follows. ^1H NMR (400 MHz, DMSO-d_6, δ, ppm): 2.08 (dd, 4H, *J* = 6.8 Hz, 13.6 Hz), 3.80 (t, 2H, *J* =4.0 Hz), 4.89 (s, 4H), 6.47 (d, 4H, *J* = 8.0 Hz), 6.70 (d, 4H, *J* = 8.0 Hz), 7.63 (s, 2H). ATR-FTIR: 3400-3250, 1650, 1505 cm^{-1}. FT-ICR MS (ESI): calcd for [M + Na, $C_{18}H_{20}N_4NaO_2]^+$, 347.14837; found, 347.14764.

2.3 Results and discussion

2.3.1 Monomer syntheses

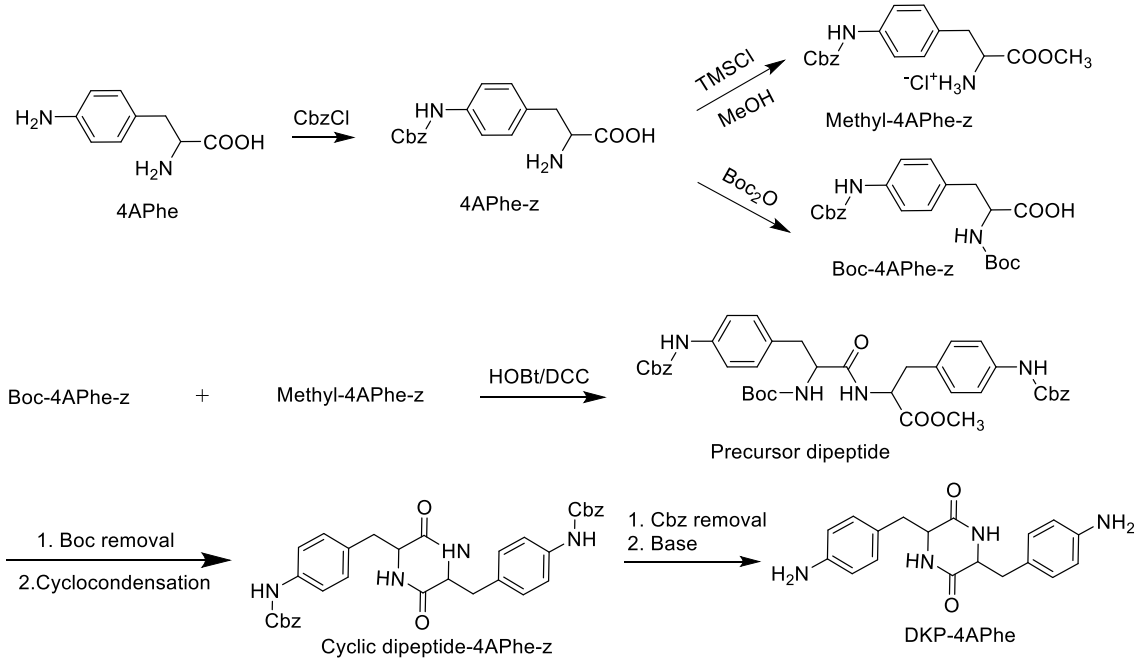

Scheme 2.1 Synthesis of bio-based aromatic diamines having diketopiperazine as a central core from 4-aminophenylalanine.

We synthesized a diamine compound from 4APhe, which not only contains the diamine for further polymerization but also the aromatic rings in its structure along with DKP moiety, which help overcome the drawback of biomass utilization due to their high rigidity, making them perfectly suitable for the syntheses of high-performance polymers.

The synthesis procedure of cyclic dipeptide formation earlier stated by Nitecki was applied to our both LL and DL-typed monomers syntheses [106]. Simply through stepwise protection and deprotection method (Scheme 2.1), the bio-based aromatic diamine composed of DKP as a central core of molecule i.e. DKP-4APhe was established. Starting with selective protection of aromatic amine group of 4APhe by benzyl chloroformate (-z), then, α-amine was protected by di-tertbutyl dicarbonate (-Boc). The protection of carboxylic acid by forming

methyl ester (Methyl-) using TMSCl was carried out separately. Following the synthesis route, the linear dipeptide was formed through simple condensation reaction, and cyclocondensation was performed successively. The condensation of L-4APhe and L-4APhe provided LL-DKP-4APhe with 35% yield, whereas the cyclodipeptide formation of L-4APhe and D-4APhe gave DL-DKP-4APhe with 45% yield.

2.3.2 Monomers characterizations

The aimed structure of aromatic diamine monomer was characterized by ^{1}H NMR, FT-IR and ESI-MS. The purity of all the intermediates was also analyzed and confirmed by the ^{1}H NMR. All the intermediates were prepared in high yield and were pure enough to proceed for the next steps. The ^{1}H NMR spectra of the intermediates synthesized along with final DKP aromatic diamine are shown in Figure 2.2.

^{1}H NMR (a) (L-4APhe-z) and (f) (LL-DKP-4APhe) (Figure 2.2) showed that the homo-coupling of L-4APhe resulted in shifting of the proton signal of β-carbons from 2.76-3.08 ppm to 2.08 ppm coupled with the appearance of proton signals of DKP at 7.63 and 3.80 ppm for amine and -CH-, respectively. The proton signal assigned to diamine appeared at 4.89 ppm.

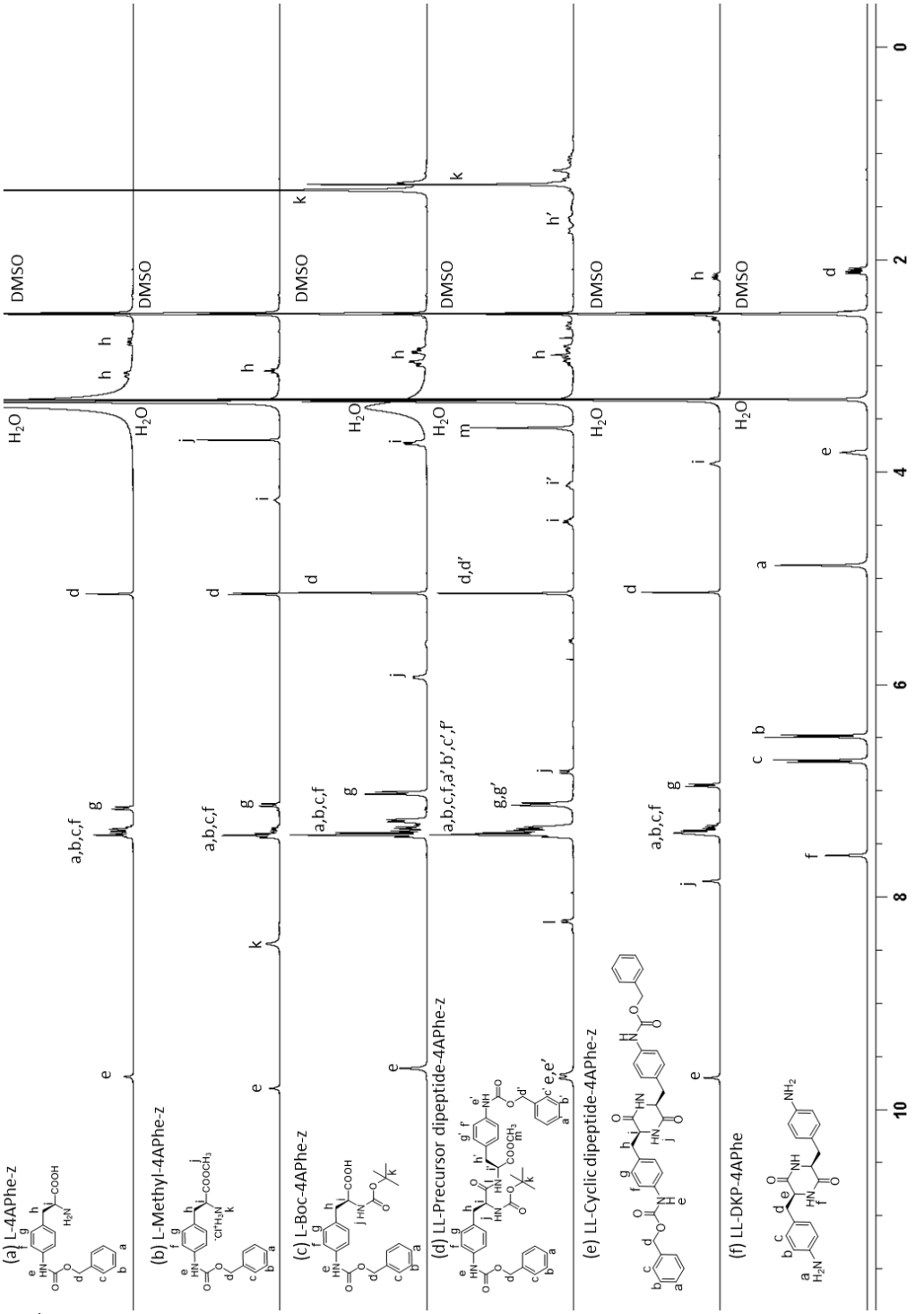

Figure 2.2 ^{1}H NMR spectra of (a) L-4APhe-z, (b) L-Methyl-4APhe-z, (c) L-Boc-4APhe-z, (d) LL-Precursor dipeptide of 4APhe-z, (e) LL-Cyclic dipeptide-4APhe-z, and (f) LL-DKP-4APhe.

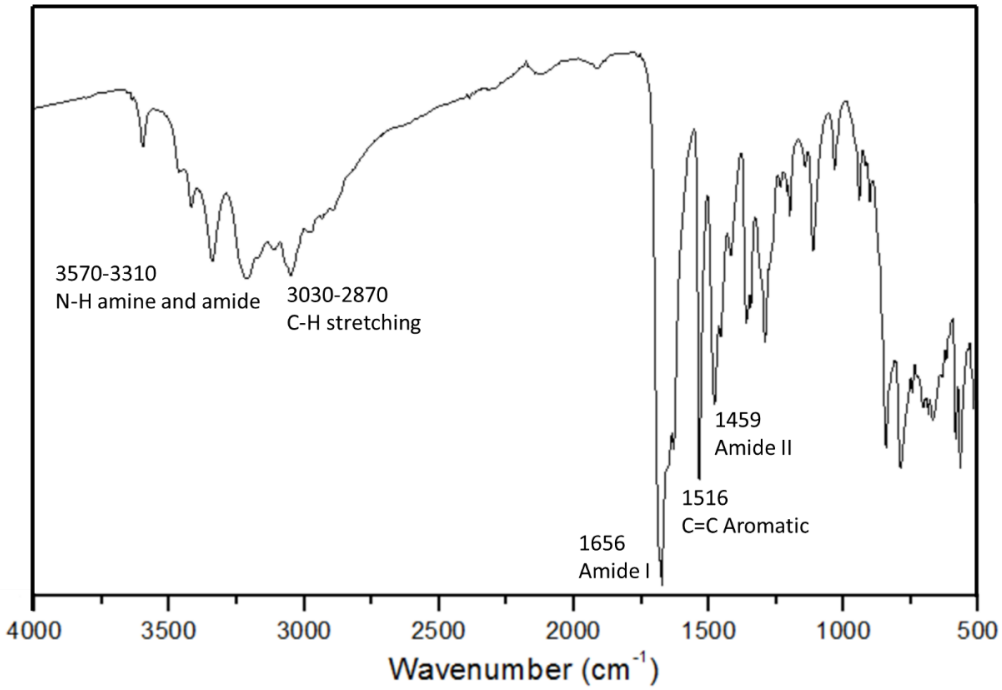

Figure 2.3 FT-IR spectrum of LL-DKP-4APhe.

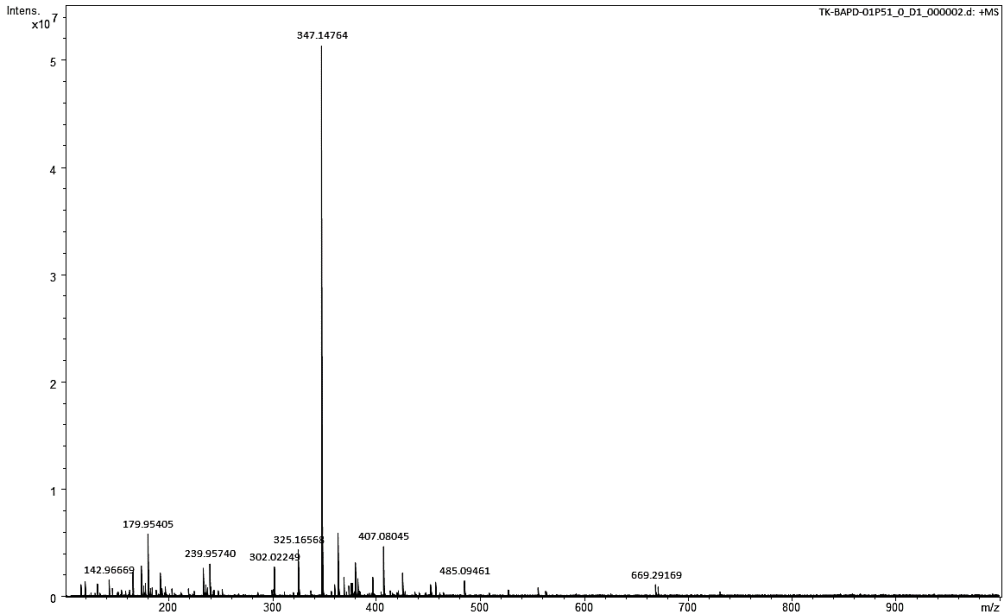

Figure 2.4 Mass spectrum of LL-DKP-4APhe.

The FT-IR spectrum (**Figure 2.3**) exhibited N-H stretching of amine at 3570-3310 cm^{-1}, N-H stretching, C=O stretching and N-H bending of amide at 3570-3310, 1656 and 1459 cm^{-1}, respectively , C=C stretching of aromatic at 1516 cm^{-1}, and C-H stretching at 3030-2870 cm^{-1}. FT-ICR MS (ESI) also confirmed the molecular weight of the synthesized LL-DKP based

diamine. The spectrum is shown the mass peak at 347.14764 corresponding to the M-Na^+ [m/z: 347.147642] (Figure 2.4) which confirmed the formation of LL-DKP-4APhe.

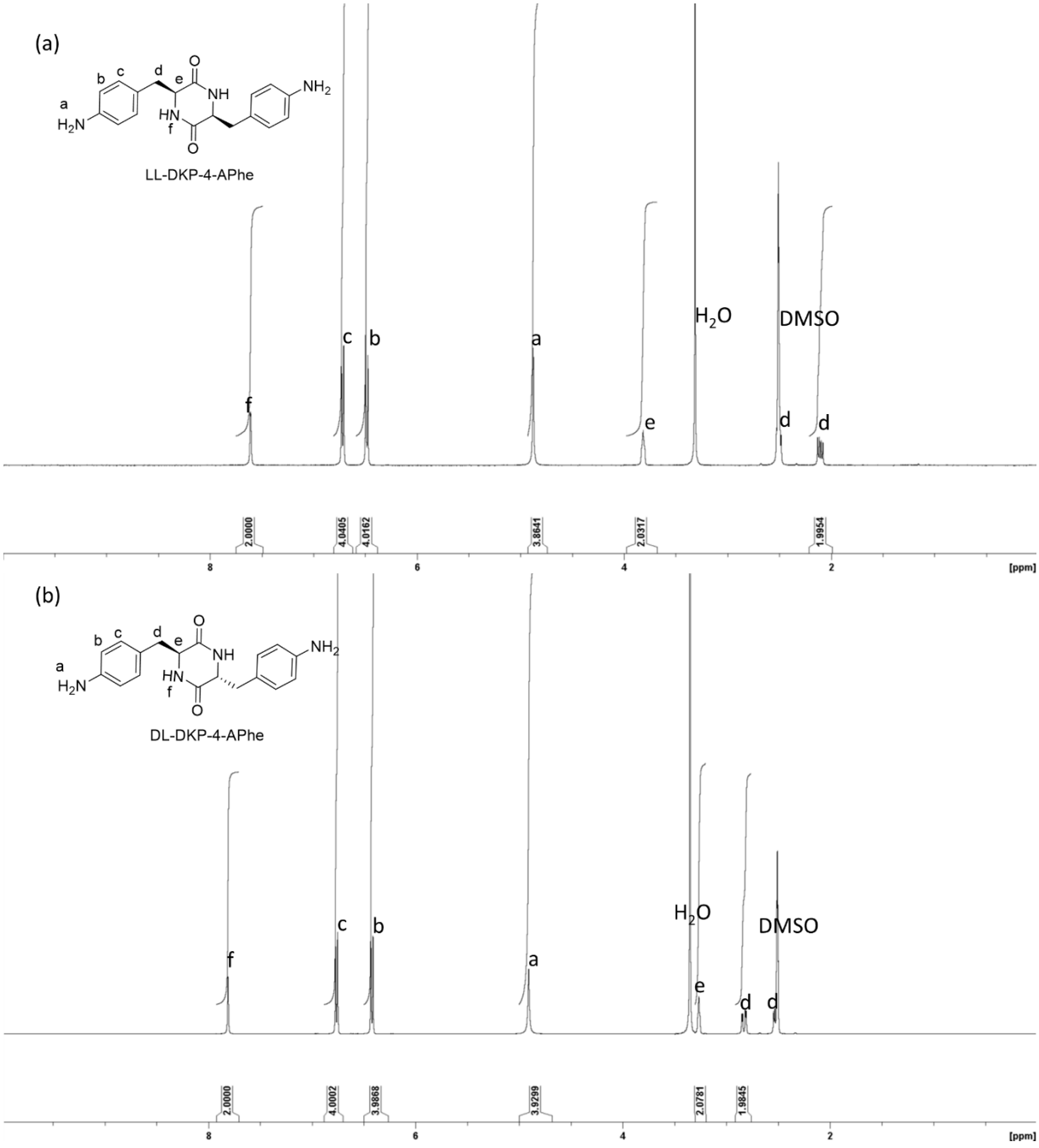

Figure 2.5 ^{1}H NMR spectra of (a) LL-DKP-4APhe and (b) DL-DKP-4APhe.

As shown in **Figure 2.5**, comparing ^{1}H NMR spectra of LL and DL-DKP-4APhe, the shifting signal of protons at α-carbon (e position) and amide (f position) in DKP ring were observed which confirmed the successful syntheses of LL and DL-DKP-4APhe monomers.

The solubility of LL and DL-DKP-4APhe was investigated. The data summarized in Table 2.1 showed that both LL and DL-DKP-4APhe had similar solubility. These two monomers could only dissolve in some polar aprotic solvent as follows: DMAc, DMF, DMSO and NMP. Pyridine could only dissolve these two monomers when heating was applied.

Table 2.1 Solubility of LL and DL-DKP-4APhe in various solvents.

Solvent	**LL-DKP-4APhe**	**DL-DKP-4APhe**
Non-polar		
Toluene	-	-
Hexane	-	-
Diethyl ether	-	-
DCM	-	-
1,4-dioxane	-	-
Polar protic		
H_2O	-	-
MeOH	-	-
EtOH	-	-
10% Acetic acid		
Polar aprotic		
Acetone	-	-
THF	-	-
EtOAc	-	-
ACN	-	-
Pyridine	±	±
DMAc	+	+
DMF	+	+
DMSO	+	+
NMP	+	+

- Not soluble / + soluble/ ± soluble when heating

The TGA showed that the stereochemistry at α-carbon had an effect on thermal stability of the monomers. As displayed in Figure 2.6, LL-DKP-4APhe showed higher thermal stability

with T_{d5} and T_{d10} of 352 and 365 °C, respectively. On the other hand, DL-DKP-4APhe had T_{d5} and T_{d10} of 341 and 355 °C, respectively.

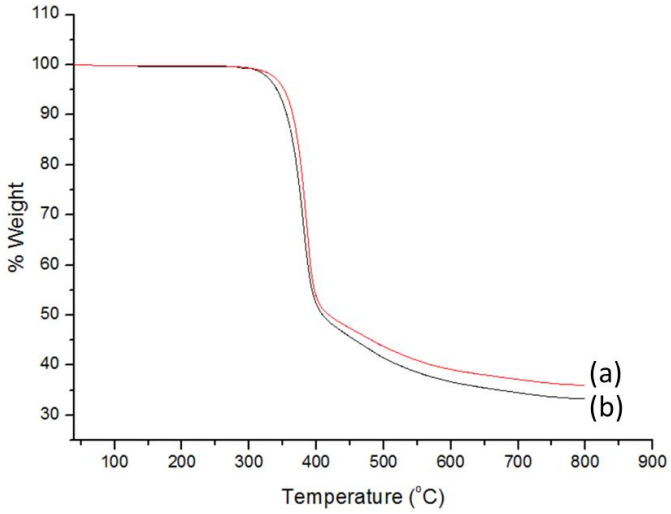

Figure 2.6 TG curves recorded under N_2 of (a) LL-DKP-4APhe, and (b) DL-DKP-4APhe.

The difference in heat resistance attributed to the different geometry of LL and DL-DKP rings. With LL stereochemistry, the six-membered ring is almost ideally flat with C-N-C(O)-C torsional angles equal to -0.07° and -0.02°. For DL stereochemistry, the corresponding torsional angles are found to be -14.02° and -5.70° [103]. Flat structure led to high densely molecular packing, resulting in higher thermal resistance.

2.4 Conclusion

In this chapter, we designed a novel bio-based diamine monomer based on the concept structure of 4ACA - having alicyclic at the core structure. The polymerization of 4ACA with various dianhydrides could introduce high rigidity from alicyclic building blocks to the polymer structures and help generate high thermoresistance polyimides. By applying this concept, DKP-4APhe, the dimerization product of biomass 4-APhe, was established. Through simple protection/deprotection reactions, this designed compound could be obtained in good yield. This synthesis approach is a template, which could be applied not only with various amino acids but also with diverse stereochemistry.

Here, two diastereomers of DKP based 4APhe, LL and DL types, were prepared. The structures of these two novel bio-based aromatic diamine were confirmed by ^{1}H NMR, FT-IR and ESI-MS.

CHAPTER III

POLYMERIZATION OF BIO-BASED DIKETOPIPERAZINE MONOMERS

3.1 Introduction

Bio-based polymers have drawn so much attention in wide fields because of serious concern for environmental problem. However, the usage of currently available bioplastics is limited due to low thermal and low mechanical properties. The introduction of aromatic rings in the polymer backbone help boost their performance and broaden their application fields. However, the availability of an aromatic diamine monomer derived from biomass is still restricted as diamine is toxic to plants

Our developed bio-based aromatic diamine (DKP-4APhe) meet all requirements as it contains reactive diamine for high-performance polymer synthesis such as polyimide and also the aromatic rings in its structure, which help overcome the drawback of biomass utilization due to their high rigidity, making them perfectly suitable for the syntheses of high-performance polymers.

In this chapter, the utilization of our bio-based aromatic diamines, DKP-4APhe, for the synthesis of high-performance polymers: polyimides and polyurea was discussed with their synthesis and characterization.

In order to prepare a series of polyimides, various available dianhydrides: 1,2,3,4-cyclobutane tetracarboxylic dianhydride (CBDA), pyromellitic anhydride (PMDA), 3,4:3’,4’-biphenyl tetracarboxylic dianhydride (BPDA), 4,4’-oxydiphthalic anhydride (OPDA), benzophenone-3,3’,4,4’-tetracarboxylic dianhydride (BTDA) and 3,3’,4,4’-diphenylsulfone

tetracarboxylic dianhydride (DSDA) and 5-(2,5-Dioxotetrahydrofuryl)-3-methyl-3-cyclohexene-1,2-dicarboxylic Anhydride (DHCDA) were used to prepare poly(amic acid)s (PAAs) and then thermally imidized to get respective polyimides.

We also described the syntheses and properties of bio-based DKP-polyurea (PUs) from our monomer via a polyaddition with various aromatic and aliphatic diisocyanates. Aliphatic diisocyanate: dicyclohexylmethane 4,4'-diisocyanate, isophorone diisocyanate, and hexamethylene diisocyanate. Aromatic diisocyanate: tolylene-2,4-diisocyanate, methylenediphenyl 4,4'-diisocyanate, 1,4-phenylene diisocyanate, and m-xylylene diisocyanate.

The different dianhydrides and diisocyanates were used because there is a drastic impact of monomer's structure on polymers' properties and for understanding the structure-property relationship.

3.2 Experimental

3.2.1 Materials

Dianhydrides such as 4,4′-oxidiphthalic anhydride (OPDA: >98.0%), 3,4,3′,4′-biphenyltetracarboxylic dianhydride (BPDA: >98.0%), and 5-(2,5-dioxotetrahydrofuryl)-3-methyl-3-cyclohexene-1,2-dicarboxylic anhydride (DHCDA: >98.0%) were purchased from Tokyo chemical industry co., LTD (TCI) and sublimed at 160^{o}C under reduced pressure and dried under vacuum at 110^{o}C prior to use. *N,N*-dimethylacetamide (DMAc: >99.8% anhydrous from Kanto chemical), 1,2,3,4-cyclobutanetetracarboxylic dianhydride (CBDA: purified by sublimation >98.0% from TCI), 3,3′,4,4′-benzophenonetetracarboxylic dianhydride (BTDA: purified by sublimation >98.0% from TCI), 3,3′,4,4′-diphenylsulfonetetracarboxylic

dianhydride (DSDA: purified by sublimation >98.0% from TCI), dicyclohexylmethane 4,4'-diisocyanate (>90.0% from TCI), isophorone diisocyanate (>99.0% from TCI), tolylene-2,4-diisocyanate (>98.0% from TCI), methylenediphenyl 4,4'-diisocyanate (>97.0% from TCI), 1,4-phenylene diisocyanate (>98.0% from TCI), hexamethylene diisocyanate (>98.0% from TCI), and m-xylylene diisocyanate (>98.0% from TCI) were used without further purification.

3.2.2 Characterizations

^{1}H nuclear magnetic resonance (^{1}H-NMR) was performed on a Bruker Biospin AG 400 MHz spectrometer using DMSO-d_6 as a solvent at 23.1 ^{o}C with 16 accumulation scans, using the proton resonance of residual non-deuterated DMSO as an internal standard (2.55 ppm). The FTIR spectra were recorded with a Perkin-Elmer Spectrum One spectrometer between 4000 and 400 cm^{-1} using a diamond-attenuated total reflection (ATR) accessory. The number-average molecular weight (M_n), weight-average molecular weight (M_w) and the molecular weight distribution (PDI, M_w/M_n) were determined by gel permeation chromatography (GPC, concentration 0.7 g/L, 10 mM LiBr/DMF eluent) after calibration with polystyrene standards. The solubility of the polymers was investigated using 1 mg of sample in 1 mL of solvent at room temperature and at 60°C. Thermogravimetric analysis (TGA) and differential scanning calorimetry (DSC) were carried out by Seiko Instruments SII, SSC/5200 and Seiko Instruments SII, X-DSC7000T, respectively, at a heating rate of 5 °C/min under a nitrogen atmosphere. Remaining solvent and absorbed moisture in polymer samples were removed at 250^{o}C for 1 hour before TGA and DSC measurement. The tension application was tested by the Instron 3365 Tension testing machine (Instron, USA) at room temperature.

3.2.3 Poly(amic acid)s (PAAs) and Polyimides (PIs) syntheses.

A typical procedure for the synthesis of PAA is shown in Scheme 3.1. A diamine of DKP-4APhe (0.20 g, 0.62 mmol) mixed with an eqimolar of dianhydrides such as CBDA (0.12 g, 0.62 mmol), BTDA (0.20 g, 0.62 mmol), DSDA (0.22 g, 0.62 mmol), OPDA(0.19 g, 0.62 mmol), BPDA (0.18 g, 0.62 mmol), and DHCDA (0.16 g, 0.62 mmol) was dissolved in DMAc (1.25 mL, 0.6 M) under nitrogen atmosphere. The reaction mixture was stirred at room temperature for 48 hours to yield a viscous PAA solution. The PAA solution was added into 1:1 mixture of water and methanol to precipitate to obtain the respective PAA polymers in quantitative yields (PAA-BTDA: Yield 93%, PAA-CBDA: Yield 91%, PAA-DSDA: Yield 93%, PAA-OPDA: Yield 90%, PAA-BPDA: Yield 92% and PAA-DHCDA: Yield 89 %). PI was obtained by thermal imidization of the PAA in an oven under vacuum by stepwise heating at 100, 150, 200 ^{o}C for 1 hour and 250 ^{o}C for 3 hours at each step.

3.2.4 Polyurea (PU) syntheses

A series of polyureas (PUs) were synthesized by a reaction of LL-DKP-4APhe, with equimolar amounts of aromatic and aliphatic diisocyanates as shown in Scheme 3.3. Representative procedures for the syntheses of PUs are shown as follows. LL-DKP-4APhe (0.20 g, 0.62 mmol) was dissolved in DMAc (1.25 mL) under nitrogen atmosphere. Diisocyanates with stoichiometric amount: dicyclohexylmethane 4,4'-diisocyanate (152 μL, 0.62 mmol), isophorone diisocyanate (130 μL, 0.62 mmol), and hexamethylene diisocyanate (99 μL, 0.62 mmol), tolylene-2,4-diisocyanate (88 μL, 0.62 mmol), methylenediphenyl 4,4'-diisocyanate (0.15 g, 0.62 mmol), 1,4-phenylene diisocyanate (0.1 g, 0.62 mmol), and m-xylylene diisocyanate (97 μL, 0.62 mmol) was added into the diamine solution with constant stirring at room temperature and the reaction solution became gradually viscous. After

polymerization for 48 h, the viscous reaction solution was poured into 1:1 water/methanol to precipitate solid PU, collected by filtration and dried in vacuum.

3.3 Results and discussion

3.3.1 Polyimides (PIs)

3.3.1.1 Synthesis and characterization

PAAs, the precursors of PIs, were prepared by the polycondensation of the prepared diamine of LL-DKP-4APhe with stoichiometric amounts of the dianhydrides: PMDA, BTDA, OPDA, DSDA, BPDA, CBDA and DHCDA (Scheme 3.1). The resulting PAAs were abbreviated as PAA-PMDA, PAA-BTDA, PAA-OPDA, PAA-DSDA, PAA-BPDA, PAA-CBDA and PAA-DHCDA. It should be noted here that "LL" was omitted from all sample names, as L is general stereochemistry of all amino acid derivatives.

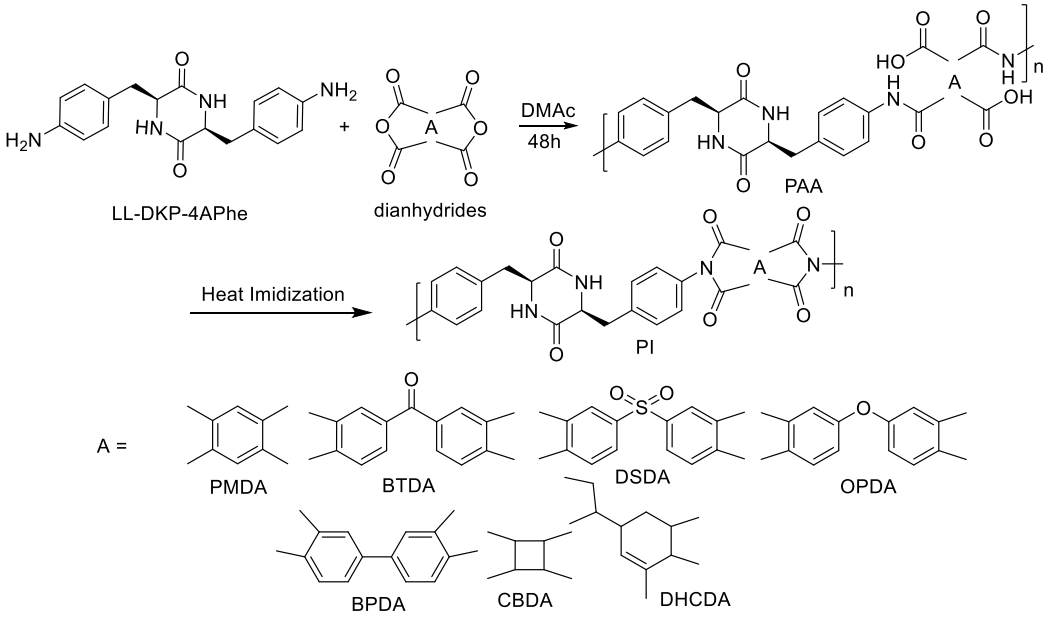

Scheme 3.1 Syntheses of bio-based aromatic poly(amic acid)s and polyimides from LL-DKP-4APhe

The ^{1}H NMR and FT-IR spectra of all PAAs are shown in Figure 3.1 and 3.2, respectively. In

^{1}H NMR spectra of PAAs, the main chain proton signals for carboxylic acid, amide, cyclic amide of DKP, and aromatic diamines appeared around 12.2-13.2, 10.4-9.8, 8.1-7.9, and 7.5-7.0 ppm. In case of dianhydride-derived aromatic PAAs, aromatic protons of dianhydrides showed signals around 8.3-7.1 ppm in addition to the above-mentioned signals, while dianhydride-derived aliphatic PAAs, PAA-CBDA and PAA-DHCDA, showed signal of cyclobutane and methyl cyclohexene at ranges of 3.9-3.4, and 3.0-1.7 ppm, respectively. A signal at 5.5 ppm is assigned to proton of double bond of DHCDA. NMR revealed the formation of PAA derived from the DKP aromatic diamine of DKP-4APhe with dianhydrides.

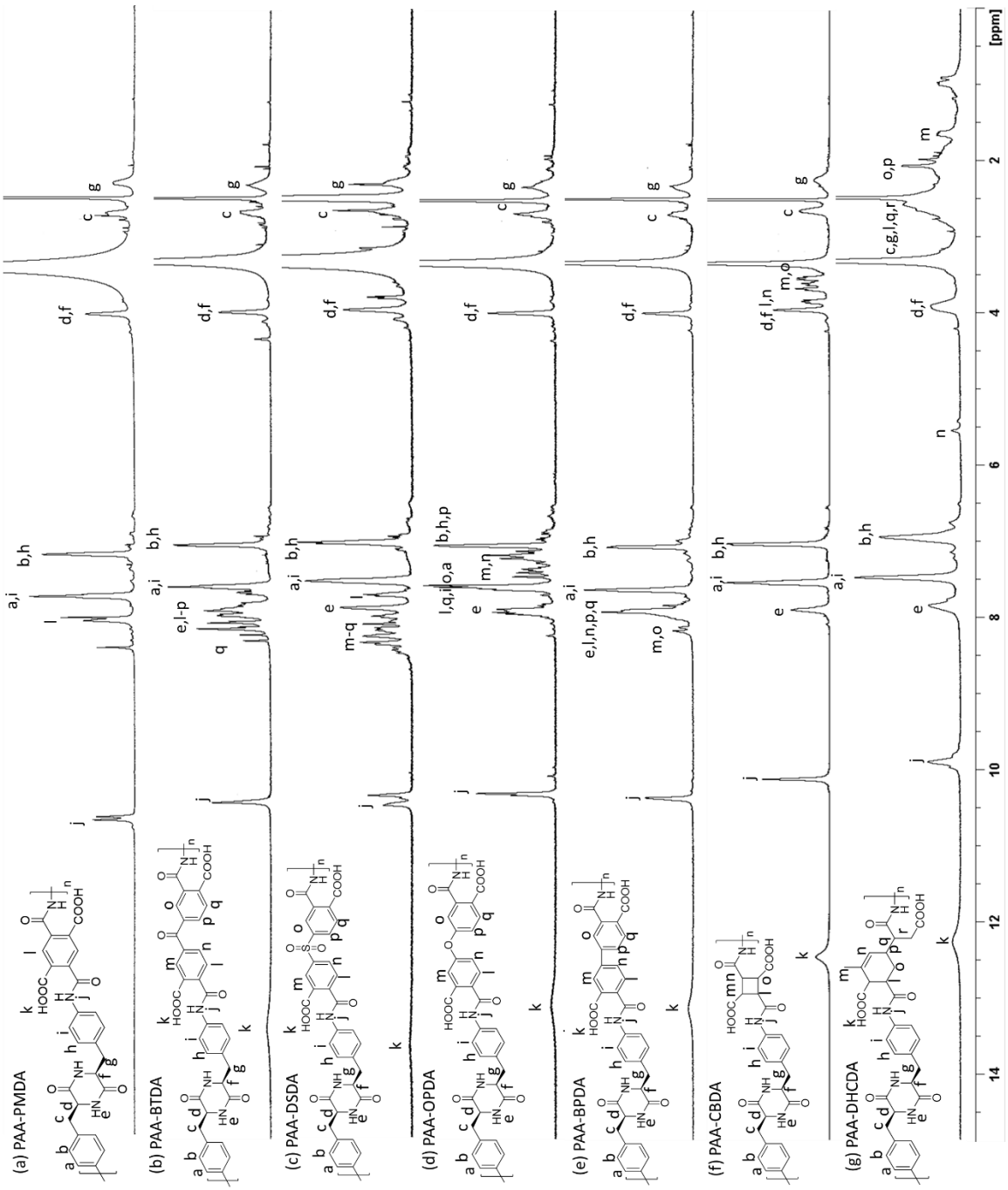

Figure 3.1 ^{1}H NMR spectra of (a) PAA-PMDA (b) PAA-BTDA, (c) PAA-DSDA, (d) PAA-OPDA, (e) PAA-BPDA, (f) PAA-CBDA, and (g) PAA-DHCDA.

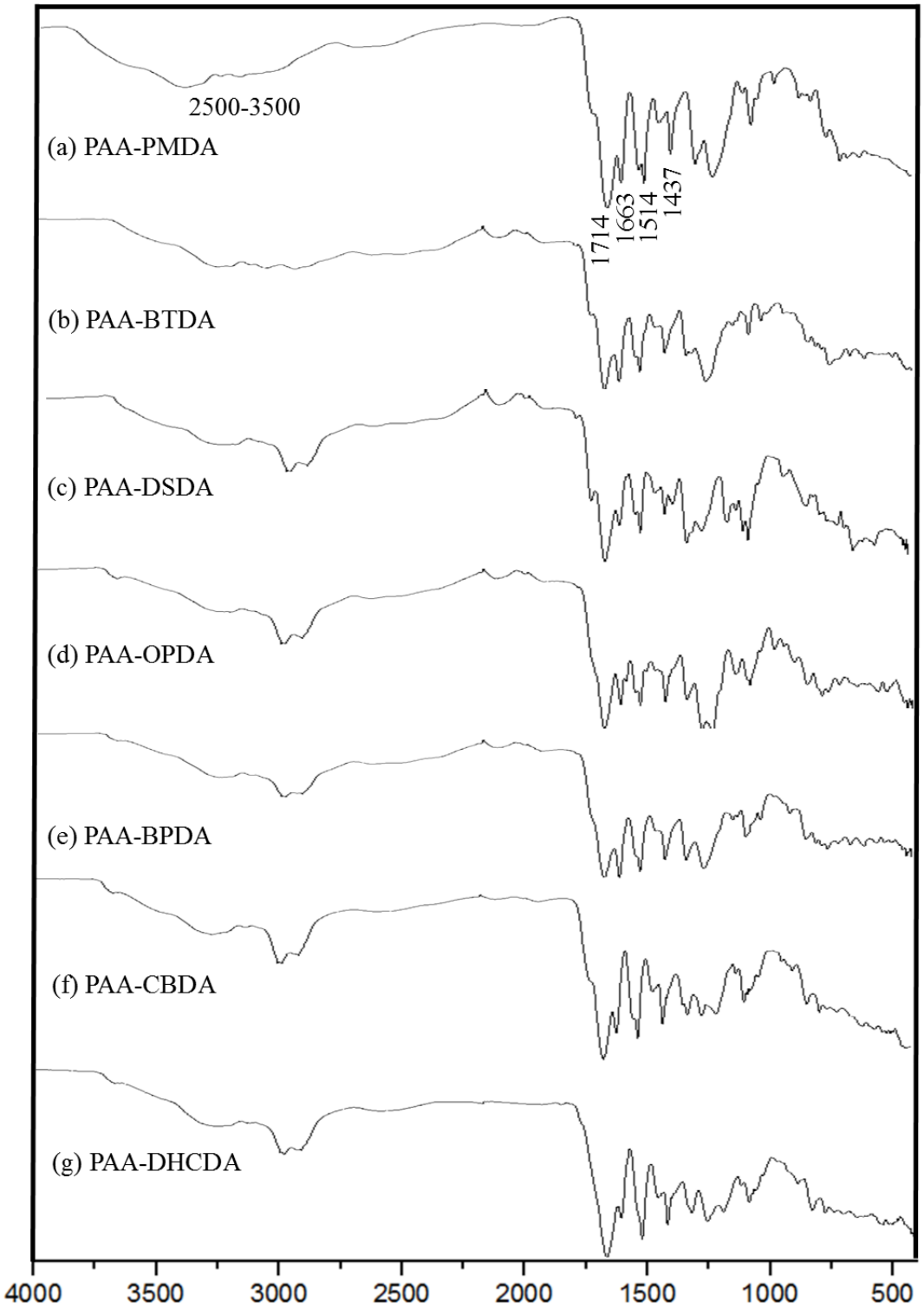

Figure 3.2 FT-IR spectra of (a) PAA-PMDA (b) PAA-BTDA, (c) PAA-DSDA, (d) PAA-OPDA, (e) PAA-BPDA, (f) PAA-CBDA, and (g) PAA-DHCDA.

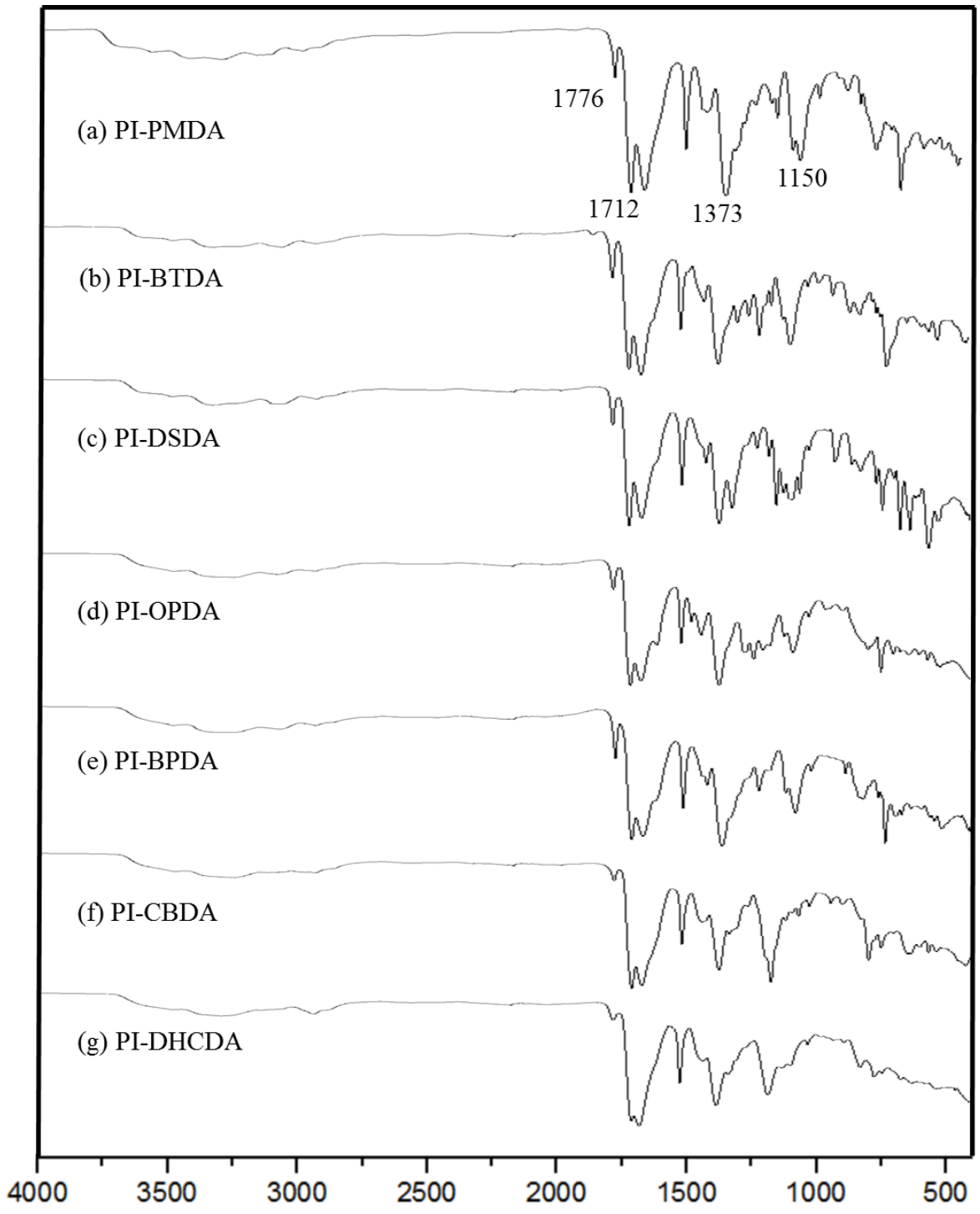

Figure 3.3 FT-IR spectra of (a) PI-PMDA, (b) PI-BTDA, (c) PI-DSDA, (d) PI-OPDA, (e) PI-BPDA, (f) PI-CBDA, and (g) PI-DHCDA.

The DMAc solution of PAAs was utilized for preparing PAAs films, by casting on silicon wafer and evaporating the solvent at 60-70 °C. However, all obtained PAAs films were brittle and fragile and no film could be fabricated from any dianhydrides.

PIs were obtained by stepwise thermal imidization by keeping the temperature at 100, 150, 200 for 1 h and 250 °C for 3 h at each step in a vacuum oven. The color of PIs became darker from yellow to dark orange than the PAAs. The color change could be explained by the densely packed aggregate structures of PI chains with the aid of intermolecular π–π interaction and charge transfer (CT) formation. The imide ring formation was confirmed by FT-IR spectroscopy (Figure 3.3).

Figure 3.2 and 3.3 show the FT-IR spectra of the PAAs and PIs respectively. In all the samples, the following peaks were observed: broad band in the range of 2500-3500 cm^{-1} (O-H stretching, carboxylic acid group's hydroxyls), two different carbonyl peaks at 1714 cm^{-1} (C=O stretching, carboxylic) and 1663 cm^{-1} (C=O stretching, amide), and 1514 and 1437 cm^{-1} (aromatic C-H overtone aromatic). After stepwise heating, all the annealed samples showed two carbonyl adsorption at 1712 cm^{-1} (C=O symmetric stretching) and a small peak at 1776 cm^{-1} (C=O asymmetric stretching), which were characteristic to PI structures. Moreover, other peaks appearing at 1373 cm^{-1} (C-N stretching of imide) and 1150 cm^{-1} (imide ring deformation) and the disappearance of characteristic amide peak found about 2980 cm^{-1}, which all indicating an imidization. Furthermore, PI-OPDA showed IR peak at 1238 cm^{-1} corresponding to ether group, PI-DSDA showed asymmetric and symmetric S=O stretching at 1310 and 1208 cm^{-1}, respectively, and PI-DHCDA showed IR peak of C=C bending at 800 cm^{-1}. These results clearly indicated the formation of the expected PIs.

The weight-average molecular weight of (M_w), number average molecular weight (M_n) and polydispersity index (PDI) were determined using PAA and were summarized in Table 3.1. PAAs had M_w and M_n values in the range of 16.8-33.2 and 24.9-14.7 kDa, respectively, and PDI

ranged from 1.1-1.4. It should be noted here that only the dissolved parts in LiBr/DMF were measured, to make the molecular weight value lower and distribution narrower.

Table 3.1 Molecular weights of PAAs polymerized from LL-DKP-4APhe and various dianhydrides.

PAA-	PMDA	BTDA	CBDA	DSDA	OPDA	BPDA	DHCDA
M_n (kDa)[a]	20.3	24.9	21.2	22.5	19.1	18.8	14.7
M_w (kDa)[a]	24.5	33.2	29.4	27.0	23.5	23.4	16.8
PDI [a]	1.2	1.3	1.4	1.2	1.3	1.2	1.1

[a]The weight-average molecular weight, M_w, the number-average molecular weight, M_n, and the distribution of polymer molecular weight, PDI, of PAA were measured by GPC.

3.3.1.2 Properties of PIs

- ***Solubility***

The solubility of all prepared PAAs and PIs was investigated in various solvents shown in Table 3.2. The solubility of the polymers was tested by dissolving them in three groups of solvent: (A) nonpolar solvent, (B) polar protic solvent, and (C) polar aprotic solvent.

Table 3.2 Solubility of LL typed PAAs and PIs in various solvents.

Solvent	**PAA-PMDA**	**PI-PMDA**	**PAA-BTDA**	**PI-BTDA**	**PAA-CBDA**	**PI-CBDA**	**PAA-DSDA**	**PI-DSDA**	**PAA-OPDA**	**PI-OPDA**	**PAA-BPDA**	**PI-BPDA**	**PAA-DHCDA**	**PI-DHCDA**
Non-polar														
Toluene	-	-	-	-	-	-	-	-	-	-	-	-	-	-
Hexane	-	-	-	-	-	-	-	-	-	-	-	-	-	-
Diethyl ether	-	-	-	-	-	-	-	-	-	-	-	-	-	-
DCM	-	-	-	-	-	-	-	-	-	-	-	-	-	-
1,4-dioxane	-	-	-	-	-	-	-	-	-	-	-	-	-	-
Polar protic														
H_2O	-	-	-	-	-	-	-	-	-	-	-	-	-	-
MeOH	-	-	-	-	-	-	-	-	-	-	-	-	-	-
EtOH	-	-	-	-	-	-	-	-	-	-	-	-	-	-
Conc. H_2SO_4	+	+	+	+	+	+	+	+	+	+	+	+	+	+
TFA	+	+	+	+	+	+	+	+	+	+	+	+	+	+
Polar aprotic														
Acetone	-	-	-	-	-	-	-	-	-	-	-	-	-	-
THF	-	-	-	-	-	-	-	-	-	-	-	-	-	-
`EtOAc	-	-	-	-	-	-	-	-	-	-	-	-	-	-
ACN	-	-	-	-	-	-	-	-	-	-	-	-	-	-
Pyridine	-	-	-	-	-	-	-	-	-	-	-	-	-	-
DMAc	+	-	+	-	+	-	+	-	+	-	+	-	+	-
DMF	±	-	±	-	±	-	±	-	±	-	±	-	±	-
DMSO	+	-	+	-	+	-	+	-	+	-	+	-	+	-
NMP	+	-	+		+	-	+	-	+	-	+	-	+	-

- Not soluble / + soluble/ ± partially soluble/

The solubility of polymers was tested; LL-PAAs were soluble in polar solvents such as NMP, DMAc and DMSO at room temperature and partially in DMF. However, all PIs were soluble in trifluoroacetic acid and concentrated sulfuric acid only.

Thermal property

TGA was utilized in order to investigate the thermal degradation of PIs in a nitrogen atmosphere using heating rate at 10°C/min, and the 5% and 10% weight-loss temperatures, T_{d5} and T_{d10}, were evaluated. As shown in Table 3.3, all of the PIs exhibited a T_{d10} range of 388-432°C and T_{d5} range of 365-420°C, which indicated the high degree of resistance towards thermal degradation; especially PI from PMDA showing a highest T_{d10} of 432°C. This result indicated high resonance energy of the benzene rings due to delocalization of π-electrons. Moreover, the strength of imide bonds, resulting from the competitive π-n conjugation between carbonyl group and the non-pair electron from the nitrogen atoms as well as from the conformation state of 5-member ring could help increase the degradation temperature. On the other hand, PI-DHCDA showed lowest T_{d10} due to the lowest amount of aromatic rings than the others, leading to more susceptible chain scission at elevated temperature.

Table 3.3 Thermal properties of PIs prepared from LL-DKP-4APhe and various dianhydrides.

PI-	PMDA	BTDA	CBDA	DSDA	OPDA	BPDA	DHCDA
T_{d5} (°C)[a]	420	411	392	383	398	401	365
T_{d10} (°C)[a]	432	427	415	397	414	414	388

[a]5% and 10% weight loss temperatures, T_{d5} and T_{d10}, were obtained from TGA curve scanned at a heating rate of 10°C/min under N_2 atmosphere.

PIs thermal transition behavior was investigated by DSC under a nitrogen atmosphere. However all PIs exhibited no distinct peaks or flections below thermal degradation temperatures, because of too high softening temperature. The charge transfer interaction characteristic to polyimides and hydrogen bonding between the imide group and DKP ring or between DKP moieties could be a reason for high thermal stability.

From our previous research, the biopolyimide derived from 4ATA and PMDA (M_w = 319 kDa) showed T_{d10} of 425 °C [59], which is lower, compared to our PI-PMDA although the

molecular weight of our PI was much lower. Higher thermal resistance could be attributed to the intermolecular forces from DKP moieties. Materials with such high T_g properties may be suitable for applications in super engineering plastics.

3.3.1.3 Effect of stereochemistry of diketopiperazine on PIs properties

To study the influence of stereochemistry of α-carbon at two positions of DKP rings in our designed aromatic diamine monomer on PIs' properties, here PIs were prepared from DL-DKP-4APhe diamines with stoichiometric amounts of various dianhydrides as follows: PMDA, BTDA, OPDA, DSDA and BPDA (Scheme 3.2). The resulting PAAs were abbreviated as DL-PAA-PMDA, DL-PAA-BTDA, DL-PAA-OPDA, DL-PAA-DSDA and DL-PAA-BPDA. In this section, the stereochemistry of all samples was clearly stated to avoid ambiguity.

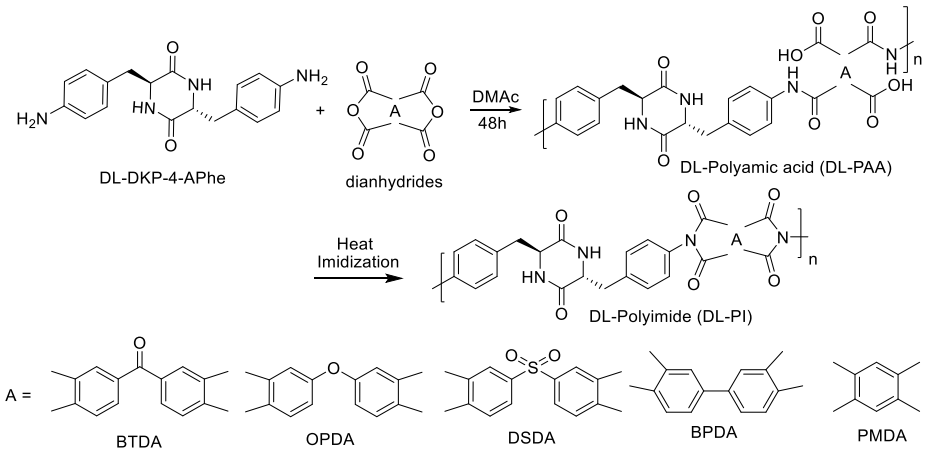

Scheme 3.2 Synthesis of bio-based aromatic poly(amic acid)s and polyimides from DL-DKP-4APhe.

After precipitation of DL-PAAs by 1:1 MeOH/H_2O, fibrils could be obtained from all DL-PAAs samples. PAAs were redissolved in DMAc and casted on glass plate for film preparation. Compared to PAAs generated from LL-DKP-4APhe, DL-PAAs could fabricate films. PIs were occurred by stepwise heat imidization via PAAs precursors at maximum temperature 250 °C. The films' color become darker in color as shown in Table 3.4. Although

the films could be fabricated in the case of DL-DKP-4APhe, the obtained films were still yet brittle except the one generated from BTDA. After imidization, the obtained DL-PI-BTDA film could be folded in four without breaking (Figure 3.4).

Table 3.4 Films images of DL-PAAs and DL-PIs

DL-Polymer-Dianhydrides	PAA films	PIs film
PMDA	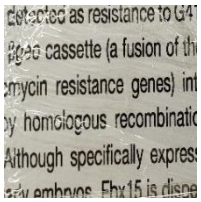	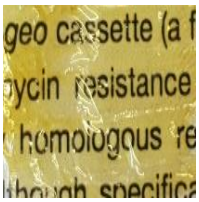
BTDA	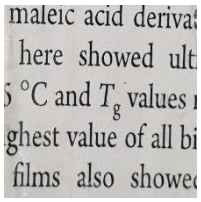	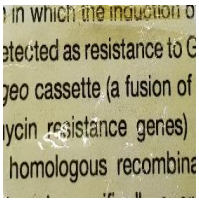
DSDA	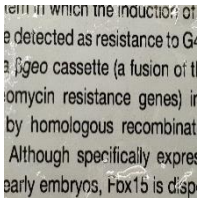	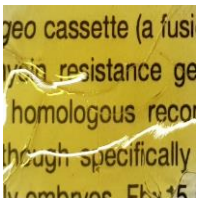
OPDA	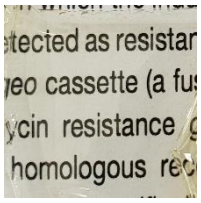	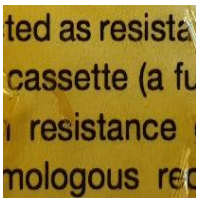
BPDA	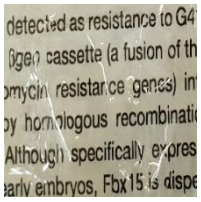	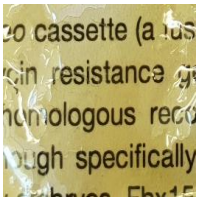

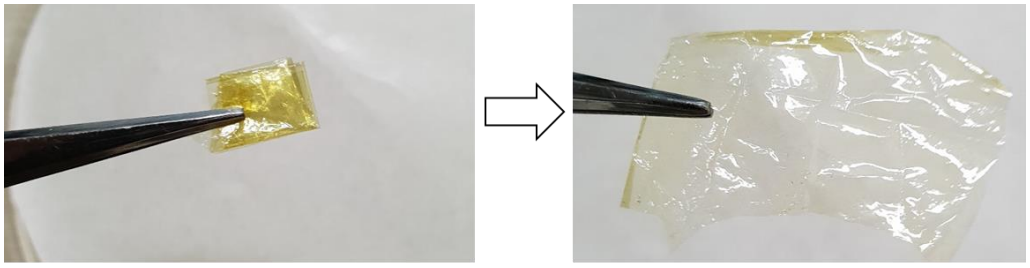

DL-PI-BTDA (4-fold)

DL-PI-BTDA (unfold)

Figure 3.4 DL-PI-BTDA films folding into four and unfolding

Structure characterization

The ^{1}H NMR and FT-IR spectra of all DL-PAAs are shown in Figure 3.5 and 3.6, respectively. In ^{1}H NMR spectra of DL-PAAs compared to LL-PAAs, only the proton signals at α- and β-carbon of DKP ring shifted. Protons at α-carbon (d, f position) shifted from 3.9 ppm to 3.5 ppm and overlapped with water peak, whereas protons at β-carbon, c position shifted from 2.6 and 3.0 ppm and at g position shifted from to 2.2 and 2.6 ppm. The shifting of proton signals attributed to the molecular orientation changing due to different structure conformation.

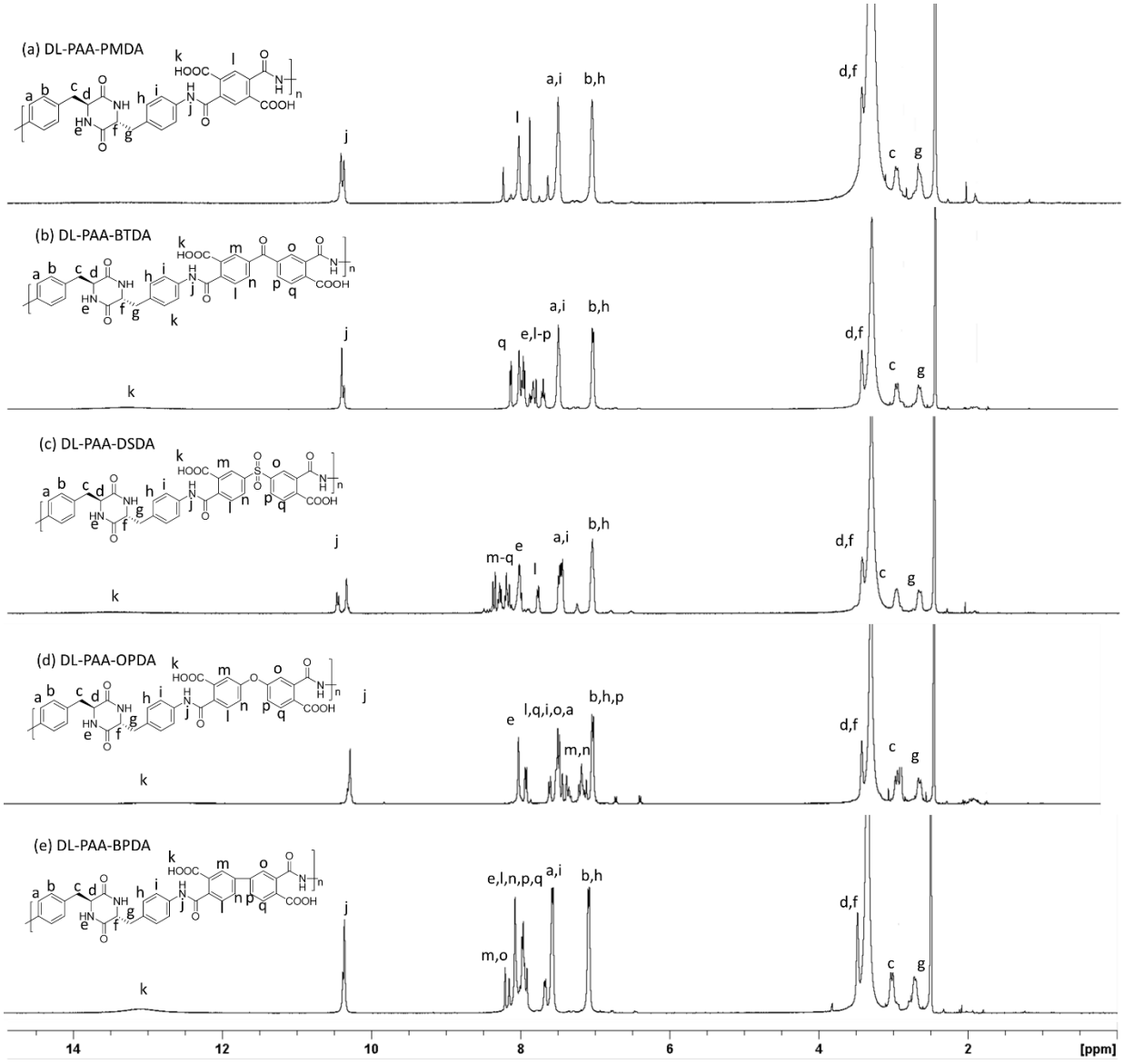

Figure 3.5 ^{1}H NMR spectra of (a) DL-PAA-PMDA (b) DL-PAA-BTDA, (c) DL-PAA-DSDA, (d) DL-PAA-OPDA, and (e) DL-PAA-BPDA.

Figure 3.6 and 3.7 show the FT-IR spectra of the DL-PAAs and DL-PIs respectively. In all the samples, the following peaks were observed: broad band in the range of 2500-3500 cm^{-1} (O-H stretching, carboxylic acid group's hydroxyls), two different carbonyl peaks at 1714 cm^{-1} (C=O stretching, carboxylic) and 1663 cm^{-1} (C=O stretching, amide), and 1514 and 1437 cm^{-1} (aromatic C-H overtone aromatic). After stepwise heating, all the annealed samples showed two carbonyl adsorption at 1712 cm^{-1} (C=O symmetric stretching) and a small peak at 1776 cm^{-1} (C=O asymmetric stretching), which were characteristic to PI structures. Moreover, other

peaks appearing at 1373 cm^{-1} (C-N stretching of imide) and 1150 cm^{-1} (imide ring deformation) and the disappearance of characteristic amide peak found about 2980 cm^{-1}, which all indicating an imidization. Furthermore, PI-OPDA showed IR peak at 1238 cm^{-1} corresponding to ether group, PI-DSDA showed asymmetric and symmetric S=O stretching at 1310 and 1208 cm^{-1}, respectively, and PI-DHCDA showed IR peak of C=C bending at 800 cm^{-1}. These results clearly indicated the formation of the expected PIs.

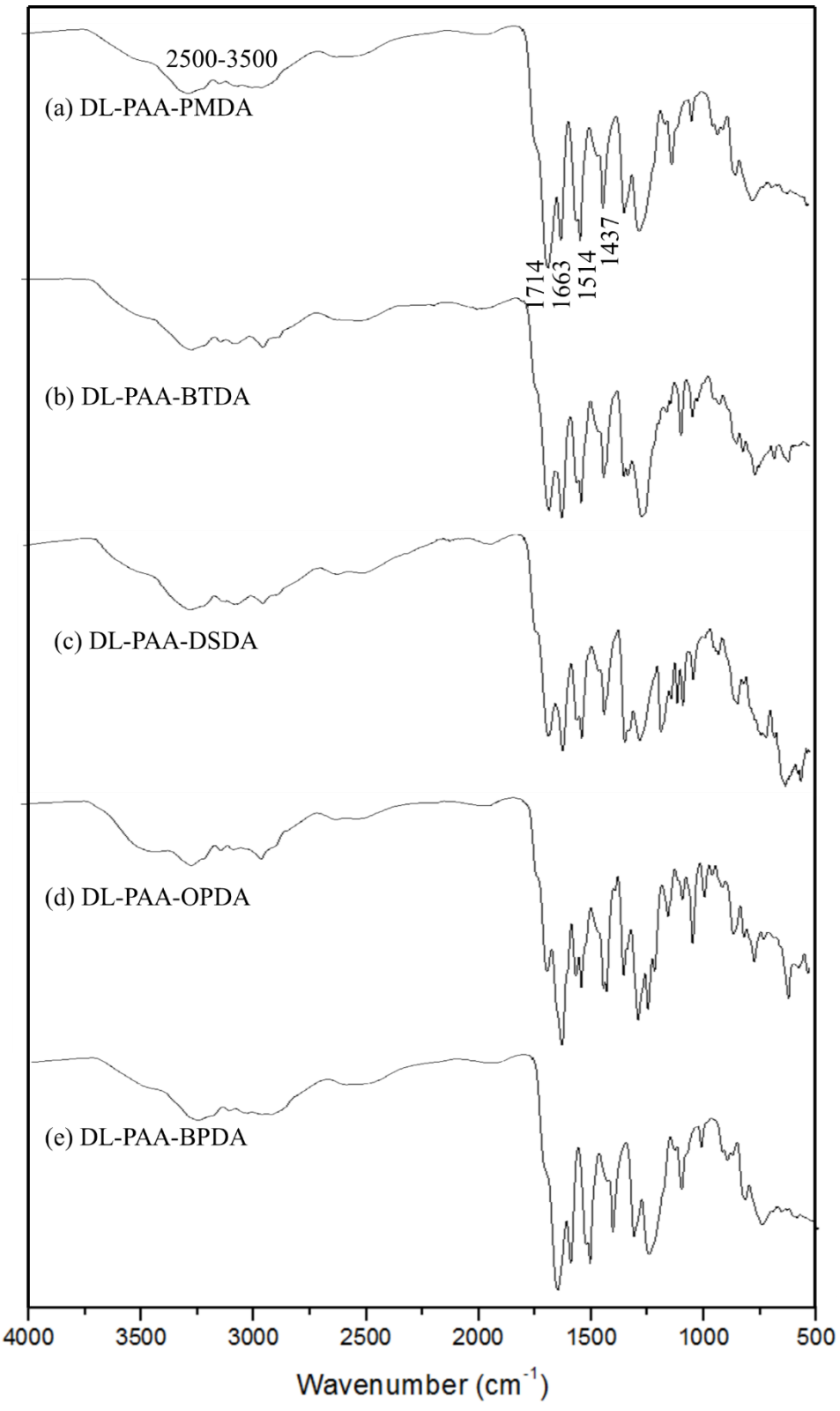

Figure 3.6 FT-IR spectra of (a) DL-PAA-PMDA (b) DL-PAA-BTDA, (c) DL-PAA-DSDA, (d) DL-PAA-OPDA, and (e) DL-PAA-BPDA.

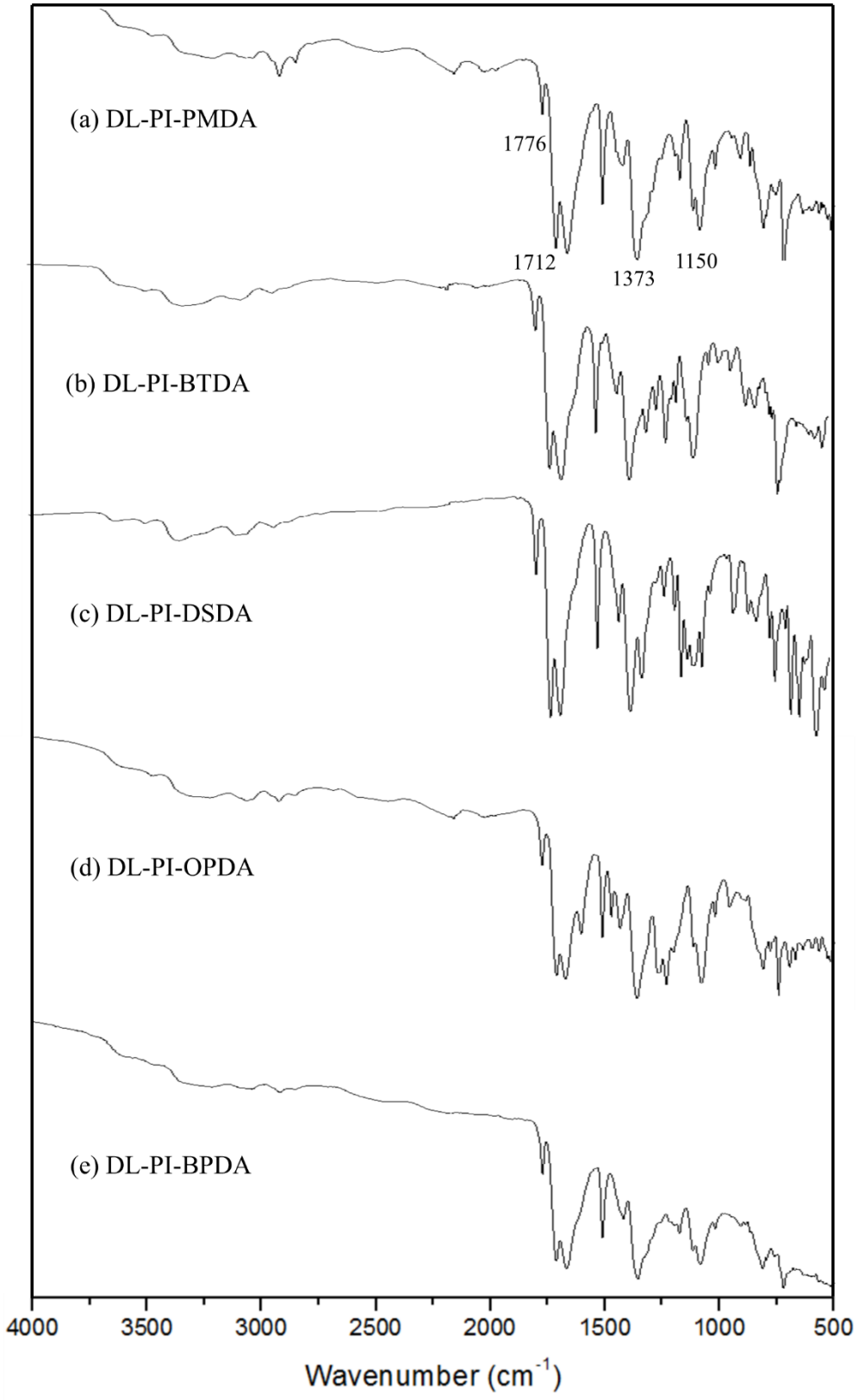

Figure 3.7 FT-IR spectra of (a) DL-PI-PMDA (b) DL-PI-BTDA, (c) DL-PI-DSDA, (d) DL-PI-OPDA, and (e) DL-PI-BPDA.

Optical property

The obtained PIs films were determined for its transparency with the UV-Visible spectroscopy at a region of 800 - 200 nm. The yellowness of the films was determined by spectrophotometer and, the results were compared with that of the glass slides as a reference.

The percent tranparency at 450 nm (cut-off wavelength) and the yellow index were shown in Table 3.5. The results show that all of DL-DKP-biopolyimide films showed higher transparency (%T at 450 nm, = 0%) and less yellow index (D1925=124.4) than Kapton®. Kapton® has strong dark brown color due to the characteristic absorption tailing from UV to visible region, caused by strong charge transfer (CT) interaction in electron-rich oxydianiline (ODA) component with dianhydride moieties. On the other hand, polyimides from DL-DKP-4APhe containing DKP alicyclic core which has less electron-rich compared to benzenes, leading to weaker CT interaction with dianhydride component than ODA in Kapton®. While comparing to 4ATA diamine monomer, all PI derived from 4ATA showed higher transparent and less coloration. This was attributed to the hydroben bonding potentail of DKP rings which could induce more densely PIs chain packing compared to alicyclic cyclobutane which has no potential sites for hydrogen bonding formation.

Table 3.5 Transparency and yellow index of DL-DKP-polyimide films

PIs-Dianhydrides	% $T_{450\ nm}$ of PI-DL-DKP-4APhe	% $T_{450\ nm}$ of PI-4ATA	Yellow index (D1925) of PI-DL-DKP-4APhe	Yellow index (D1925) of PI-4ATA
BPDA	58.0	N/A	42.13	N/A
DSDA	60.7	77	54.74	18.0
OPDA	52.2	80	55.49	7.1
BTDA	79.0	82	35.57	8.39
PMDA	75.5	N/A	47.50	N/A

Solubility

The solubility of all prepared DL-PAAs and DL-PIs was investigated in various solvents shown in Table 3.6. The solubility of the polymers was tested by dissolving them in three groups of solvent: (A) nonpolar solvent, (B) polar protic solvent, and (C) polar aprotic solvent.

Table 3.6 Solubility of DL-type PAAs and PIs in various solvents.

Solvent	PAA-PMDA	PI-PMDA	PAA-BTDA	PI-BTDA	PAA-DSDA	PI-DSDA	PAA-OPDA	PI-OPDA	PAA-BPDA	PI-BPDA
Non-polar										
Toluene	-	-	-	-	-	-	-	-	-	-
Hexane	-	-	-	-	-	-	-	-	-	-
Diethyl ether	-	-	-	-	-	-	-	-	-	-
DCM	-	-	-	-	-	-	-	-	-	-
1,4-dioxane	-	-	-	-	-	-	-	-	-	-
Polar protic										
H_2O	-	-	-	-	-	-	-	-	-	-
MeOH	-	-	-	-	-	-	-	-	-	-
EtOH	-	-	-	-	-	-	-	-	-	-
Conc. H_2SO_4	+	+	+	+	+	+	+	+	+	+
TFA	+	+	+	+	+	+	+	+	+	+
Polar aprotic										
Acetone	-	-	-	-	-	-	-	-	-	-
THF	-	-	-	-	-	-	-	-	-	-
`EtOAc	-	-	-	-	-	-	-	-	-	-
ACN	-	-	-	-	-	-	-	-	-	-
Pyridine	-	-	-	-	-	-	-	-	-	-
DMAc	+	-	+	-	+	-	+	-	+	-
DMF	+	-	+	-	+	-	+	-	+	-
DMSO	+	-	+	-	+	-	+	-	+	-
NMP	+	-	+		+	-	+	-	+	-

- Not soluble / + soluble/ ± partially soluble/

The solubility of polymers was tested; DL-PAAs were soluble in polar solvents such as NMP, DMAc, DMSO and DMF at room temperature. However, all PIs were soluble in trifluoroacetic acid and concentrated sulfuric acid only.

Table 3.7 Molecular weights of DL-PAAs polymerized from DL-DKP-4APhe and various dianhydrides.

DL-PAA-	PMDA	BTDA	DSDA	OPDA	BPDA
M_n (kDa)[a]	72.8	135.7	61.9	35.2	75.1
M_w (kDa)[a]	299.7	659.2	304.3	197.8	392.0
PDI [a]	4.1	4.8	4.9	5.6	5.2

[a]The weight-average molecular weight, M_w, the number-average molecular weight, M_n, and the distribution of polymer molecular weight, PDI, of PAA were measured by GPC.

The weight-average molecular weight of (M_w), number average molecular weight (M_n) and polydispersity index (PDI) were determined using DL-PAA and were summarized in Table 3.7. PAAs had M_w and M_n values in the range of 659.2-197.8 and 135.7-35.2 kDa, respectively, and PDI ranging from 4.1-5.6. For all DL-PAA, the polymer could dissolve well in DMF/LiBr. Presumably, due to less densely packing of DL-PAA polymer chains, the solvation could take place more easily compared to LL-PAA.

By changing the stereochemistry from L to D at one α-carbon position of DKP-4APhe monomer, polyimide with greatly increased molecular weights could be generated. The low molecular weight of LL-PAA could be the result from polymer aggregation/packing during reaction and consequently low efficiency in polymerization.

Thermal properties

Degradation temperature (T_d) of polyimide was determined at 5% and 10% weight loss by thermogravimetric analysis (TGA) under nitrogen atmosphere. Glass transition temperature (T_g) of polyimides were determined by differential scanning calorimetry (DSC). The results from both LL and DL typed PI were summarized in Table 3.8 for compararison.

Table 3.8 Thermal Properties of PIs prepared from LL and DL-DKP-4APhe and various dianhydrides

Dianhydrides	DKP-4APhe	T_{d5} (°C)	T_{d10} (°C)	T_g (°C)
PMDA	LL	420	432	ND
	DL	423	433	ND
DSDA	LL	383	397	ND
	DL	400	411	ND
ODPA	LL	398	414	ND
	DL	404	416	ND
BTDA	LL	411	427	ND
	DL	423	447	ND
BPDA	LL	401	414	ND
	DL	423	433	ND

[a]5% and 10% weight loss temperatures, T_{d5} and T_{d10}, were obtained from TGA curve scanned at a heating rate of 10°C/min under N_2 atmosphere. ND refers to not determined.

TGA was utilized in order to investigate the thermal degradation of PIs in a nitrogen atmosphere using heating rate at 10°C/min, and the 5% and 10% weight-loss temperatures, T_{d5} and T_{d10}, were evaluated. As shown in Table 3.8, all PIs prepared from DL-DKP aromatic diamine monomers exhibited a T_{d10} range of 411-433°C and T_{d5} range of 391-423°C, which indicated the high degree of resistance towards thermal degradation; especially PI from PMDA showing a highest T_{d10} of 433 °C. Thermal property of DL-PIs; however, was quite comparable to that of LL-PIs despite their much higher molecular weight. The DL conformation possibly depromoted CT interaction in DL-PIs chains.

DL-PIs thermal transition behavior was investigated by DSC under a nitrogen atmosphere. However all DL-PIs also exhibited no distinct peaks below thermal degradation temperatures same as LL-PIs, which possibly attributed to the charge transfer interaction and hydrogen bonding formations between PIs chains

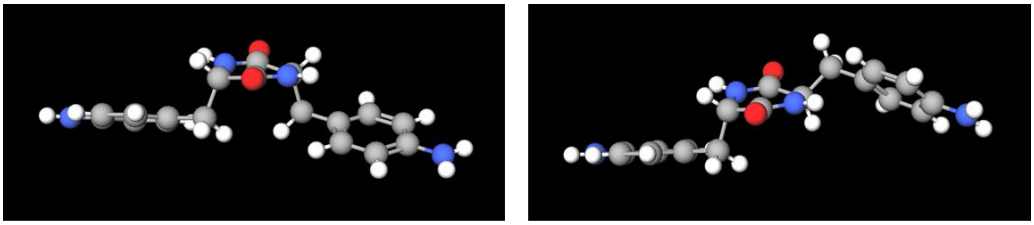

LL-DKP-4APhe LD-DKP-4APhe

Figure 3.8 Molecular structure of LL and DL-DKP-4APhe

As seen from Figure 3.8, the molecules of LL- and DL- typed DKP monomers were oriented differently. It seems that the structure of LL-DKP-4APhe could help induce polymer chain packing more easily and impart higher rigidity to the polymer chains compared to DL type, resulting in higher thermal stability. Unfortunately, due to the strong intermolecular forces between DKP units and nearly flat structure, LL-polymers tended to aggregate/pack during polymerization leading to low molecular weight. This is probably one reason that we could not fabricate film from LL-type PAAs. In order to balance these two properties, here, the polymerization of BTDA with the mixture of both LL and DL-DKP-4APhe at various ratio was also studied. Their thermal property were evaluated and the data shown in Table 3.9.

However, from Table 3.9, we could not detect any significant difference of thermal stability of each PI-BTDA obtained from a mixture of LL and DL-DKP-4APhe vat various ratio.

Table 3.9 Thermal Properties of PIs prepared a mixture of LL and DL-DKP-4APhe with BTDA.

DKP-4APhe	T_{d5} (°C)	T_{d10} (°C)
LL 100 DL 0	411	427
LL 80 DL 20	396	415
LL 50 DL 50	402	422
LL 20 DL 80	404	419
LL 0 DL 100	423	447

Mechanical property

The mechanical properties of the DL-PI-BTDA films was measured by a tensile test (other DL-PIs films were too brittle to take a mechanical test). The DL-PI-BTDA films had tensile strength values of 74.0 MPa, % elongation of 10.5% and tensile modulus of 1.1 GPa. The mechanical data shown in Figure 3.9 indicated that DL-PI-BTDA film had ductile property.

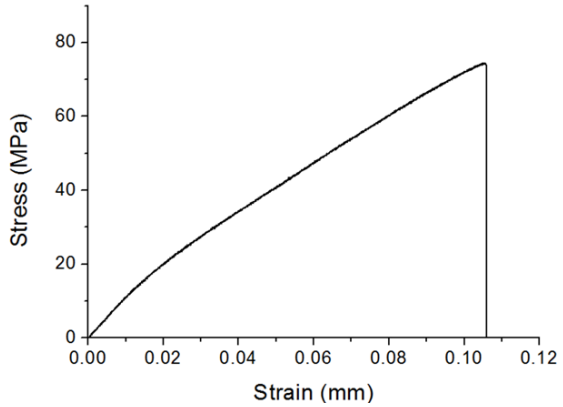

Figure 3.9 The mechanical property of DL-PI-BTDA film.

3.3.2 Polyurea (PUs) syntheses and characterization

3.3.2.1 Syntheses and characterization

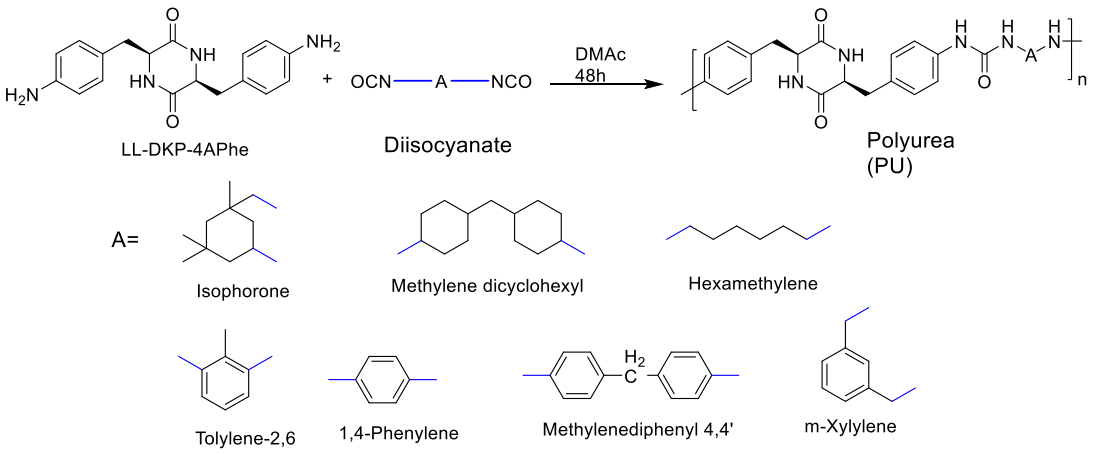

Scheme 3.3 Syntheses of polyurea from LL-DKP-4APhe

A series of PU were prepared by polyadditions of our LL-type diamine monomer with stoichiometric amounts of aromatic diisocyantes and aliphatic diisocyanate. We found that using DMAc as a polymerization solvent, when aromatic diisocyanate was polymerized with LL-DKP-4APhe, after about an hour the polymer solution became turbid and precipitate out of the reaction. On the other hand, with aliphatic diisocyante, after 48 hour the clear viscous solution could be obtained without any precipitates. This was possibly attributed to the presence of carbamide function groups along the PU chains. Carbamide had hydrogen bonding formation potential, which strengthened the intermolecular force, leading to polymer aggregates.

We considered only aliphatic diisocyanate. In this chapter, PUs with isophorone diisocyanate., methylene dicyclohexyl diisocyanate and hexanethylene diisocyanate are abbreviated as PU-Iso, PU-Cyclo and PU-Hexa, respectively.

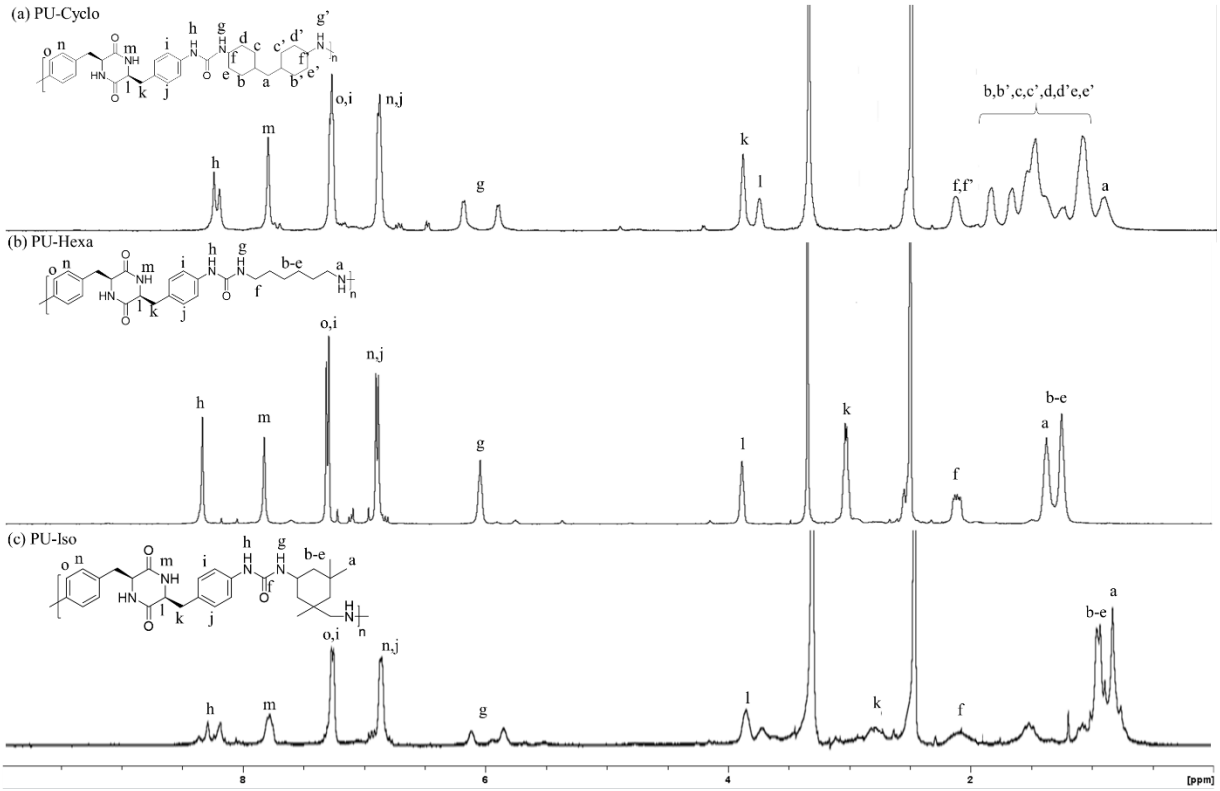

Figure 3.10 ^{1}H NMR spectra of (a) PU-Cyclo (b) PU-Hexa, and (c) PU-Iso.

The ^{1}HnNMR spectra of these PUs indicated the proton signals for aromatic region and ureas around 7.0–7.5 and 8.5–8.7, respectively. Proton of aliphatic diisocyanate moieties appeared around 0.8-2.3 ppm (Figure 3.10).

Table 3.10 Molecular weights of PUs polymerized from LL-DKP-4APhe and aliphatic diisocyanate

	PU-Hexa	PU-Iso	PU-Cyclo
M_n (kDa)[a]	10.5	17.2	7.1
M_w (kDa)[a]	40.7	42.9	17.2
PDI [a]	3.9	2.5	2.4

[a]The weight-average molecular weight, M_w, the number-average molecular weight, M_n, and the distribution of polymer molecular weight, PDI, of PUs were measured by GPC.

3.3.2.2 Properties of synthesized PUs

Solubility

All aliphatic PUs were soluble in polar solvents such as NMP, DMAc, DMSO at room temperature and in DMF partially.

Thermal property

Table 3.11 Thermal properties of PUs prepared from LL-DKP-4APhe and aliphatic diisocyanate

DKP-4APhe	T_{d5} **(°C)**	T_{d10} **(°C)**
PU-Iso	317	331
PU-Cyclo	291	327
PU-Hexa	284	319

The thermal degradation of all the synthesized PUs was analyzed by thermogravimetric analysis under nitrogen atmosphere at a heating rate of 5 ^{o}C/min, and the values of 5 and 10% weight-loss temperatures (T_{d5} and T_{d10}) were determined, which were summarized in Table 3.11. TGA analyses were made up to 800 ^{o}C to evaluate. The T_{d5} values lie above 280 ^{o}C for all PUs, while T_{d10} ranged between 319 and 331 ^{o}C which are much higher than conventional bioplastics such as poly(lactic acid)s (PLA, ca. 300 ^{o}C) and polyhydroxybutyrate (PHB, 260 ^{o}C).

3.4 Conclusion

Our novel bio-based DKP-4Phe could polymerized with various dianhydrides to generate high thermal resistance polyimides. All LL-DKP-based PI prepared here showed high thermal resistance, especially PI from PMDA showing a highest T_{d10} of 432 °C and T_g values above thermal degradation temperatures. Such high thermal property could be attributed to the charge transfer interaction characteristic to polyimides and hydrogen bonding between the imide group and DKP ring or between DKP moieties could be a reason for high thermal stability.

By changing the stereochemistry from L to D at one α-carbon position, the intermolecular forces in polyimides became weaken. DL-DKP-4APhe could provide DL-polyimide with significantly increased molecular weight due to less densely polymer packing during polymerization. All DL-PIs had thermal stability comparable to that of LL-PIs. Due to less electron density in DKP aliphatic ring, all DL-PI films exhibited higher transparency and less coloration compared to a classic PI Kapton®. Additonally, DL-PI film derived from BTDA showed ductile property. With aliphatic diisocyanates, our DKP-based aromatic monomers could also generate PUs with high thermal resistance feature.

.

CHAPTER IV

SELF-ASSEMBLY PROPERTY OF BIO-BASED DIKETOPIPERAZINE POLYMERS

4.1 Introduction

2,5-Diketopiperazines (DKPs) are semi-rigid molecules, and although they are conformationally constrained heterocycles, they are flexible because the six-membered ring can exist in an essentially flat conformation or a slightly puckered boat form, with only a few kcal/mol difference in energy between the boat and planar forms. They contain 2 cis-amide bonds and as a result possess 2 H-bond acceptor and 2 H-bond donor sites important for binding to enzymes and receptors. The cis-amide functionality in the 2,5-diketopiperazine ring forms intermolecular hydrogen bonds (N−H···O) between adjacent molecules that enable 2,5-diketopiperazines to take up higher-ordered supramolecular structures that are important in crystal engineering and as liquid gelators.

Considering our design of monomers, the presence of symmetrical amide functionality in DKP ring, and aromatic rings in the monomer structure was expected to induce self-assembly of DKP-based polymer through hydrogen bonding and π-π interaction [90], [92], [102], [103]. As a result, the incorporation of DKP could render high-performance PIs with higher ordered supramolecular structures, which lead to the widening of the polymer applications. To the best of our knowledge, the preparation of DKP embedded in PIs and their self-assembly studies had not been reported thus far.

4.2 Experimental

4.2.1 Materials

Pyromellitic dianhydride (PMDA: >98.0%) were purchased from Tokyo chemical industry co., LTD (TCI) and sublimed at 160^{o}C under reduced pressure and dried under vacuum at 110^{o}C prior to use. *N*,*N*-dimethylacetamide (DMAc: >99.8% anhydrous from Kanto chemical), 1,2,3,4-cyclobutanetetracarboxylic dianhydride (CBDA: purified by sublimation >98.0% from TCI), 3,3′,4,4′-benzophenonetetracarboxylic dianhydride (BTDA: purified by sublimation >98.0% from TCI), 3,3′,4,4′-diphenylsulfonetetracarboxylic dianhydride (DSDA: purified by sublimation >98.0% from TCI), dicyclohexylmethane 4,4'-diisocyanate, isophorone diisocyanate, and hexamethylene diisocyanate, triton X-100 (from Acros), acetic anhydride (>95.0% from Kanto chemical) and pyridine (anhydrous >99.5% from Kanto chemical) were used without further purification.

4.2.2 Characterization

The FT-IR spectra were recorded with a Perkin-Elmer Spectrum One spectrometer between 4000 and 400 cm^{-1} using a diamond-attenuated total reflection (ATR) accessory. Thermogravimetric analysis (TGA) were carried out by Seiko Instruments SII, SSC/5200 at a heating rate of 5 °C/min under a nitrogen atmosphere. Remaining solvent and absorbed moisture in polymer samples were removed at 250^{o}C for 1 hour before TGA measurement. Poly(amic acid) (PAA) and polyimide (PI) particles morphology were characterized with scanning electron microscope (JCM-6000Plus Versatile Benchtop SEM). To prepare a sample, a droplet of the dispersion liquid (5 μL) was casted on a glass slide and air-dried at room temperature; the glass slide was fixed on the sample holder using double-faced carbon tape and coated with a thin layer of gold with a sputter coater (Magnetron sputter MSP-1S). SEM

instrument was operated at an acceleration voltage of 15kV and an emission current of 10μA. ImageJ software was used to analyze average particle diameters from the SEM images. Hydrodynamic size and zeta potential were analyzed with dynamic light scattering (Zetasizer Nano ZS90). The calculation of size distribution from light scattering measurements is based on the assumptions that the particles are spherical.

4.2.3 Preparation of polymer particles.

In a typical solvent displacement method, a PAA solution in DMAc (4% w/v, 100 μL) was injected into vigorously magnetically stirred Triton X-100 aqueous solution (1% w/v, 10 mL) as the poor solvent at room temperature to obtain PAA particles. Collecting PAA by centrifuge, the two-step imidization was subsequently performed to convert PAA to PI. Firstly, PAA was chemically imidized using a mixture of pyridine and acetic anhydride (1:1 molar ratio, 100 μL). After 3 hours, the chemicals were removed by centrifuge, and the thermal imidization was performed at 250 ^{o}C for 3 hours, resulting in a yellowish powder of PI particles.

4.2.4 Evaluation of particle formulation variables.

Various factors during particle formation could govern the properties of fabricated particles (e.g. particle size). Effect of formulation variables (polymer concentration: 0.5, 1, 2, 4, 6 % (w/v); surfactant concentration: 0.1, 0.5, 1, 3 % (w/v); polymer structure with various dianhydrides: BTDA, CBDA, DSDA, PMDA) on particle size were studied in this investigation. Only one variable was studied at a time while keeping all other variable constant.

To study the particulation control of PIs, PAA particles collected by centrifuge were redispersed in different solvent systems such as acetone/water mixture, methanol/water mixture, and cyclohexane and further sonicated for 5 hours. After that, subsequent imidization to convert PAA to PI was made by chemical procedure and thermal treatment. The redispersed

particles of PAA and PI were observed their morphology by SEM as illustrated in Figure 4.1. Here, PI-BTDA was chosen as an example for study.

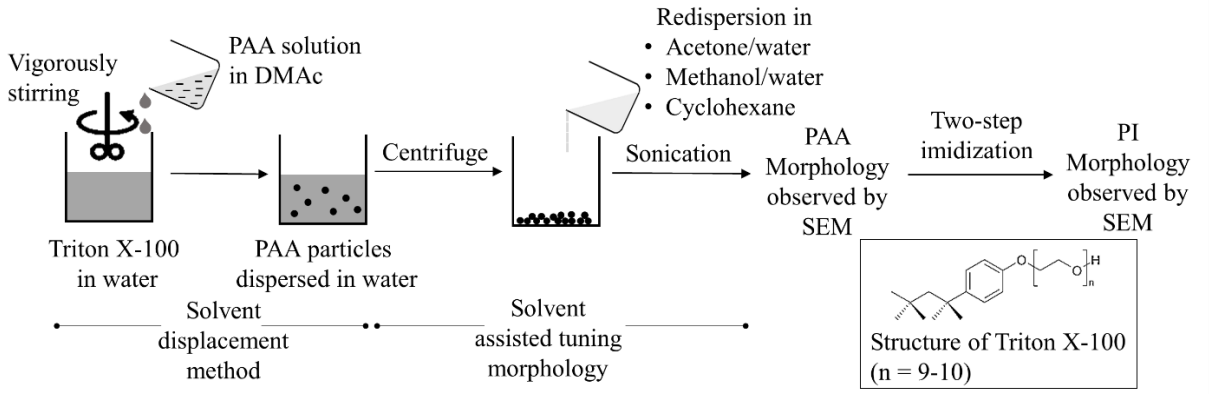

Figure 4.1. Schematic illustration of particle formation and deformation of PAA and PI by solvent assisted approach (the inset picture: the structure of triton X-100).

4.3 Results and discussion

4.3.1 Self-assembly study of bio-based diketopiperazine polymers

4.3.1.1 Polyamic acid and Polyimide particles

The self-assembly behavior of the synthesized polymers was investigated. The polymers synthesized in this study have a DKP six-membered ring with two amide groups as well as other sites such as the amide and acid groups, and the aromatic ring, all of which can trigger various noncovalent interchain interactions.

One of well-known techniques utilized preformed PAA polymer to prepare spherical particles is solvent displacement method [107], [108]. The solvent displacement method, also called as reprecipitation method, is a convenient technique for fabricating organic and polymer particles in a dispersion medium. Under the relatively small shear forces of vigorous stirring,

finely dispersed polymer droplets in a poor solvent could be obtained with the help of a surfactant to reduce the surface tension and stabilize the droplet phase during the process.

The PAAs derived from DKP-4APhe diamine with a series of dianhydrides, PMDA, BTDA, DSDA and CBDA were taken for self-assembly (PAA-PMDA, PAA-BTDA, PAA-DSDA, PAA-CBDA, respectively). Using 1% triton X-100 aqueous solution as the poor solvent in reprecipitation method, 4% PAAs of those dissolved in DMAc could form into spherical nanoparticles with narrow size distribution (Table 4.1 and Figure 4.2).

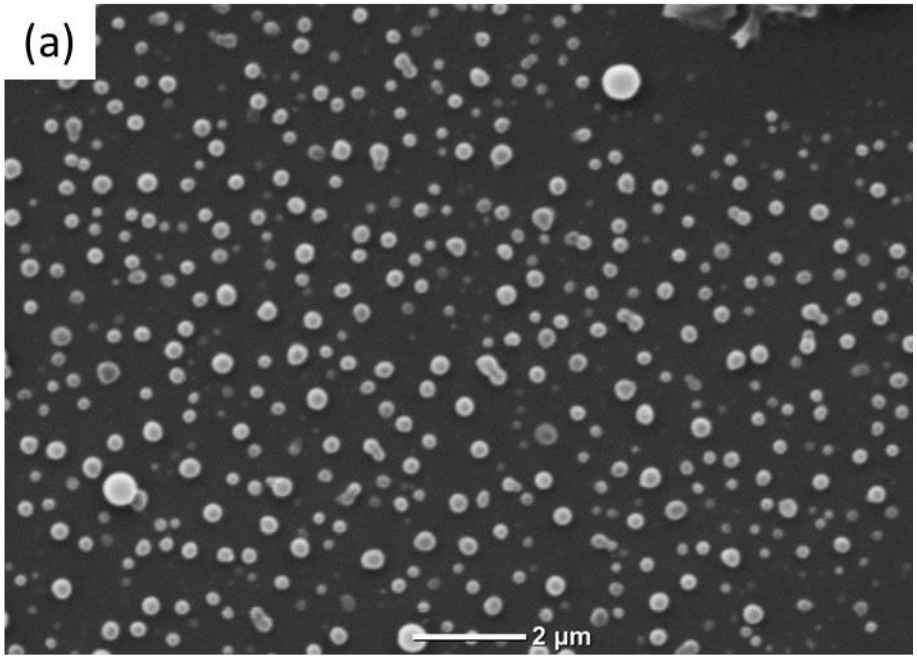
(a)
2 µm

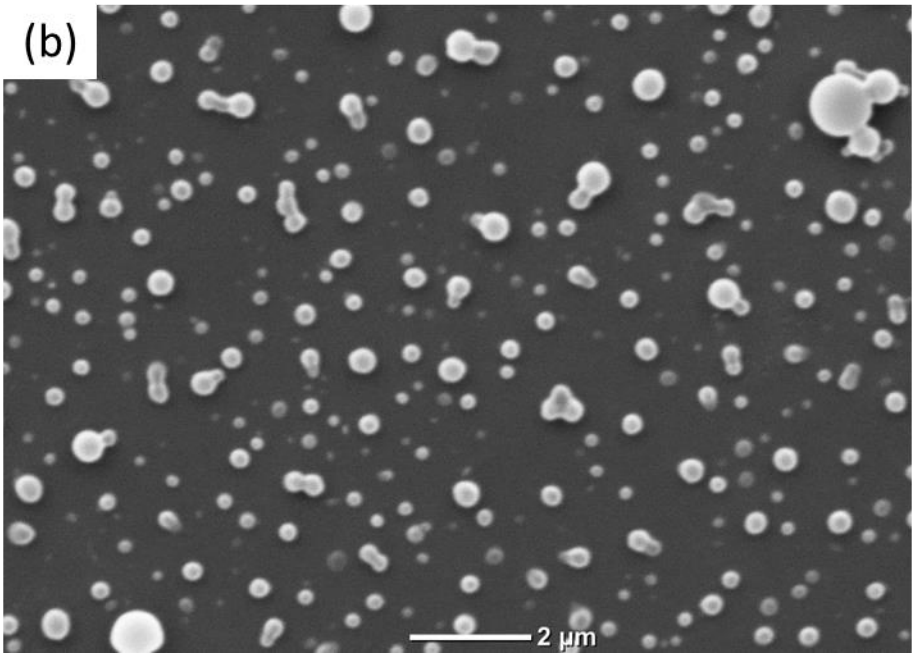
(b)
2 µm

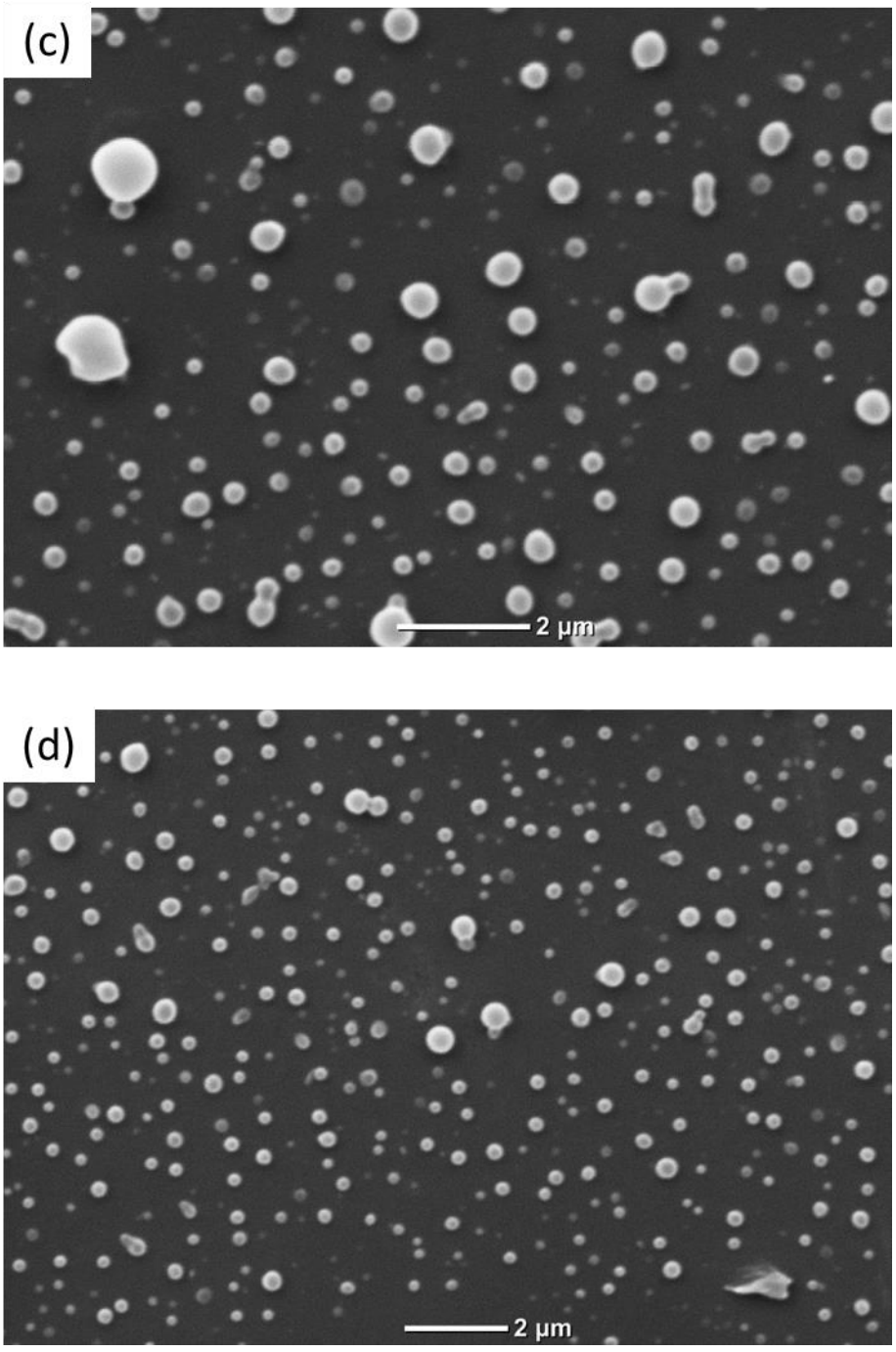

Figure 4.2 SEM images of (a) PAA-BTDA, (b) PAA-CBDA, (c) PAA-DSDA and (d) PAA-PMDA. PAA concentration of 4 wt% and triton X-100 of 1 wt% were used to formulate PAA particles. The diameter of PAA particles were as follows: of (a) 284±82, (b) 375±128, (c) 448±159 and (d) 279±69 nm.

Table 4.1. Particle size and PDI of PAAs and PIs nanoparticles measured by DLS

Nanoparticles	Particle size (nm)	PDI
PAA-BTDA	295.1±86.9	0.100
PAA-CBDA	396.5±88.6	0.194
PAA-DSDA	531.3±95.3	0.219
PAA-PMDA	302.6±78.2	0.150
PI-BTDA	396.0±115.9	0.214
PI-CBDA	458.6±173.9	0.259
PI-DSDA	531.2±323.1	0.349
PI-PMDA	779.7±585.2	0.472

Typically, a preformed PAA polymer solved in DMAc, a water-miscible solvent, was slowly introduced drop by drop to an aqueous phase containing triton X-100 as the emulsifier under vigorous magnetic stirring. After adding the organic phase into the watery phase, a slight turbidity could be observed. PAA-surfactant in water formed aggregated structures with a hydrophilic exterior and a hydrophobic interior. Subsequent self-assembly was initiated by the fast diffusion of the organic solvent (DMAc) into the aqueous medium, which progressively enriched the concentration of the polymers in emulsion droplets. To counteract the loss of the configurational entropy, cooperative noncovalent interactions of PAA chains and polymer self-assembly were induced within surfactant aggregates giving rise to uniform nanoparticles [109].

The PAA particles could remain suspended in water for several days without aggregations. The zeta potentials of the prepared PAAs particles, as measured by dynamic light scattering (DLS), indicate that the surfaces of all particles were negatively charged, irrespective of the nature of the dianhydride (Table 4.2). This result suggests that the carboxyl groups in each PAA are self-arranged on the exterior surface of particles, which would help stabilize the dispersion in the aqueous colloidal system.

Table 4.2. Zeta potential of PAAs nanoparticles dispersed in water measured by DLS

Nanoparticles	Zeta potential (mV)
PAA-BTDA	-39.9±7.7
PAA-CBDA	-23.7±4.8
PAA-DSDA	-38.1±4.8
PAA-PMDA	-26.3±4.7

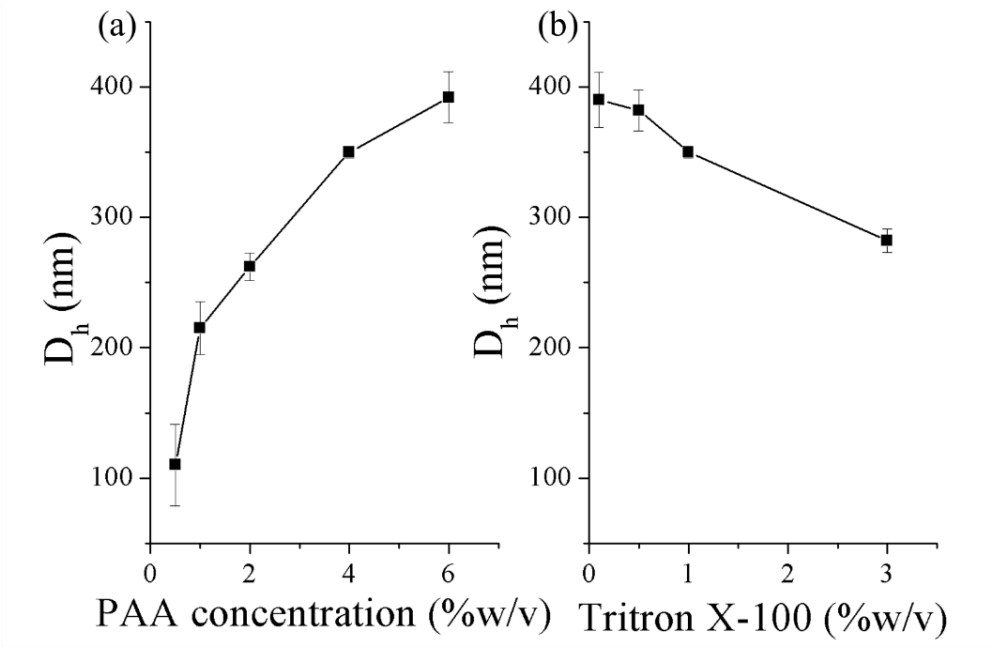

Figure 4.3 Hydrodynamic diameter, D_h, of PAA-BTDA particles measured by dynamic light scattering. (a) D_h dependence on polymer concentration under a constant Triton X-100 concentration of 1 wt%. (b) D_h dependence on Triton X-100 concentration under a constant polymer concentration of 4 wt%.

Figure 4.3 shows changes in hydrodynamic diameter, D_h, of PAA-BTDA particles as a function of PAA concentration and Triton X-100 concentration. The PAA particles with the smallest hydrodynamic size of 110 nm were formed at a PAA concentration of 0.5 wt%. A monotonous increase in D_h with increase in PAA concentration can be clearly seen in Figure 4.3 (a). When a dilute solution of the PAA was dropped into stirred surfactant solution,

nucleation and growth was initiated. The increased concentration resulted in the formation of large particles by enhanced growth. In contrast, when a very dilute PAA solution (lower than 0.5 wt%) was used, it was impossible to evaluate the particle size by either DLS or SEM, because of the particle yield was very low. Conversely, when PAA concentration was higher than 6 wt%, the precipitation occurred macroscopically immediately after dropping the PAA solution. To summarize, the concentration range between 0.5 wt % and 6 wt% was found to be suitable in order to obtain well-dispersed and size-controlled PAA particles.

Figure 4.3 (b) shows a decrease in D_h with an increase in the concentration of Triton X-100, from 0.1 wt% to 3.0 wt%. The surfactant plays an important role because it can retard the aggregation of the droplets by lowering the surface tension. A higher amount of surfactant made the droplet smaller since a large surface area could be stabilized. In solutions with very low concentrations of Triton X-100 (lower than 0.1 wt%), DLS was unable to supply the particle size data, indicating that there was very little surfactant to stabilize the polymer droplets, which resulted in aggregation. The size distribution of the PAA particles was the lowest when the concentration of the PAA and Triton X-100 were 4 wt% and 1 wt%, respectively, suggesting that this range of concentrations should be used for investigating factors that could control particle morphologies.

To convert PAAs to PIs particles, we employed two-step imidization: chemical imidization using pyridine/acetic anhydride mixture (1:1 mole ratio) followed by stepwise thermal imidization. The characteristic peaks of imide formation appeared in the FT-IR spectrum (Figure 4.4) confirmed the conversion as following: the peaks at 1781 and 1713 cm^{-1} corresponding to the in-phase and out-of-phase stretching vibrations of imide carbonyl group, respectively, the peak at 1373 cm^{-1} corresponding to the C-N imide stretching, and the peak at 712 cm^{-1} corresponding to the bending of C-N.

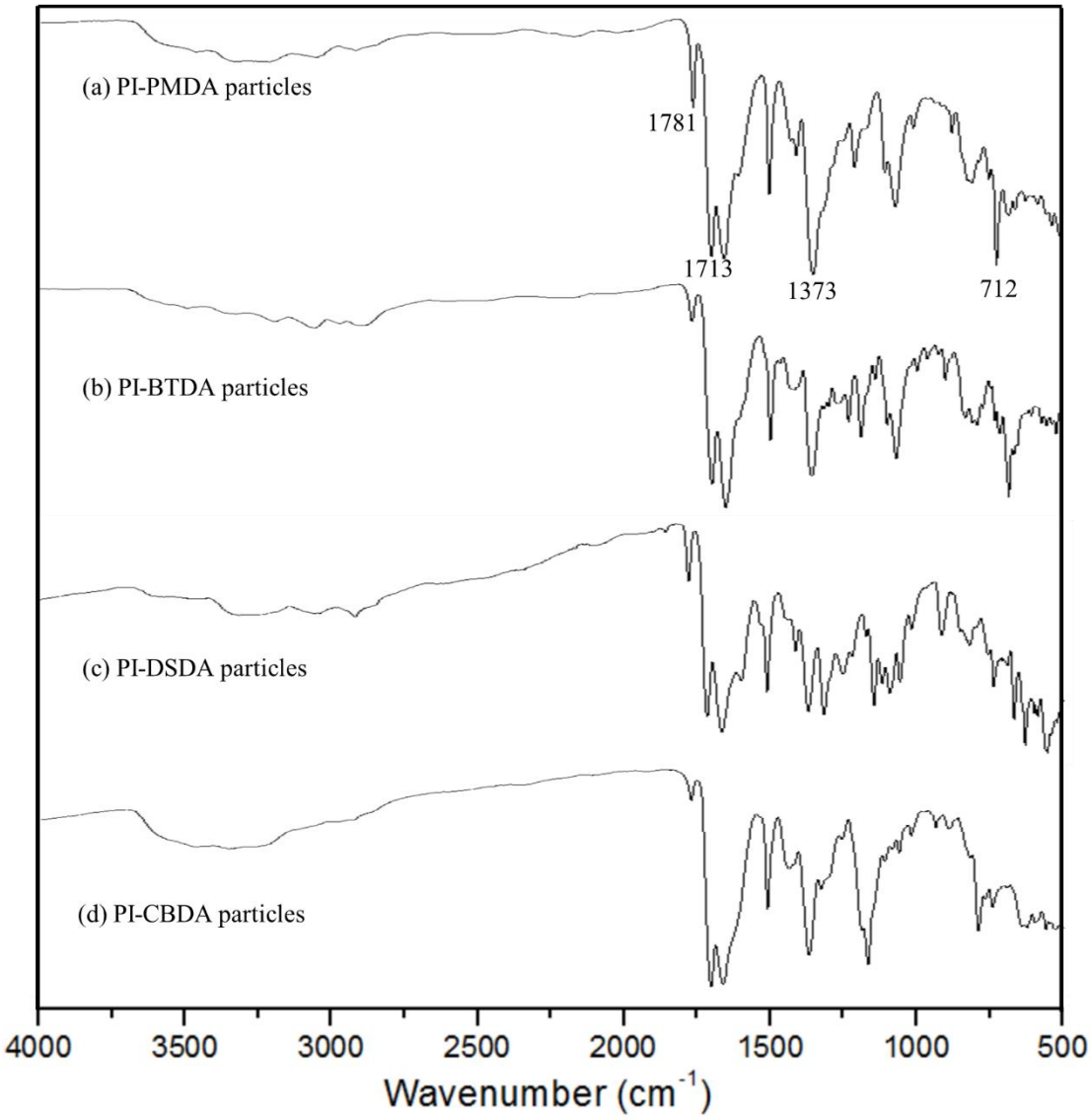

Figure 4.4 FT-IR spectra of PIs particles (a) PI-PMDA, (b) PI-BTDA, (c) PI-DSDA, and (d) PI-CBDA.

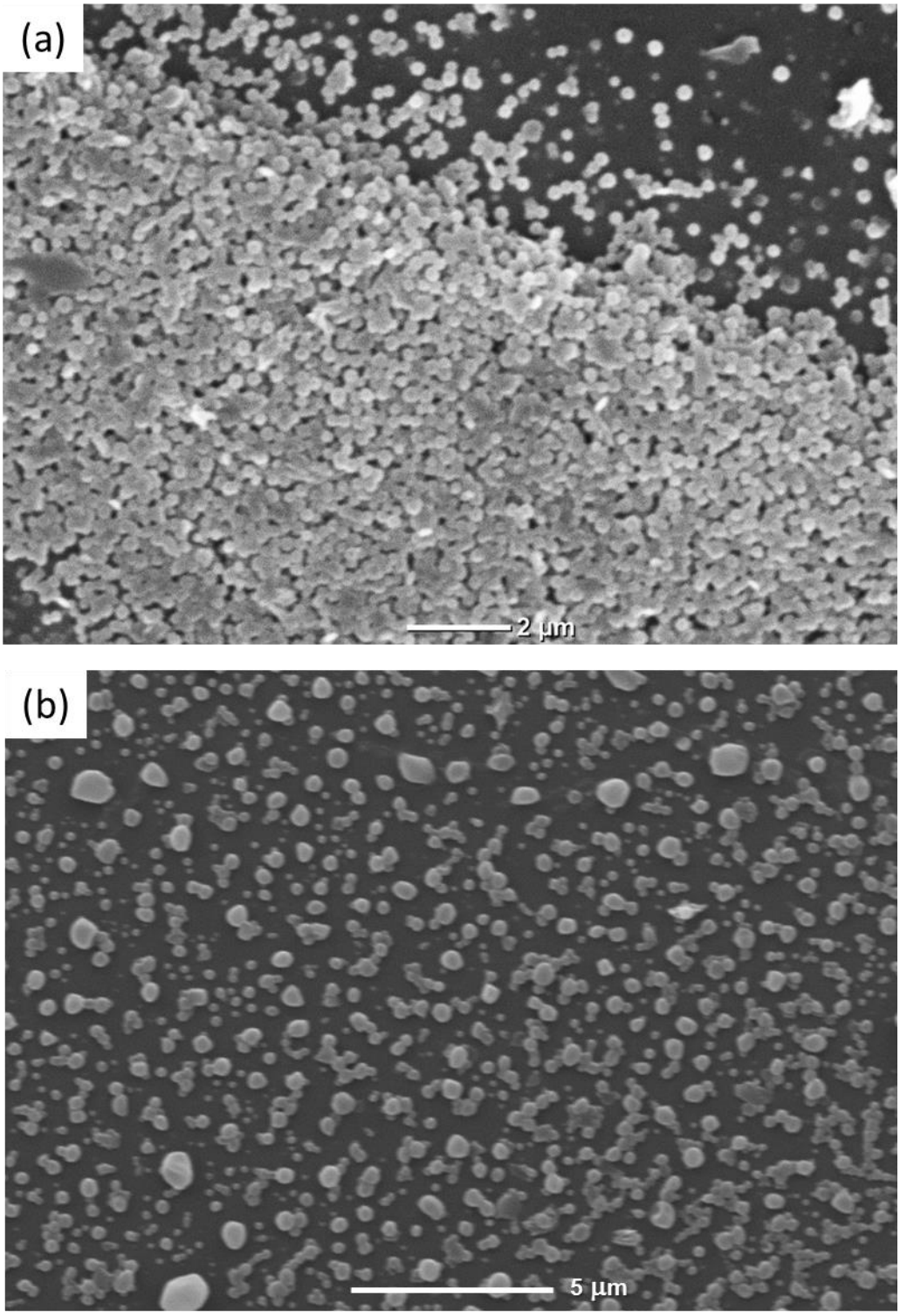
(a)
2 µm
(b)
5 µm

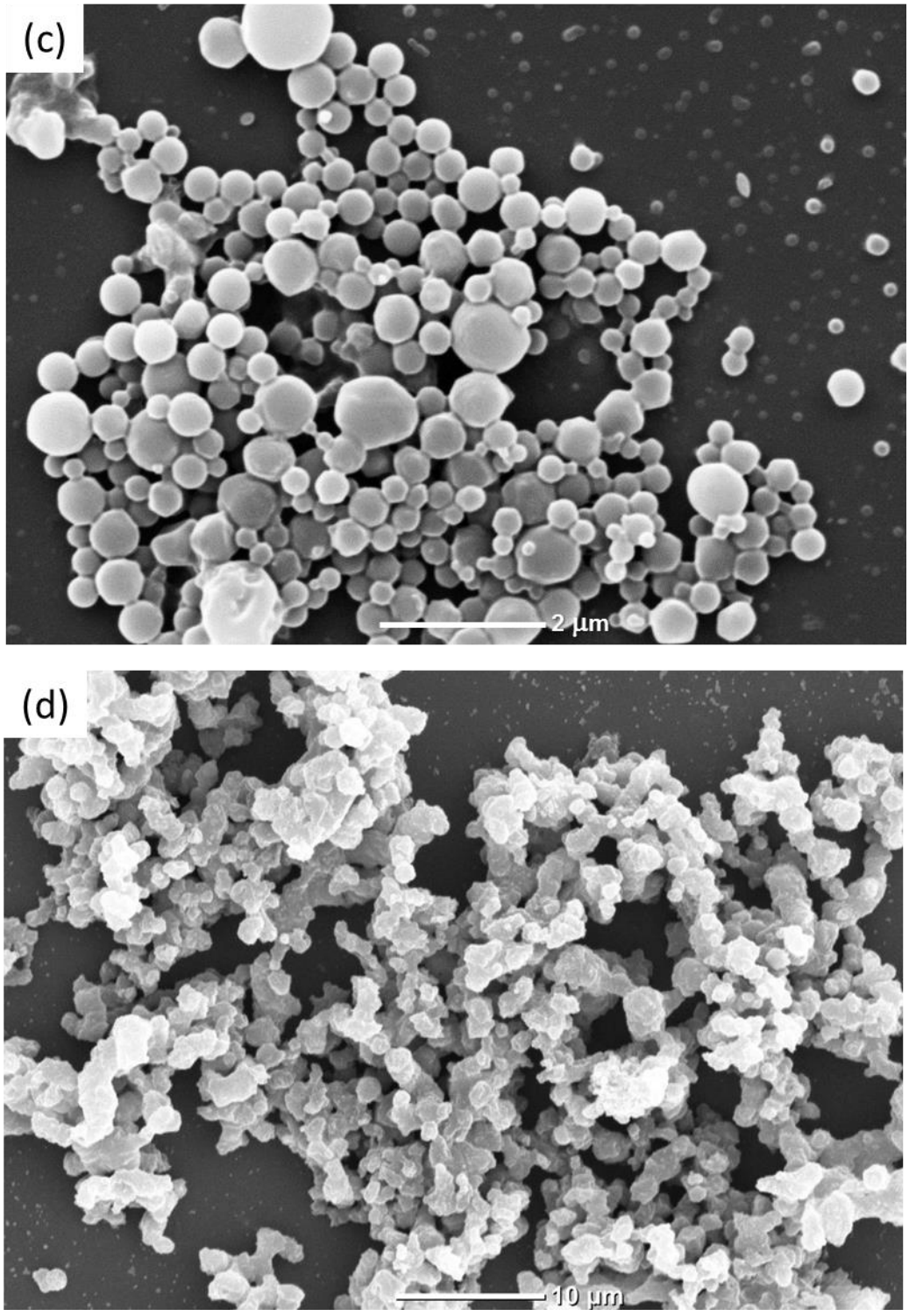

Figure 4.5 SEM images of PIs particles prepared from DKP-4APhe with various dianhydrides (a) BTDA, (b) CBDA, (c) DSDA, and (d) PMDA.

After two-step imidization, Figure 4.5 exhibited that the spherical nano-sized PIs were still formed with the diameter of 309±38, 471±110, and 499±171 nm for PI-BTDA, PI-CBDA and PI-DSDA, respectively, which corresponding to the hydrodynamic diameter measured by DLS (Table 4.1). The morphology of PI-PMDA was not clear as others because of particle agglomeration forming irregular particle clusters. Although the PI-PMDA size were difficult to determine from the SEM image, the hydrodynamic diameter from DLS was 779.7±585.2 nm. Due to imide formation, there was no negatively-charged repulsion to prevent aggregates forming. It could be observed by DLS that PIs particles dispersed in water exhibited broader size distribution compared to PAAs particles (Table 4.1).

Figure 4.6 shows the results of TGA measurements of PIs nanoparticles. The data demonstrated that the thermal behavior of the two-step imidized PIs nanoparticles is comparable to those of PIs in Table 3.2 with 5% weight loss started at about 400 ^{o}C in most cases, indicating the high degree of thermal resistance. The PI-DSDA particles showed the lowest heat resistance among them. Containing the sulfone group of DSDA in the structure, PI-DSDA is slightly flexible, so the heat resistance of the particles generated from PI-DSDA may show lower than the others.

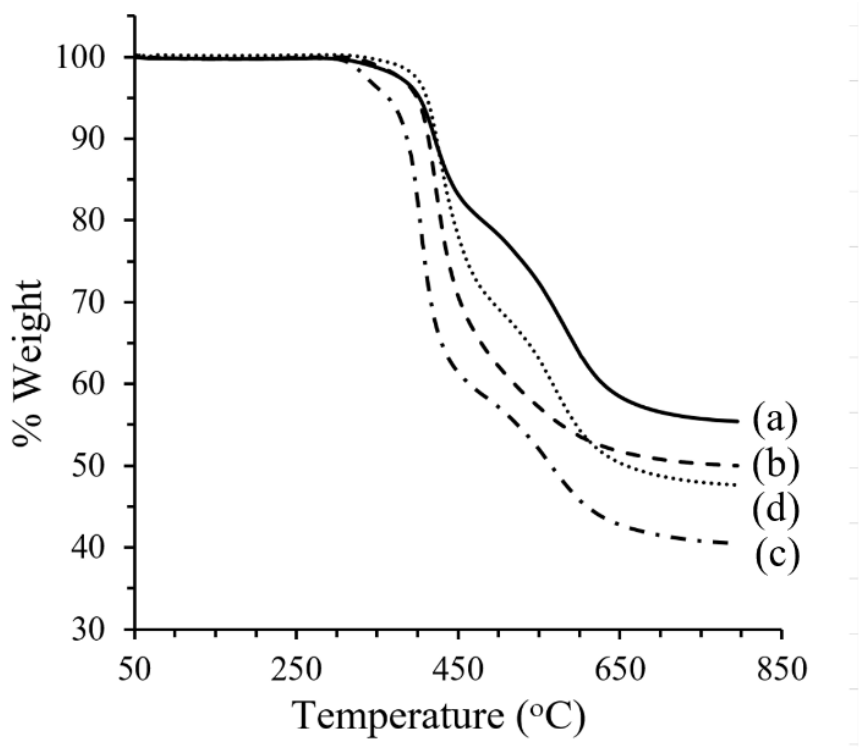

Figure 4.6 TG curves recorded under N_2 of PIs particles prepared from DKP-4APhe with various dianhydrides (a) BTDA, (b) CBDA, (c) DSDA, and (d) PMDA.

Particle morphologies of DKP-based PIs were controlled by external stimuli, namely, variation of the solvent polarity. After collecting the PAA microspheres from aqueous medium by centrifuge, they were redispersed in three solvent systems, acetone/water mixture, methanol/water mixture, and cyclohexane, followed by sonication for 5 h. Figure 4.7 shows SEM images of the PAA-BTDA particles after treatment by different solvents, clearly revealing morphology changes. When 20% acetone/80% water mixture was used, microparticles like spiky balls were formed (8.6±1.0 μm) (Figure 4.7(a)). The spiky ball can be regarded as consisting of secondary aggregates, with needles on their surface. We propose that the needles could be formed as a result of interchain self-assembly via DKP interactions. When the proportion of acetone was changed in the mixed solvent, the secondary aggregates were formed but needles were formed to some extent only at 2 compositions, with 10% and 50 % acetone (Figures 4.8 (a2) and (a3), respectively). The introduction of PAA nanospheres into

a less polar solvent, such as acetone/water mixed solvent seemed to induce polymer aggregation, with a consequent increase in particle size. Under sonication, the polymers could rearrange themselves into more highly ordered structures. It is possible that solvent polarity may be fine-tuned to cause the formation of needle-like structures on the secondary aggregate surfaces. When a 40% methanol/ 60% water mixture was used, rod-like microparticles, whose lengths ranged from 10-60 μm (with aspect ratios ranging from 1-6), were formed. The volumes of the rods were much higher than those of the pretreated spheres and this is attributed to efficient self-assembly by using the mixed solvent (methanol/water) of the right polarity. The rod content in a SEM image seemed to be related to the proportion of methanol in the mixed solvent (Figure 4.8 (b1) and (b2)). This suggests that when PAA spheres were plasticized by an appropriate composition of methanol/water, the PAA chains were able to self-assemble efficiently to form the rods.

When cyclohexane was used as a solvent, flake-like microparticles were formed. If the PAA was partially dissolved in cyclohexane under ultrasonication, the brittle and thin film formed was cast over cyclohexane solution and seen to be flake-like particles. After the two-step imidization, the PAA particle morphologies were still maintained in the corresponding PIs (see Figure 4.7 (a2), (b2) and (c2)). The morphology of the PI particles were then fine-tuned by the use of mixed solvents of different polarities.

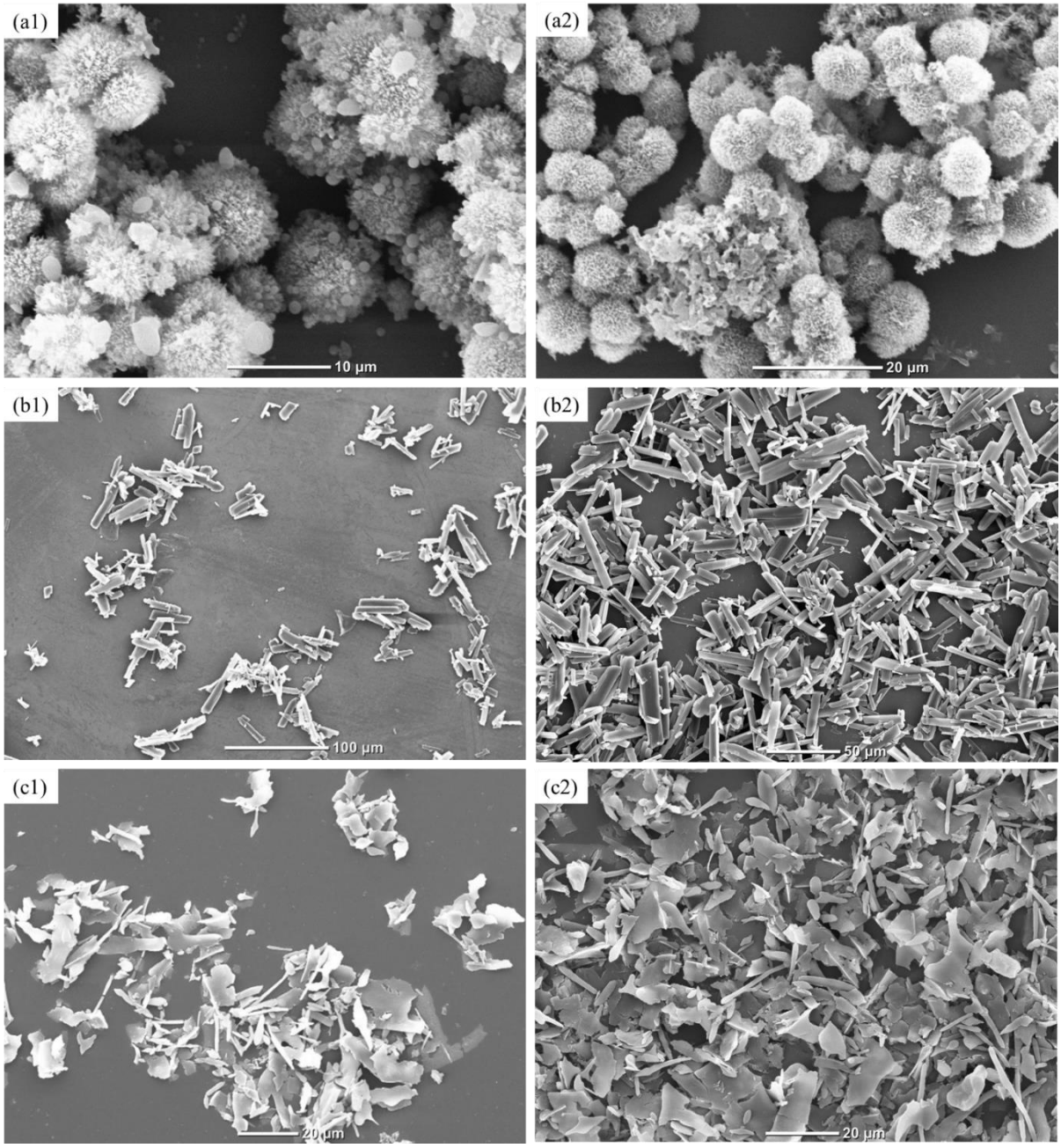

Figure 4.7 SEM images of PAA-BTDA obtained by redispersion of PAA spheres into (a1) 20% acetone/water, (b1) 40% methanol/water and (c1) cyclohexane, following sonication and conversion to PI by two-step imidization given (a2), (b2) and (c2), respectively.

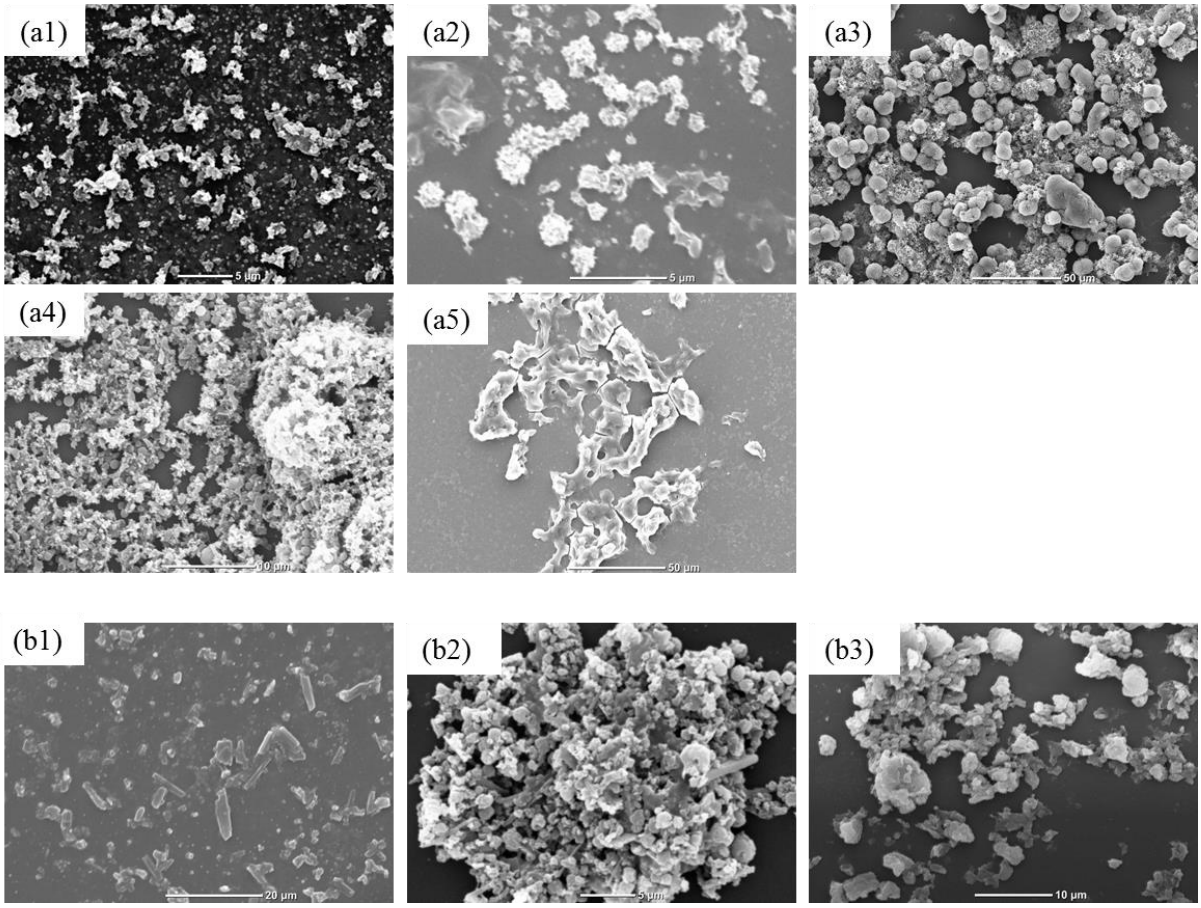

Figure 4.8 SEM images of PI-BTDA obtained by redispersion of PAAs spheres into a various mix ratio of acetone in water: (a1) 5%, (a2) 10%, (a3) 50%, (a4) 70% and (a5) 100%, and into a various mix ratio of methanol in water: (b1) 20%, (b2) 70% and (b3) 100%, following the sonication and conversion to PI by two-step imidization.

The self-assembly was investigated in terms of hydrogen bonding by FTIR techniques. Figure 4.9(b) shows the FTIR spectrum of the PI-BTDA spherical particles obtained by solvent displacement and subsequent imidization, showing five specific vibrations at 1780, 1718, 1667, 1516, and 1375 cm^{-1}, which were assigned to C=O of benzophenone, C=O of the imide ring (Imide I), C=O stretching of DKP (Amide I), N-H bending of DKP (Amide II), and C-N of imide (Imide II), respectively. The FTIR peaks of the spiky balls were not very different from those of the spheres (Figure 4.9(c)), although the C=O of imide ring showed a slight shift towards higher wavenumbers. The absence of any significant change of FTIR spectrum

suggests that there is no distinct change in the hydrogen bonding patterns during the morphology conversion from spheres to spiky balls. Although the transformation from a smooth to a spiky surface could have resulted from an enhancement in hydrogen bonding, the percentage change was too small. On the other hand, rods formed by the methanol/water stimulus showed the broadening of amide I, as well as the red shifts of amide II, C=O of benzophenone, and imide II peaks, clearly indicating the enhanced hydrogen bonding in stacked polymer chains [91], [110] via DKP interactions, even after imidization (see Figure 4.9(d)). Regarding the flakes formed by cyclohexane stimulus, the blue shifts of amide I, and imide I were observed (Figure 4.9(a)), which implied that the hydrogen bonds became weaker after drying over cyclohexane. The IR analyses support the notion of solvent casting of particles to be film-like structures.

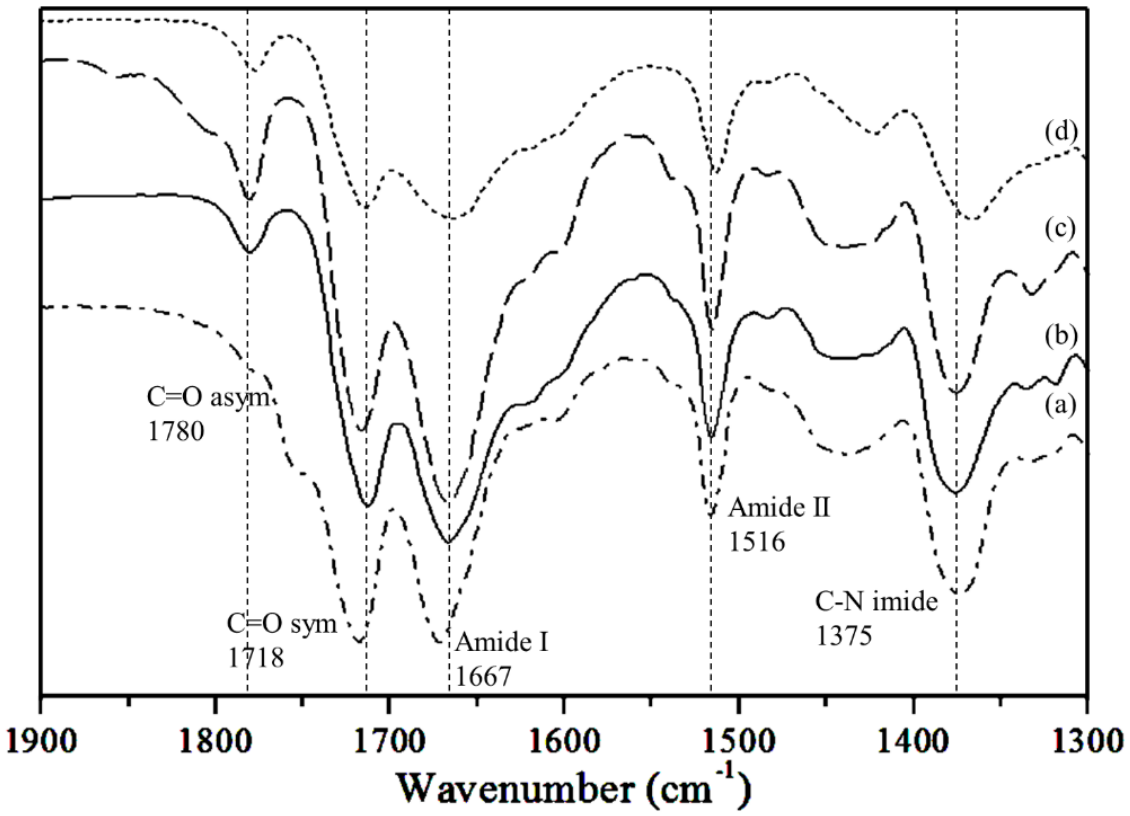

Figure 4.9 FT-IR spectra of PI-BTDA in various forms: (a) particles, (b) spiky ball, and (c) microsheet.

The solvent effects for the previously reported [59] PAA-BTDA particles, derived from 4ATA dimethyl ester, were investigated for comparison. 4ATA dimethyl ester is a diamine monomer having a central cyclobutane ring sandwiched by aromatic rings similar to DKP-4APhe monomers, but having no amide linkage which makes it different from DKP. The particle morphologies were observed by SEM (Figure 4.10). Although spherical particles (605±157 nm) were obtained by the solvent displacement method (Figure 4.10 (a)), particles were broken into diffuse shapes after redispersion into solvent mixtures of 20% acetone/80% water, 40% methanol/60% water, and cyclohexane, and following sonication (Figure 4.10 (b), (c), and (d), respectively). This suggests that DKP units could play a key role in solvent-assisted morphological change in the present PAA and PI systems. Thus, the thermoresistant biopolyamide particles have the ability to transform into different shapes by external stimuli of

solvent exchange, and the morphology change can help to add to their functionality. This could in turn increase the number of possible applications for such molecules, e.g., as fillers reinforcing a polymer matrix.

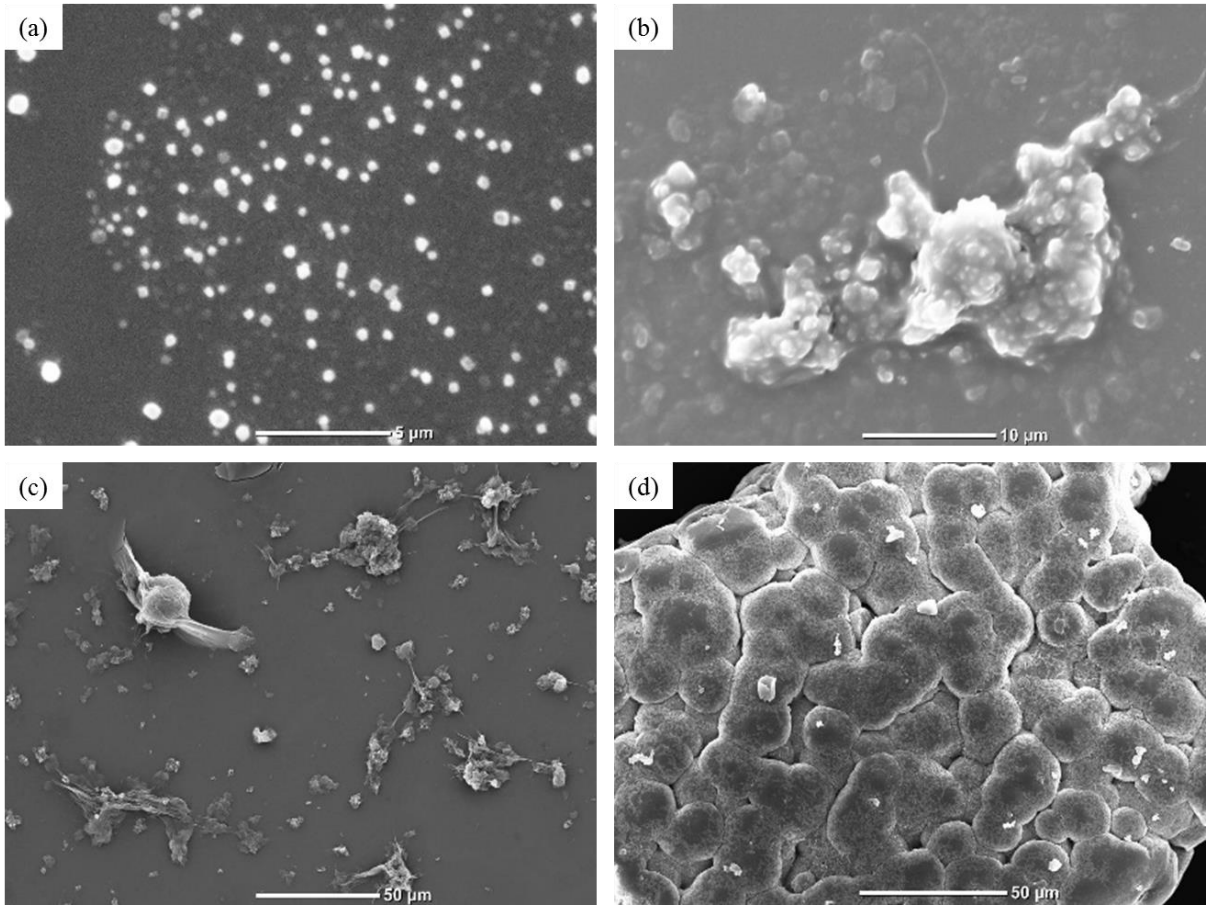

Figure 4.10. SEM images of PAA-BTDA based 4ATA obtained by (a) solvent displacement method and subsequent redispersion into (b) 20% acetone/water, (c) 40% methanol/water and (d) cyclohexane, and following sonication.

4.4 Conclusion

Due to superior hydrogen bonding ability of DKP and the embedded aromatic in the polymer chains, the self-assembly property could be bestowed on the developed PAAs and PIs. Here, the self-assembly of the DKP-based PIs was demonstrated. The uniform PIs

nanoparticles with various dianhydrides could be obtained using simple solvent displacement method and following two-step imidization. The high thermal resistance property of the generated PI particles still maintained. The morphology control of the developed PIs was also achieved by adjusting the polarity of the dispersed solvent system given higher ordered self-assembled structure. The morphology of self-assembled PIs could be tuned into either spiky ball or microsheet by adjusting the polarity of the dispersed solvent system prior to imidization. Such high-performance PIs with controllable high ordered supramolecular structure property could lead to the widening of the PI applications.

CHAPTER V

GENERAL CONCLUSION

In this work, we designed a novel bio-based diamine monomer based on the concept structure of 4-aminocinnamic acid (4ACA), having alicyclic at the structure core. The polymerization of 4ACA with various dianhydrides could introduce high rigidity from alicyclic building blocks to the polymer structures and help generate high thermoresistance polyimides. By applying this concept, the dimerization of biomass 4-aminophenylalanine (4-APhe), 2,5-diketopiperazine (DKP), 6-membered alicyclic ring containing 2 *cis*-amide bonds embedded in the structure, could be formed as the monomer core, rendering DKP-4APhe. Through simple protection/deprotection reactions, this designed compound could be obtained in good yield. This synthesis approach is a template, which could be applied not only with various amino acids but also with diverse stereochemistry.

The prepared bio-based DKP-4Phe could polymerized with various dianhydrides to generate high thermal resistance polyimides. All DKP-based PI prepared here showed high thermal resistance, especially PI from PMDA showing a highest T_{d10} of 432 °C and T_g values above thermal degradation temperatures. Altering the stereochemistry at one site of α-carbon from L to D, given LD-DKP-4APhe could provide not only polymer films but also the molecular weights high enough to evaluate the thermal and mechanical properties. Polymerization of DKP-4APhe with diisocyanate to prepare polyurea was also demonstrated. With only aliphatic diisocyanates could polymerize with our DKP-based aromatic monomers without precipitation occurred. The obtained PUs also exhibited high thermal resistance.

Due to superior hydrogen bonding ability of DKP and the embedded aromatic in the polymer chains, the self-assembly property could be bestowed on the developed PAAs and PIs. Using simple solvent displacement method, PAAs and PIs spheres could formed in uniform size in water. The morphology of self-assembled PIs could be tuned into either spiky ball or microsheet by adjusting the polarity of the dispersed solvent system prior to imidization. Such high-performance PIs with controllable high ordered supramolecular structure property could lead to the widening of the PI applications.

REFERENCES

[1] J. G. B. Derraik, “The pollution of the marine environment by plastic debris: a review,” *Mar. Pollut. Bull.*, vol. 44, no. 9, pp. 842–852, 2002.

[2] F. Parrenin *et al.*, “Synchronous Change of Atmospheric CO₂ and Antarctic Temperature During the Last Deglacial Warming,” *Science (80-.).*, vol. 339, no. 6123, pp. 1060 LP – 1063, Mar. 2013.

[3] R. P. Babu, K. O’Connor, and R. Seeram, “Current progress on bio-based polymers and their future trends,” *Prog. Biomater.*, vol. 2, no. 1, p. 8, Mar. 2013.

[4] M. Jamshidian, E. A. Tehrany, M. Imran, M. Jacquot, and S. Desobry, “Poly-Lactic Acid: Production, Applications, Nanocomposites, and Release Studies,” *Compr. Rev. Food Sci. Food Saf.*, vol. 9, no. 5, pp. 552–571, Sep. 2010.

[5] G. L. Fiore, F. Jing, J. Young Victor G., C. J. Cramer, and M. A. Hillmyer, “High Tg aliphatic polyesters by the polymerization of spirolactide derivatives,” *Polym. Chem.*, vol. 1, no. 6, pp. 870–877, 2010.

[6] Y. Furuhashi, Y. Kimura, N. Yoshie, and H. Yamane, “Higher-order structures and mechanical properties of stereocomplex-type poly(lactic acid) melt spun fibers,” *Polymer (Guildf).*, vol. 47, no. 16, pp. 5965–5972, 2006.

[7] A. Basu, M. Nazarkovsky, R. Ghadi, W. Khan, and A. Domb, *Poly(lactic acid)-based nanocomposites: Polylactide-based Nanocomposites*, vol. 28. 2017.

[8] K. KAN, H. AJIRO, and M. AKASHI, “Chain End Modification of Polylactide Biomaterials and Investigation of Their Polymer-Polymer Interaction,” *KOBUNSHI RONBUNSHU*, vol. advpub, 2017.

[9] M. Chauzar *et al.*, “Hydrotalcites Catalyze the Acidolysis Polymerization of Phenolic Acid to Create Highly Heat-Resistant Bioplastics,” *Adv. Funct. Mater.*, vol. 22, no. 16, pp. 3438–3444, Aug. 2012.

[10] T. Kaneko, T. H. Thi, D. J. Shi, and M. Akashi, “Environmentally degradable, high-performance thermoplastics from phenolic phytomonomers,” *Nat. Mater.*, vol. 5, no. 12, pp. 966–970, 2006.

[11] Y. Wang, S. M. Chiao, T.-F. Hung, and S.-Y. Yang, “Improvement in toughness and

heat resistance of poly(lactic acid)/polycarbonate blend through twin-screw blending: Influence of compatibilizer type," *J. Appl. Polym. Sci.*, vol. 125, no. S2, pp. E402–E412, Sep. 2012.

[12] C.-H. Lee, M. Kato, and A. Usuki, "Preparation and properties of bio-based polycarbonate/clay nanocomposites," *J. Mater. Chem.*, vol. 21, no. 19, pp. 6844–6847, 2011.

[13] C. W. J. McChalicher and F. Srienc, "Investigating the structure–property relationship of bacterial PHA block copolymers," *J. Biotechnol.*, vol. 132, no. 3, pp. 296–302, 2007.

[14] K. C. Reis, J. Pereira, A. C. Smith, C. W. P. Carvalho, N. Wellner, and I. Yakimets, "Characterization of polyhydroxybutyrate-hydroxyvalerate (PHB-HV)/maize starch blend films," *J. Food Eng.*, vol. 89, no. 4, pp. 361–369, 2008.

[15] U. J. Hänggi, "Requirements on bacterial polyesters as future substitute for conventional plastics for consumer goods," *FEMS Microbiol. Rev.*, vol. 16, no. 2-3, pp. 213–220, Feb. 1995.

[16] H. Eslami and M. R. Kamal, "Elongational rheology of biodegradable poly(lactic acid)/poly[(butylene succinate)-co-adipate] binary blends and poly(lactic acid)/poly[(butylene succinate)-co-adipate]/clay ternary nanocomposites," *J. Appl. Polym. Sci.*, vol. 127, no. 3, pp. 2290–2306, Feb. 2013.

[17] J. Ren, P. Zhao, W. Liu, and Q. Wu, "Preparation, mechanical, and thermal properties of biodegradable polyesters/poly(Lactic Acid) blends," *J. Nanomater.*, vol. 2010, 2010.

[18] C. H. R. M. Wilsens, B. A. J. Noordover, and S. Rastogi, "Aromatic thermotropic polyesters based on 2,5-furandicarboxylic acid and vanillic acid," *Polymer (Guildf).*, vol. 55, no. 10, pp. 2432–2439, 2014.

[19] G. N. Short, H. T. H. Nguyen, P. I. Scheurle, and S. A. Miller, "Aromatic polyesters from biosuccinic acid," *Polym. Chem.*, vol. 9, no. 30, pp. 4113–4119, 2018.

[20] M. AOYAGI, K. MURAI, and M. FUNAOKA, "Thermal Behavior of Lignophenol Ester," *KOBUNSHI RONBUNSHU*, vol. 70, no. 12, pp. 722–730, 2013.

[21] "Syntheses of hyperbranched liquid-crystalline biopolymers with strong adhesion from

phenolic phytomonomers," *Pure and Applied Chemistry*, vol. 84. p. 2559, 2012.

[22] V. Mittal, "High Performance Polymers: An Overview," *High Performance Polymers and Engineering Plastics*. pp. 1–20, 29-Aug-2011.

[23] P. M. Hergenrother, "The Use, Design, Synthesis, and Properties of High Performance/High Temperature Polymers: An Overview," *High Perform. Polym.*, vol. 15, no. 1, pp. 3–45, Mar. 2003.

[24] J. R. Klaehn, C. J. Orme, E. S. Peterson, F. F. Stewart, and J. M. Urban-Klaehn, "Chapter 13 - High Temperature Gas Separations Using High Performance Polymers," in *Inorganic Polymeric and Composite Membranes*, vol. 14, S. T. Oyama and S. M. B. T.-M. S. and T. Stagg-Williams, Eds. Elsevier, 2011, pp. 295–307.

[25] M. Katz and R. J. Theis, "New high temperature polyimide insulation for partial discharge resistance in harsh environments," *IEEE Electr. Insul. Mag.*, vol. 13, no. 4, pp. 24–30, 1997.

[26] M. Matsuguchi, T. Kuroiwa, T. Miyagishi, S. Suzuki, T. Ogura, and Y. Sakai, "Stability and reliability of capacitive-type relative humidity sensors using crosslinked polyimide films," *Sensors Actuators B Chem.*, vol. 52, no. 1, pp. 53–57, 1998.

[27] R. Yokota, R. Horiuchi, M. Kochi, H. Soma, and I. Mita, "High strength and high modulus aromatic polyimide/polyimide molecular composite films," *J. Polym. Sci. Part C Polym. Lett.*, vol. 26, no. 5, pp. 215–223, May 1988.

[28] S. Numata, S. Oohara, K. Fujisaki, J. Imaizumi, and N. Kinjo, "Thermal expansion behavior of various aromatic polyimides," *J. Appl. Polym. Sci.*, vol. 31, no. 1, pp. 101–110, Jan. 1986.

[29] D. J. Liaw, K. L. Wang, Y. C. Huang, K. R. Lee, J. Y. Lai, and C. S. Ha, "Advanced polyimide materials: Syntheses, physical properties and applications," *Prog. Polym. Sci.*, vol. 37, no. 7, pp. 907–974, 2012.

[30] I. K. Spiliopoulos, J. A. Mikroyannidis, and G. M. Tsivgoulis, "Rigid-Rod Polyamides and Polyimides Derived from 4,3‘‘-Diamino-2‘,6‘-diphenyl- or Di(4-biphenylyl)-p-terphenyl and 4-Amino-4‘‘-carboxy-2‘,6‘-diphenyl-p-terphenyl," *Macromolecules*, vol. 31, no. 2, pp. 522–529, Jan. 1998.

[31] R. S. Irwin, "Polyimides–thermally stable polymers, by M. I. Bessonov, M. M. Koton,

V. V. Kudryavtsev, and L. A. Laius, Consultants Bureau, New York, 1987, 318 pp. Price: $75.00," *J. Polym. Sci. Part C Polym. Lett.*, vol. 26, no. 3, pp. 159–163, Mar. 1988.

[32] C. E. Sroog, "Polyimides," *Prog. Polym. Sci.*, vol. 16, no. 4, pp. 561–694, 1991.

[33] G. F. L. Ehlers, K. R. Fisch, and W. R. Powell, "Thermal degradation of polymers with phenylene units in the chain. IV. Aromatic polyamides and polyimides," *J. Polym. Sci. Part A-1 Polym. Chem.*, vol. 8, no. 12, pp. 3511–3527, Dec. 1970.

[34] Y. Imai, "Rapid Synthesis of Polyimides from Nylon-Salt-Type Monomers BT - Progress in Polyimide Chemistry I," H. R. Kricheldorf, Ed. Berlin, Heidelberg: Springer Berlin Heidelberg, 1999, pp. 1–22.

[35] M. Jean, *HIGH PERFORMANCE POLYMERS – POLYIMIDES BASED – FROM CHEMISTRY TO APPLICATIONS Edited by Marc Jean Médard Abadie*. .

[36] D. W. Taylor and J. F. Kennedy, "Polyimides Edited by D. Wilson, H. D. Stenzenberger and P. M. Hergenrother, Blackie & Son Limited, Glasgow, 1990. pp. x + 297, price £62.00. ISBN 0-2 16-92680-7," *Polym. Int.*, vol. 25, no. 3, p. 199, Jan. 1991.

[37] M. Fryd, *Structure –Tg relationships in Polyimides: Synthesis, Characterization and Properties*. Plenum New York, 1984.

[38] B. V Kotov, T. A. Gordina, V. S. Voishchev, O. V Kolninov, and A. N. Pravednikov, "Aromatic polyimides as charge transfer complexes," *Polym. Sci. U.S.S.R.*, vol. 19, no. 3, pp. 711–716, 1977.

[39] S. Ando, T. Matsuura, and S. Sasaki, "Coloration of Aromatic Polyimides and Electronic Properties of Their Source Materials," *Polym. J.*, vol. 29, no. 1, pp. 69–76, 2005.

[40] Q. Wang, Y. Bai, Y. Chen, J. Ju, F. Zheng, and T. Wang, "High performance shape memory polyimides based on π–π interactions," *J. Mater. Chem. A*, vol. 3, no. 1, pp. 352–359, 2015.

[41] I. A. Ronova and M. Bruma, "Influence of chemical structure on glass transition temperature of polyimides," *Struct. Chem.*, vol. 21, no. 5, pp. 1013–1020, 2010.

[42] H. Lim *et al.*, “Flexible Organic Electroluminescent Devices Based on Fluorine-Containing Colorless Polyimide Substrates,” *Adv. Mater.*, vol. 14, no. 18, pp. 1275–1279, Sep. 2002.

[43] T. Sekitani, U. Zschieschang, H. Klauk, and T. Someya, “Flexible organic transistors and circuits with extreme bending stability,” *Nat. Mater.*, vol. 9, p. 1015, Nov. 2010.

[44] K.-I. Min *et al.*, “Monolithic and Flexible Polyimide Film Microreactors for Organic Microchemical Applications Fabricated by Laser Ablation,” *Angew. Chemie Int. Ed.*, vol. 49, no. 39, pp. 7063–7067, Sep. 2010.

[45] J. A. Kreuz and J. R. Edman, “Polyimide Films,” *Adv. Mater.*, vol. 10, no. 15, pp. 1229–1232, Oct. 1998.

[46] D.-J. Liaw, K.-L. Wang, Y.-C. Huang, K.-R. Lee, J.-Y. Lai, and C.-S. Ha, “Advanced polyimide materials: Syntheses, physical properties and applications,” *Prog. Polym. Sci.*, vol. 37, no. 7, pp. 907–974, 2012.

[47] F. Ke, N. Song, D. Liang, and H. Xu, “A method to break charge transfer complex of polyimide: A study on solution behavior,” *J. Appl. Polym. Sci.*, vol. 127, no. 1, pp. 797–803, Jan. 2013.

[48] S. Ando, T. Matsuura, and S. Sasaki, “Coloration of Aromatic Polyimides and Electronic Properties of Their Source Materials,” *Polym. J.*, vol. 29, no. 1, pp. 69–76, 1997.

[49] H. Ni, J. Liu, Z. Wang, and S. Yang, “A review on colorless and optically transparent polyimide films: Chemistry, process and engineering applications,” *J. Ind. Eng. Chem.*, vol. 28, pp. 16–27, 2015.

[50] J.-Y. Xiong, X.-Y. Liu, S. B. Chen, and T.-S. Chung, “Preferential Solvation Stabilization for Hydrophobic Polymeric Nanoparticle Fabrication,” *J. Phys. Chem. B*, vol. 109, no. 29, pp. 13877–13882, Jul. 2005.

[51] S. Omi, A. Matsuda, K. Imamura, M. Nagai, and G.-H. Ma, “Synthesis of monodisperse polymeric microspheres including polyimide prepolymer by using SPG emulsification technique,” *Colloids Surfaces A Physicochem. Eng. Asp.*, vol. 153, no. 1, pp. 373–381, 1999.

[52] T. Ishizaka, A. Ishigaki, M. Chatterjee, A. Suzuki, T. M. Suzuki, and H. Kawanami,

"Continuous process for fabrication of size controlled polyimide nanoparticles using microfluidic system," *Chem. Commun.*, vol. 46, no. 38, pp. 7214–7216, 2010.

[53] S. Watanabe, K. Ueno, K. Kudoh, M. Murata, and Y. Masuda, "Preparation of core-shell polystyrene-polyimide particles by dispersion polymerization of styrene using poly(amic acid) as a stabilizer," *Macromol. Rapid Commun.*, vol. 21, no. 18, pp. 1323–1326, Dec. 2000.

[54] T. Lin *et al.*, "Preparation of submicrometre polyimide particles by precipitation from solution," *Polymer (Guildf).*, vol. 34, no. 4, pp. 772–777, 1993.

[55] T. Brock and D. C. Sherrington, "Preparation of spherical aromatic polyimide particulates," *J. Mater. Chem.*, vol. 1, no. 1, pp. 151–152, 1991.

[56] Z. Chai, X. Zheng, and X. Sun, "Preparation of polymer microspheres from solutions," *J. Polym. Sci. Part B Polym. Phys.*, vol. 41, no. 2, pp. 159–165, Jan. 2003.

[57] Y. J. Xiong, "Surfactant free fabrication of polyimide nanoparticles," vol. 5733, no. December 2004, 2010.

[58] M. Suzuki *et al.*, "Fabrication of Size-Controlled Polyimide Nanoparticles," *J. Nanosci. Nanotechnol.*, vol. 7, no. 8, pp. 2748–2752, Aug. 2007.

[59] P. Suvannasara *et al.*, "Biobased polyimides from 4-aminocinnamic acid photodimer," *Macromolecules*, vol. 47, no. 5, pp. 1586–1593, 2014.

[60] J. Liu *et al.*, "Novel partially bio-based fluorinated polyimides from dimer fatty diamine for UV-cured coating," *J. Coatings Technol. Res.*, vol. 14, no. 6, pp. 1325–1334, 2017.

[61] K. Ma *et al.*, "Partially bio-based aromatic polyimides derived from 2,5-furandicarboxylic acid with high thermal and mechanical properties," *J. Polym. Sci. Part A Polym. Chem.*, vol. 56, no. 10, pp. 1058–1066, 2018.

[62] J. Hu *et al.*, "Bio-based adenine-containing high performance polyimide," *Polymer (Guildf).*, vol. 119, pp. 59–65, 2017.

[63] S. S. Kuhire, A. B. Ichake, E. Grau, H. Cramail, and P. P. Wadgaonkar, "Synthesis and characterization of partially bio-based polyimides based on biphenylene-containing diisocyanate derived from vanillic acid," *Eur. Polym. J.*, vol. 109, no. September, pp.

257–264, 2018.

[64] X. Ji, Z. Wang, J. Yan, and Z. Wang, “Partially bio-based polyimides from isohexide-derived diamines,” *Polymer (Guildf).*, vol. 74, pp. 38–45, 2015.

[65] A. Susa, J. Bijleveld, M. Hernandez Santana, and S. J. Garcia, “Understanding the Effect of the Dianhydride Structure on the Properties of Semiaromatic Polyimides Containing a Biobased Fatty Diamine,” *ACS Sustain. Chem. Eng.*, vol. 6, no. 1, pp. 668–678, 2018.

[66] J. C. Root and P. J. Scruton, “Second generation multi-purpose polyureas and marketing 101,” *NLGI Spokesm.*, vol. 59, no. 5, pp. 28–32, 1995.

[67] D. J. Primeaux II, “Application of 100% Solids, Plural Component Aliphatic Polyurea Spray Elastomer Systems,” *J. Prot. Coatings Linings Mag.*, pp. 26–32, 2001.

[68] V. Sendijarevic, A. Sendijarevic, I. Sendijarevic, R. E. Bailey, D. Pemberton, and K. A. Reimann, “Hydrolytic Stability of Toluene Diisocyanate and Polymeric Methylenediphenyl Diisocyanate Based Polyureas under Environmental Conditions,” *Environ. Sci. Technol.*, vol. 38, no. 4, pp. 1066–1072, Feb. 2004.

[69] J. L. Stanford, R. H. Still, and A. N. Wilkinson, “Effects of soft-segment prepolymer functionality on the thermal and mechanical properties of RIM copolymers,” *Polym. Int.*, vol. 41, no. 3, pp. 283–292, Nov. 1996.

[70] A. Mahammad Ibrahim, V. Mahadevan, and M. Srinivasan, “Synthetic studies on aliphatic-aromatic co-polyureas,” *Eur. Polym. J.*, vol. 25, no. 4, pp. 427–429, 1989.

[71] W. Sakai, K. Chiga, and N. Tsutsumi, “Nonlinear optical (NLO) polymers. IV. Second-order optical nonlinearity of NLO polyurea and copolyurea with NLO dipole moments aligned transverse to the main backbone,” *J. Polym. Sci. Part B Polym. Phys.*, vol. 39, no. 2, pp. 247–255, Jan. 2001.

[72] J. R. Hwu and K. Y. King, “Design, Synthesis, and Photodegradation of Silicon-Containing Polyureas,” *Chem. – A Eur. J.*, vol. 11, no. 13, pp. 3805–3815, Jun. 2005.

[73] B. Shiwei and W. Guan, “100% Solids Polyurethane and Polyurea Coatings Technology,” no. March, pp. 49–58, 2003.

[74] H. J. Fabris, “Advances in urethane science and technology,” *Technomic, New York*,

1976.

[75] M. E. Kazmierczak, R. E. Fornes, D. R. Buchanan, and R. D. Gilbert, “Investigations of a series of PPDI-based polyurethane block copolymers. II. Annealing effects,” *J. Polym. Sci. Part B Polym. Phys.*, vol. 27, no. 11, pp. 2189–2202, Oct. 1989.

[76] Q. Zhu, S. Feng, and C. Zhang, “Synthesis and thermal properties of polyurethane–polysiloxane crosslinked polymer networks,” *J. Appl. Polym. Sci.*, vol. 90, no. 1, pp. 310–315, Oct. 2003.

[77] P. J. HARRIS and R. D. HARTLEY, “Detection of bound ferulic acid in cell walls of the Gramineae by ultraviolet fluorescence microscopy,” *Nature*, vol. 259, no. 5543, pp. 508–510, 1976.

[78] K. Yanai, N. Sumida, K. Okakura, T. Moriya, M. Watanabe, and T. Murakami, “Para-position derivatives of fungal anthelmintic cyclodepsipeptides engineered with Streptomyces venezuelae antibiotic biosynthetic genes,” *Nat. Biotechnol.*, vol. 22, no. 7, pp. 848–855, 2004.

[79] R. A. Mehl *et al.*, “Generation of a Bacterium with a 21 Amino Acid Genetic Code,” *J. Am. Chem. Soc.*, vol. 125, no. 4, pp. 935–939, Jan. 2003.

[80] M. Piraee, N. Magarvey, J. He, and L. C. Vining, “The gene cluster for chloramphenicol biosynthesis in Streptomyces venezuelae ISP5230 includes novel shikimate pathway homologues and a monomodular non-ribosomal peptide synthetase gene,” *Microbiology*, vol. 147, no. 10, pp. 2817–2829, Oct. 2001.

[81] E. Fischer and E. Koenigs, “Synthese von Polypeptiden. XVIII. Derivate der Asparaginsäure,” *Berichte der Dtsch. Chem. Gesellschaft*, vol. 40, no. 2, pp. 2048–2061, Mar. 1907.

[82] R. J. Bergeron, O. Phanstiel, G. W. Yao, W. R. Weimar, and S. Milstein, “Macromolecular Self-Assembly of Diketopiperazine Tetrapeptides,” *J. Am. Chem. Soc.*, vol. 116, no. 19, pp. 8479–8484, 1994.

[83] A. D. Borthwick, “2,5-Diketopiperazines: Synthesis, Reactions, Medicinal Chemistry, and Bioactive Natural Products,” *Chem. Rev.*, vol. 112, no. 7, pp. 3641–3716, 2012.

[84] G. T. R. Palmore and M. T. McBride, “Engineering layers in molecular solids with the cyclic dipeptide of (S)-aspartic acid,” *Chem. Commun.*, no. 1, pp. 145–146, 1998.

[85] S. Palacin *et al.*, “Hydrogen-Bonded Tapes Based on Symmetrically Substituted Diketopiperazines: A Robust Structural Motif for the Engineering of Molecular Solids,” *J. Am. Chem. Soc.*, vol. 119, no. 49, pp. 11807–11816, Dec. 1997.

[86] Y. Yang, M. Suzuki, M. Kimura, H. Shirai, and K. Hanabusa, “Preparation of cotton-like silica,” *Chem. Commun.*, no. 11, pp. 1332–1333, 2004.

[87] Z. Xie, A. Zhang, L. Ye, and Z. G. Feng, “Organo- and hydrogels derived from cyclo(L-Tyr-L-Lys) and its ε-amino derivatives,” *Soft Matter*, vol. 5, no. 7, pp. 1474–1482, 2009.

[88] H. Hoshizawa, Y. Minemura, K. Yoshikawa, M. Suzuki, and K. Hanabusa, “Thixotropic hydrogelators based on a cyclo(dipeptide) derivative,” *Langmuir*, vol. 29, no. 47, pp. 14666–14673, 2013.

[89] J. C. MacDonald and G. M. Whitesides, “Solid-State Structures of Hydrogen-Bonded Tapes Based on Cyclic Secondary Diamides,” *Chem. Rev.*, vol. 94, no. 8, pp. 2383–2420, Dec. 1994.

[90] T. Govindaraju, “Spontaneous self-assembly of aromatic cyclic dipeptide into fibre bundles with high thermal stability and propensity for gelation,” *Supramol. Chem.*, vol. 23, no. 11, pp. 759–767, 2011.

[91] A. Jeziorna *et al.*, “Cyclic Dipeptides as Building Units of Nano- and Microdevices: Synthesis, Properties, and Structural Studies,” *Cryst. Growth Des.*, vol. 15, no. 10, pp. 5138–5148, Oct. 2015.

[92] K. B. Joshi and S. Verma, “Participation of aromatic side chains in diketopiperazine ensembles,” *Tetrahedron Lett.*, vol. 49, no. 27, pp. 4231–4234, 2008.

[93] A. K. Barman and S. Verma, “Solid state structures and solution phase self-assembly of clicked mannosylated diketopiperazines,” *RSC Adv.*, vol. 3, no. 34, pp. 14691–14700, 2013.

[94] N. Shimazaki, I. Shima, M. Okamoto, K. Yoshida, K. Hemmi, and M. Hashimoto, “PAF inhibitory activity of diketopiperazines: Structure-activity relationships,” *Lipids*, vol. 26, no. 12, pp. 1175–1178, 1991.

[95] P. G. Wyatt *et al.*, “2,5-Diketopiperazines as potent and selective oxytocin antagonists 1: identification, stereochemistry and initial SAR,” *Bioorg. Med. Chem. Lett.*, vol. 15,

no. 10, pp. 2579–2582, 2005.

[96] K. Terada, E. B. Berda, K. B. Wagener, F. Sanda, and T. Masuda, “ADMET polycondensation of diketopiperazine-based dienes. Polymerization behavior and effect of diketopiperazine on the properties of the formed polymers,” *Macromolecules*, vol. 41, no. 16, pp. 6041–6046, 2008.

[97] K. Takada, H. Yin, T. Matsui, M. A. Ali, and T. Kaneko, “Bio-based mesoporous sponges of chitosan conjugated with amino acid-diketopiperazine through oil-in-water emulsions,” *J. Polym. Res.*, vol. 24, no. 12, 2017.

[98] M. Sohail *et al.*, “Synthesis and hydrolysis-condensation study of water-soluble self-assembled pentacoordinate polysilylamides,” *Organometallics*, vol. 32, no. 6, pp. 1721–1731, 2013.

[99] F. Rafiemanzelat, A. Fathollahi Zonouz, and G. Emtiazi, “Synthesis and characterization of poly(ether-urethane)s derived from 3,6-diisobutyl-2,5-diketopiperazine and PTMG and study of their degradability in environment,” *Polym. Degrad. Stab.*, vol. 97, no. 1, pp. 72–80, 2012.

[100] M. Vert, “Aliphatic polyesters: Great degradable polymers that cannot do everything,” *Biomacromolecules*, vol. 6, no. 2, pp. 538–546, 2005.

[101] O. Hauenstein, S. Agarwal, and A. Greiner, “Bio-based polycarbonate as synthetic toolbox,” *Nat. Commun.*, vol. 7, no. May, pp. 1–7, 2016.

[102] S. Manchineella and T. Govindaraju, “Hydrogen bond directed self-assembly of cyclic dipeptide derivatives: Gelation and ordered hierarchical architectures,” *RSC Adv.*, vol. 2, no. 13, pp. 5539–5542, 2012.

[103] A. Jeziorna *et al.*, “Cyclic dipeptides as building units of nano- and microdevices: Synthesis, properties, and structural studies,” *Cryst. Growth Des.*, vol. 15, no. 10, pp. 5138–5148, 2015.

[104] J. Y. Park, K. O. Oh, J. C. Won, H. Han, H. M. Jung, and Y. S. Kim, “Facile fabrication of superhydrophobic coatings with polyimide particles using a reactive electrospraying process,” *J. Mater. Chem.*, vol. 22, no. 31, pp. 16005–16010, 2012.

[105] G. Zhao *et al.*, “Ultralow-Dielectric-Constant Films Prepared from Hollow Polyimide Nanoparticles Possessing Controllable Core Sizes,” *Chem. Mater.*, vol. 21, no. 2, pp.

419–424, Jan. 2009.

[106] D. E. Nitecki, B. Halpern, and J. W. Westley, “Simple route to sterically pure diketopiperazines,” *J. Org. Chem.*, vol. 33, no. 2, pp. 864–866, Feb. 1968.

[107] M. Suzuki *et al.*, “PREPARATION OF POLYIMIDE ULTRAFINE PARTICLES,” *Mol. Cryst. Liq. Cryst.*, vol. 406, no. 1, pp. 151–157, Jan. 2003.

[108] G. Zhao, T. Ishizaka, H. Kasai, H. Oikawa, and H. Nakanishi, “Fabrication of Unique Porous Polyimide Nanoparticles Using a Reprecipitation Method,” *Chem. Mater.*, vol. 19, no. 8, pp. 1901–1905, Apr. 2007.

[109] W. Wei, F. Bai, and H. Fan, “Surfactant-Assisted Cooperative Self-Assembly of Nanoparticles into Active Nanostructures,” *ISCIENCE*, vol. 11, pp. 272–293, 2019.

[110] T. Govindaraju, M. Pandeeswar, K. Jayaramulu, G. Jaipuria, and H. S. Atreya, “Spontaneous self-assembly of designed cyclic dipeptide (Phg-Phg) into two-dimensional nano- and mesosheets,” *Supramol. Chem.*, vol. 23, no. 7, pp. 487–492, 2011.

LIST OF PUBLICATIONS

Journals

T. Hirayama, A. Kumar, K.Takada, T. Kaneko, Morphology-controlled Self-assembly and Synthesis of Biopolyimide Particles from 4-Amino-L-phenylalanine, *ACS Omega*, accepted.

International conferences

1. Spring 2019 ACS National Meeting & Exposition

March 31-April 4, 2019, Orlando, Florida, USA

Title: Bio-based amino acid polymers and their self-assembly properties (Oral presentation)

Domestic conferences:

1. JAIST Japan-India Symposium on Advanced Science 2019

March 7, 2019, JAIST, Ishikawa, Japan

Title: Synthesis, characterization and self-assembly study of novel diketopiperazine based polymer (Poster presentation)

2. Symposium on Macromolecules (SPSJ)

20-22 September 2017, Ehime

Titile: Fabribation of polyimide nanoparticles from building blocks of amino-acid dimers (Poster presentation)

3. CSJKINKI

1 Dec 2017, JAIST High-tech center

Title: Fabribation of polyimide nanoparticles based amino-acid dimers (Poster presentation)

4. JAIST world conference (JWC) 2018

27-28 Feb 2018 JAIST High-tech center

Title: Fabribation of polyimide nanoparticles based amino-acid building blocks (Poster presentation)